Functional analysis of FtsZ1-2 in the cytoplasm of *Physcomitrella patens*. (Hedw.) B.S.G.

Zur Erlangung des akademischen Grades eines

DOKTORS DER NATURWISSENSCHAFTEN

(Dr. rer. nat.)

der Fakultät für Chemie und Biowissenschaften der
Universität Karlsruhe (TH)
vorgelegte

DISSERTATION

Von

Marianne Neumann

aus Bühl

Dekan: Prof. Dr. Stefan Bräse
Referent: Prof. Dr. Peter Nick
Korreferent: Priv. Doz. Frank Hartung
Tag der mündlichen Prüfung: 20. Oktober 2008

Zusammenfassung

Das Moos *Physcomitrella patens* ist evolutionsbiologisch gesehen ein Organismus von der Basis der Landpflanzen Entwicklung. Durch die einfachen Gewebe und den überschaubaren Entwicklungszyklus, und die genau bekannten Reaktionen auf Umwelt und Wachstumsbedingungen, ist es ein optimaler Modelorganismus für Entwicklungsbiologie und physiologische Studien. Seit einiger Zeit ist das Genom von *Physcomitrella* entschlüsselt und da es einer der wenigen bekannten pflanzlichen Organismus mit effektiver homologer Transformierbarkeit ist, ist *Physcomitrella* auch in der Genetik optimal für Studien einzusetzen.
FtsZ1-2 Protein, ist als einziges der fünf in *Physcomitrella* vorkommenden FtsZ Proteine nicht nur an der Chloroplastenteilung beteiligt ist, sondern besitzt auch ein Transitpeptid Motiv, mit dem es im Cytoplasma der Pflanzenzelle zum Einsatz kommt.
Für diese Studie wurden drei Mooslinien verwendet, die alle drei im Biotechnologischen Institut der Universität Freiburg von Dr. Anja Martin erstellt wurden. Es handelt sich dabei um eine Zelllinie die unter einem 35s Promotor FtsZ1-2:GFP überexprimiert, einen Wildtyp und die Knockout Zelllinie Δ114.
Um zu ergründen, was dieses ursprünglichen prokaryotischen Zellteilungsprotein in der Pflanzenzelle außerhalb des Chloroplasten bewirkt, wurden mehrere Wachstumsfaktoren, die Einfluss auf die Zellmorphologie von *Physcomitrella patens* nehmen, eingesetzt. Diese Faktoren waren Phytohormone, Zytoskelettdrogen, Hemmstoffe, die bakterielles FtsZ *in vivo* hemmen, sowie Lichtqualität und Quantität.
Diese Studie konnte einige neue Einflüsse benennen, die in Bezug auf FtsZ1-2 die Zellmorphologie verändern.
Der Einfluss von Lichtqualität auf die korrekte Entwicklung und Positionierung von Seitenzweiginitialen konnte in Abhängigkeit von FtsZ1-2 gezeigt werden. Rotlicht fördert eine unkontrollierte Verzweigung der Protonemazellen der Knockoutzelllinie, während die Anwesenheit von FtsZ1-2 im Plasma die Zahl der Verzweigungen verringert. Der differenzielle Einfluss von Abscisinsäure auf die Differenzierung der protonemalen Gewebe in Abhängigkeit von FtsZ1-2 konnte deutlich gemacht werden. ABA verhindert die Bildung von Caulonemazellen und fördert die Bildung von Chloronemata und Brachyzyten (Dauerzellen) in der Knockoutzelllinie und im Wildtyp, während die Überexpression von FtsZ1-2 die Reaktion auf ABA stark abschwächt.
Ein Einfluss von Kalzium auf die Zellmorphologie in Abhängigkeit von FtsZ1-2 konnte gezeigt werden. Durch den Einsatz der Kalziuminhibitoren EGTA (ein Chelator) und Verapamil (ein Kalzium Transport Blocker) konnte die FtsZ1-2:GFP bedingte Fluoreszenz im Cytoplasma verhindert werden, was auf den Einfluss von Kalzium auf die Polymerisierung von FtsZ1-2 *in vivo* schließen lässt. Außerdem beeinflusst Kalziummangel die Verzweigung in der Überexpressionslinie und in der Knockoutzelllinie auf die gleiche Weise, indem es unregelmäßige Verzweigungen erzeugt. Dieser Effekt war im Wildtyp nicht so stark ausgeprägt.
Sanguinarin und Zantrin Z3 sind Inhibitoren der bakteriellen Zellteilung durch ihre Interaktion mit FtsZ. Z3 stabilisiert FtsZ auf Taxol artige Weise, während Sanguinarin dir Polymerisierung der Monomere verhindert. In allen drei Zelllinien führte die Inkubation mit den FtsZ- Inhibitoren zur Produktion von kürzeren Zellen. In der Überexpressionslinie war der Effekt allerdings gedämpft.Den stärksten Einfluss auf FtsZ1-2:GFP hatten starkes Weißlicht und Cytokinin, besonders in Kombination, da durch die Inkubation mit diesen Faktoren die Bildung von FtsZ1-2 Filamenten im Cytoplasma und fluoreszente Strukturen in den Chloroplasten gezielt herbeigeführt werden konnten.

Table of Contents

1. Introduction

1.1. FtsZ in evolution, an old protein in a new job?

Modern plants evolved from primitive organisms residing in the Ordovician oceans. They underwent significant changes in their metabolism and growth in order to enable their adaptation to the constantly changing and adverse environmental conditions existing on land

Plants had already acquired an important tool for this colonialization millions of years before. During one or more endosymbiosis events (McFadden, 2001) the first photosynthetically active prokaryote was engulfed by an early eukaryote cell and was transformed into a fully functioning symbiont instead of being digested.

The development of chloroplasts signified a radical change in life on our planet, since these photosynthetic organisms, were now able to use a completely new energy source.

The harmonized interaction of all metabolism-related components and functions was of great importance in this new situation. A responsive sensory apparatus and a superordinate messenger and regulatory system made a fast and effective reaction to environmental changes possible.

Of central importance to plants now and then is the synchronization of their own growth and division with that of their symbionts. Since no chloroplast can be synthesized *de novo*, cells not capable of this synchronization end up without symbionts and the possibility to "synthesize food from sunlight" (Mc Fadden, 2001).

This means that a regulation system for chloroplast division had to be established. For that the transfer of genetic material from the plastids to the nucleus of the host cell (reviewed in Kuroiwa *et al*. 1998) was an important step. Most of the division proteins of the chloroplast are now encoded in the nucleus and have to be reimported into the plastid.

The ideal target for regulation through the host cell is FtsZ ("filamentous thermo sensitive Z"). This protein has been inherited from the bacterial ancestors of our chloroplasts. Its central role in chloroplast division results from the fact that it is the first protein that is recruited to the division site in bacteria and chloroplasts.

1.2. The FtsZ protein, a prokaryotic homologue of eukaryotic tubulin

One of the few division proteins of the bacterial divisome identified in plants so far is FtsZ (Stokes and Osteryoung 2003, Miyagishima *et al.* 2004). Its crystal structure shows that it possesses four distinct domains including a highly conserved core region, a variable N-terminal segment, a spacer region and a conserved C-terminal peptide (Figure 1.2.1, Margolin 2005). The core region consists of two further segments that fold separately, namely the N-terminal segment (NT core) and C-terminal segment (CT core). Both core segments are important in FtsZ monomer binding.

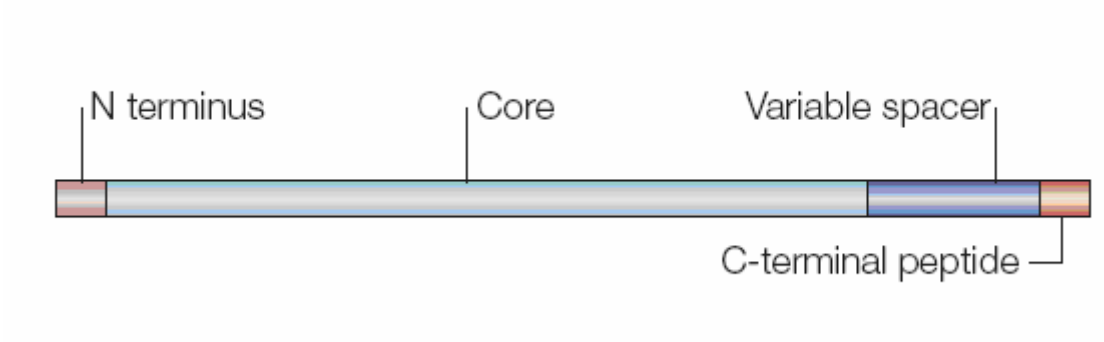

Figure 1.2.1 Domain structure of FtsZ (Margolin 2005)

Since FtsZ and tubulin show many similarities in their tertiary structures, it is claimed that FtsZ is a tubulin homologue (Löwe and Amos 1998), even though sequential similarity is only about 20% (Burns 1998). Apart from their crystal structure, tubulin and FtsZ share important features. For example, FtsZ contains the tubulin signature GTP-binding motif, GGGTG(T/S)G at the N-terminal core region and is able to hydrolyze GTP (Erickson 1997).
It was also shown to form asters (Figure 1.2.2) and protofilaments, but whereas tubulin depolymerizes in the presence of Ca^{2+}, GTP dependent FtsZ assembly is mediated by Ca^{2+} (Yu and Margolin 1997) at millimolar concentrations.

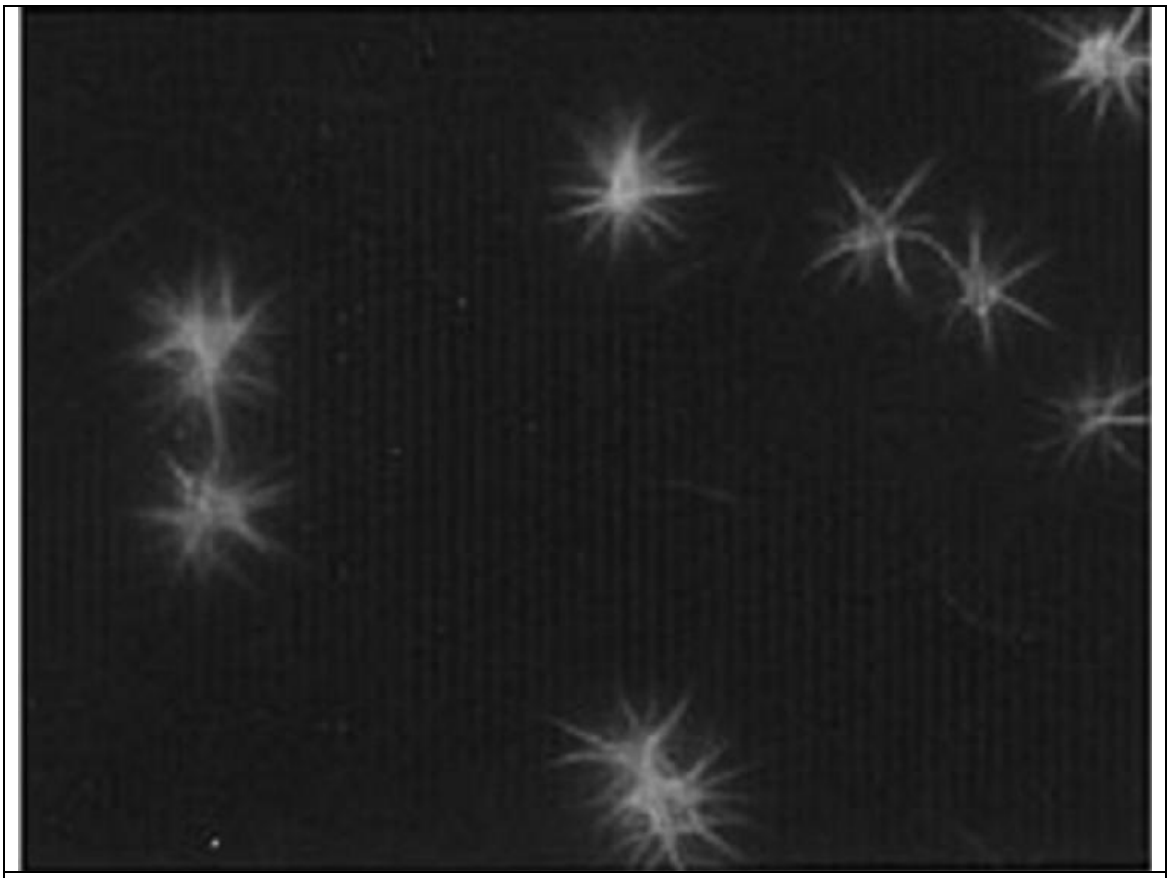

Figure 1.2.2 FtsZ:GFP asters (Yu and Margolin, 1997)

FtsZ self assembles into filamentous tubules, minirings and protofilament sheets, thus resembling tubulin behavior *in vitro* (Erickson *et al.*1996). FtsZ binds GTP and GDP at micromolar concentrations. Mg^{2+} is needed for GTP hydrolysis but not for GTP binding (Lutkenhouse and Addinall 1997).

FtsZ and tubulin both share important features during cell division.
All these similarities led to the suggestion, that FtsZ might be the evolutionary precursor of tubulin (Erickson 1995). New FtsZ-like proteins have been identified in bacteria, like tubZ from *Bacillus thuringiensis*, which shares properties with FtsZ and tubulin, but is only distantly related to both. Phylogenetic analysis suggests that all three proteins form distinct groups which share an ancient ancestor, rather than being descended from each other (Larson *et al.* 2007).

1.3. Binary fission: How prokaryotes divide

Bacteria divide through binary fission, which at first glance seems to be a simple process. When a certain cell size is reached a constriction appears at the division site of the bacterium. This constriction narrows further and divides the mother cell into two identical daughter cells (Vincente *et al.* 2006).
In the rod shaped *E. coli*, possibly the best studied bacterium, division is a highly ordered and strictly regulated process. It starts with the binding of FtsZ protein to the membrane at midcell, where it forms the highly dynamic and energy dependent scaffold (or Z-ring) that allows the other 16 so far identified division proteins to assemble at the right time and space and form the division ring (divisome).
The divisome is a constrictive multiprotein complex that leads the way for the constriction of the cell membrane. How this constriction is achieved is controversially discussed. One model proposes a spiral or coil of FtsZ protein that constricts by forming tighter loops. This tightening might be brought about by conformational changes induced through GTP- hydrolysis of FtsZ itself (Erickson 1997) or may be mediated through hitherto unknown motorproteins.
By redirecting peptidoglycan synthesis to follow the constricting membrane, septation is finally achieved (Vincente *et al.* 2006). A complex of FtsB, FtsL and FtsQ is suggested to influence the peptidoglycan synthesis machinery to that end (Buddelmeijer and Beckwith, 2004). These three proteins are also located at the division site (Figure 1.2.1)

Figure 1.2.1 Dividing *E. coli* cell. Z-ring labeled by FtsL:GFP fusion protein (Ghigo *et al.* 2000)

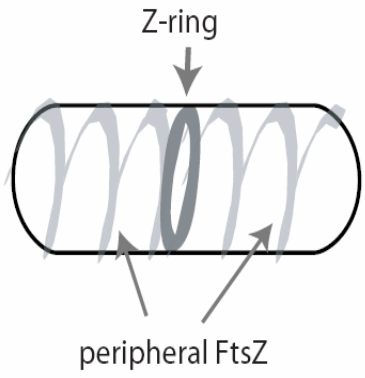

Figure 1.2.2 Two sub-populations of *E. coli* FtsZ, with distinct diffusion properties. (Niu & Yu 2008)

Niu and Yu (2008) described two separate populations of FtsZ during divisome formation of *E. coli*. They observed that the polymerized protein inside the ring is mostly stationary and is accompanied by another sub- population of monomeric and dimeric FtsZ molecules with different diffusion properties, oscillating between cell poles on helical paths (Figure 1.2.2). Helical patterns were observed earlier (Z-spiral, Thanedar and Margolin 2004) and taken as evidence for filamentation of the protein inside the cytoplasm of *E. coli* and *B. subtilis*. This led to the postulation of cytoskeleton-like structures in bacteria.

The concentration of FtsZ protein inside the bacterial cell is about five times higher than the critical concentration necessary for assembly. This implies the presence of inhibitors to safeguard the correct function of the protein (Margolin 2005).
One of those factors, which also shows oscillatory behavior has been described for the MinCDE system, which guides FtsZ to midcell position (Rothfield *et al.* 2001)
By an intricate pattern of membrane binding and mutual inhibition the MinCD proteins oscillate from cell pole to cell pole keeping FtsZ in the cytoplasm, until Min E forms a ring like structure which wanders towards the poles pushing MinCD ahead, and clearing the midcell region for FtsZ binding. MinE is doing this in oscillating waves with a period of about 90 seconds.
Since FtsZ only polymerizes in time for cell division, another mechanism is needed, to keep it from assembling in the absence of MinCD. Woldringh (1990) proposed nucleoid occlusion as the mechanism that prevents FtsZ to polymerize over unreplicated and unsegregated DNA. It is proposed that Noc (*B. subtilis*) and SlmA (*E. coli*) keep FtsZ from polymerizing in the presence of the nucleoid (Wu and Errington 2004; Bernardt and de Boer 2005). When Plasmid segregation is completed and the mid-cell region is cleared from DNA, FtsZ is needed to polymerize. Liu *et al.* (1998) proposed that FtsK might link these two processes together.
The first protein to interact with FtsZ at midcell position is ZapA, which is a positive regulatory factor needed for bundling of the protofilaments. ZipA and FtsA come next. Both proteins are thought to anchor the Z-ring at the cell membrane. It is known, that ZipA binds to the C-terminal peptide domain described earlier (Reviewed in Margolin 2005).
The concentration ratio of FtsZ to FtsA and ZipA are crucial for correct cell division. A slight overexpression of FtsZ leads to minicell formation via increased division frequency. Overexpression of FtsZ inhibits cell division completely and leads to long unseparated bacterial filaments. (Hale and de Boer 1997; Dai and Lutkenhaus 1992; Ward and Lutkenhaus 1985).
Another important factor inhibiting cell division is the SOS response protein SulA that is induced at DNA damage. It binds directly to FtsZ and thus delays protofilament assembly until it is cleaved again by the Lon protease (Margolin 2005).

Even though the function of most bacterial division proteins is as yet unclear, the time and place of their recruitment to the Z-ring has been established (Figure 1.3.1). Without the correct sequence of binding, the divisome assembly cannot be completed and division cannot take place.

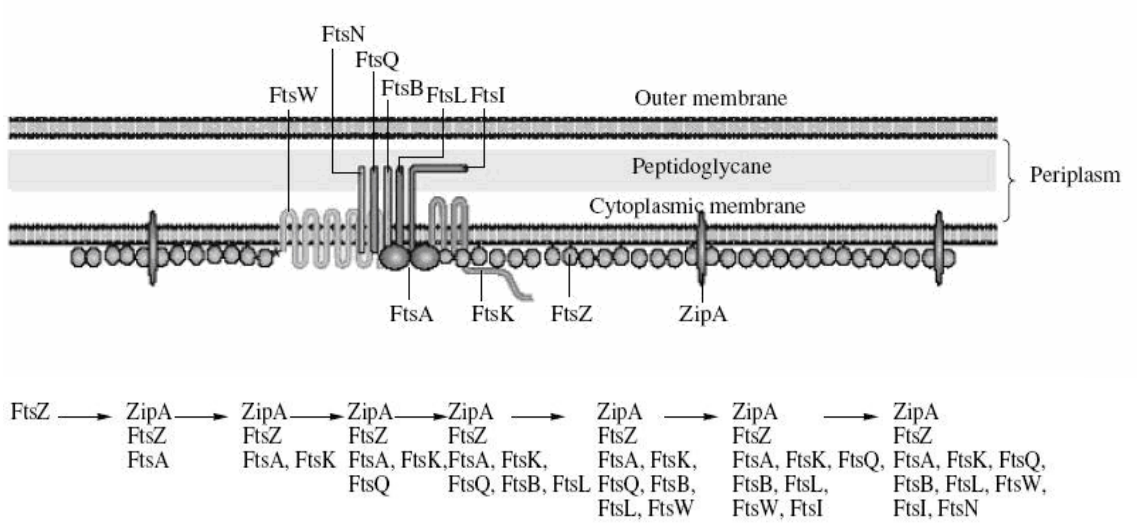

Figure 1.3.1 The bacterial divisome (Figures taken from Margolin 2005)
The upper picture shows the placement of some Z-ring associated proteins at their putative binding sites, the lower picture shows the temporal and spatial placement of the divisome proteins in relation to FtsZ.

1.4. Chloroplast division and FtsZ

As proposed by Schimper as early as 1883, chloroplasts also divide via binary fission. Chloroplast division is just as complex as bacterial division and less is known about the processes leading to the separation of the daughter plastids. Unlike bacteria, chloroplasts possess two division rings. The membrane systems of the chloroplasts are complex and highly structured and consist of the outer envelope, the inner envelope and the thylakoid membranes, which have to be coordinately severed. For this purpose, a cytosol-oriented division ring is formed at the outer envelope membrane of the chloroplast and a second, inner ring is formed at the stromal side of the inner envelope membrane (Kuroiwa *et al.* 1998; Miyagishima *et al.* 2001). The composition of these two rings is not yet clear, but some components of the plastid division machinery have been identified. As in bacteria, the first protein to bind to the future division site is FtsZ. Unlike bacteria, there are two distinct FtsZ families present in plants, FtsZ1 and FtsZ2 (see below), that interact mutually and with other proteins of the plastid division machinery. El Kafafi *et al.* (2005) have shown that FtsZ2 is tightly associated with the inner envelope membrane and that FtsZ1 is located mostly as a soluble protein in the stroma. The meaning of this localization is not yet understood.
Apart from FtsZ, so far three homologues of prokaryotic divisome proteins have been identified, MinD, (Colletti *et al.* 2000; Dinkins *et al.* 2001), MinE (Maple *et al.* 2004; Reddy *et al.*, 2002) and GC1/ Sul A (Maple *et al.* 2004; Raynaud *et al.* 2004)
The Min system, which is missing its bacterial MinC component, again is necessary for correct placement of FtsZ to the division site. Mutations of MinD in *Arabidopsis* lead to multiple asymmetric constriction events reminiscent of *E. coli* MinD mutations (Colletti *et al.* 2000, Maple *et al.* 2002). The role of MinC might have been taken over by Arc3, which is a plant specific protein with some similarities to FtsZ that has been shown to interact with MinD/E and FtsZ1 in *Arabidopsis*. (Shimada *et al.* 2004).

The function of GC1 is not clear, since it misses the *Ec*SulA specific FtsZ binding site, but it has been shown to associate with the inner envelope. GC1 has been proposed to be an indirect regulator of the Z- ring (Reviewed in Glynn *et al.* 2007)
Other proteins are recruited to the Z- ring in chloroplasts. A positive regulating factor is Arc6, an inner envelope membrane protein (Vitha *et al.* 2003). *Arc6* mutants possess only short FtsZ filaments in *Arabidopsis* macrochloroplasts. Overexpression leads to abnormally long branched FtsZ filaments inside oversized chloroplasts (Glynn *et al.* 2007). It has been shown by the same author that Arc6 binds to a specific short C-terminal motif in FtsZ2 which FtsZ1 does not possess. It has also been shown to localize to the division site in *Arabidopsis* chloroplasts.
Neither timing nor components of the division ring assembly are so far completely understood, but a further difference to bacterial division has been shown for chloroplasts, in that dynamins form another ring, distinct from the inner and outer division-ring during constriction of the plastid (Miyagishima *et al.* 2003). The dynamin like protein is Arc5, and has first been characterized at the division site of the rhodophyte *Cyanidioschyzon merolae* (Gao *et al*. 2003; Miyagishima *et al*. 2001). In *Arabidopsis* and *Physcomitrella*, Arc5 is recruited to the division site only in the presence of PDV1 and PDV2 at a late stage of division (Miyagishima *et al.* 2006). PDV1 and PDV2 are anchored to the outer envelope membrane through membrane spanning domains in both their sequences. They form a discontinuous ring at the constriction site, similar to that of Arc5. A tentative model of the supposed sites of action (Mapel *et al.* 2005) is given in Figure 1.4.1.

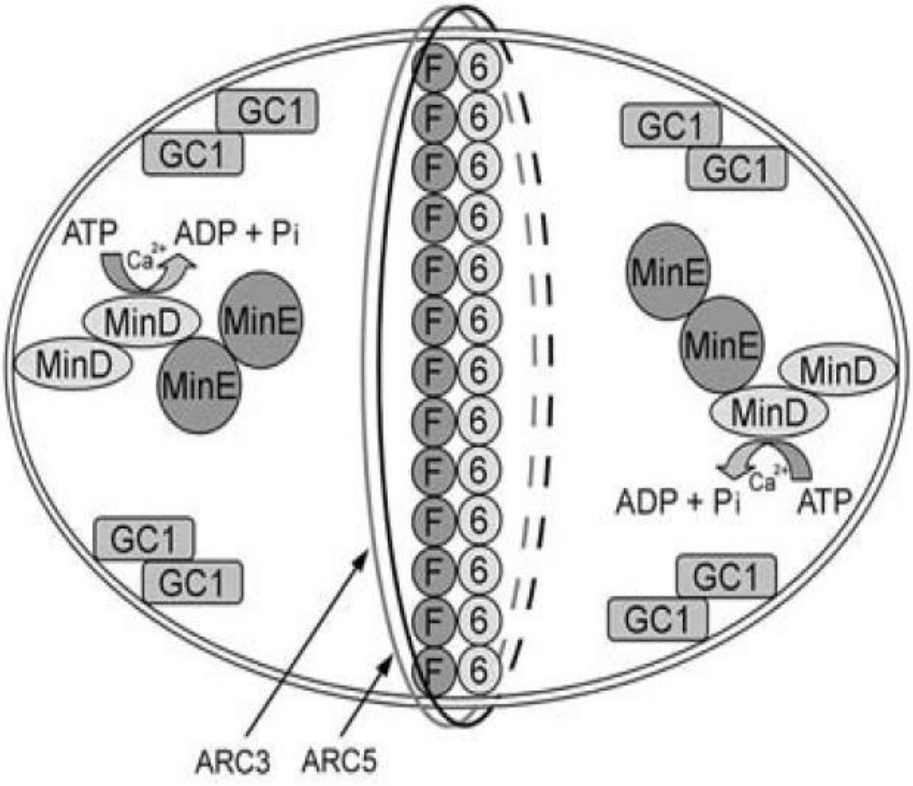

Figure 1.4.1 Tentative model of the plastid division machinery, indicate the supposed sites of action of the known components. Figure taken from Mapel *et al.* (2005).

1.5. FtsZ inside the plant cell

Plant FtsZ was first identified in the nuclear genome of *Arabidopsis thaliana* (Osteryoung and Vierling 1995) In contrast to bacteria, plant cells possess various paralogues of the *ftsZ* gene, which cluster in two distinct families (FtsZ1 and FtsZ2) with different structure and functionality (Osteryoung and McAndrew 2001; Rensing *et al.* 2004). Stokes and Osteryoung (2003) postulated that the cyanobacterial progenitor of chloroplasts first procured a duplicated FtsZ gene between the divergence of red and green algae.
First evidence of a function of FtsZ in chloroplast division was given by Strepp *et al.* (1998), who showed, that the deletion of *ftsZ* in the genome of *P. patens* leads to inhibition of chloroplast division and the formation of one giant chloroplast per cell. This was confirmed by Osteryoung *et al.* (1998) who demonstrated a similar phenotype in *Arabidopsis* chloroplasts expressing an *ftsZ* antisense transgene.
Functionality in chloroplast division of the different FtsZ paralogues have been shown in *Physcomitrella patens* (Kiessling *et al.* 2004) and *Arabidopsis* (Stokes *et al*. 2000).
Arabidopsis harbors three paralogue *ftsZ* genes (*Atfts*Z2-1, *Atfts*Z2-2, *Atfts*Z1-1). Vitha *et al.* could show that GFP-fusion proteins of FtsZ1 and FtsZ2 formed co-aligned rings at the division site in *Arabidopsis*, pea and tobacco chloroplasts.

So far, five FtsZ paralogues have been identified in *Physcomitrella patens*. FtsZ1-1 has been shown to localize to the plastid where it assembles into filamentous networks.
Ftsz1-3 has only recently been described. It possesses high sequence similarity with FtsZ1-1 and also assembles into networks inside of the chloroplast. FtsZ1-1 and FtsZ1-3 are also both present inside stromules, which are tubular stroma-filled outgrowths of the plastid membranes (Gremillon *et al.* 2007)
FtsZ1-2 has been shown to be dually targeted to the chloroplast and the cytosol and to form ring like and filamentous structures in the cytosol and at the division site in chloroplasts (Kiessling *et al.* 2004). It has also been shown that *ftsZ*1-2 knock out plants have an altered cell shape and size (Martin 2007). Because of this it is proposed that Ftsz1-2 is a molecular link between cell and plastid division in mosses (Kiessling *et al.* 2004).
FtsZ2-1 and FtsZ2-2 do not have a targeting motif to the cytosol. They interact inside the chloroplasts where they form filamentous networks that have been termed plastoskeleton because of their similarity to the cytoskeleton of eukaryotes (Reski 2002). It is further believed that these two proteins hold the chloroplasts in shape since they have lost their peptidoglycan support (McFadden 2000).
Fluorescence resonance energy transfer (FRET) analyses of *P. patens* proteins FtsZ1-1, FtsZ1-2, FtsZ2-1, and FtsZ2-2 could demonstrate specific interaction of all four proteins in the cytosol and the chloroplasts of *P. patens* (Figure 1.5.1 Gremillon *et al.* 2007).

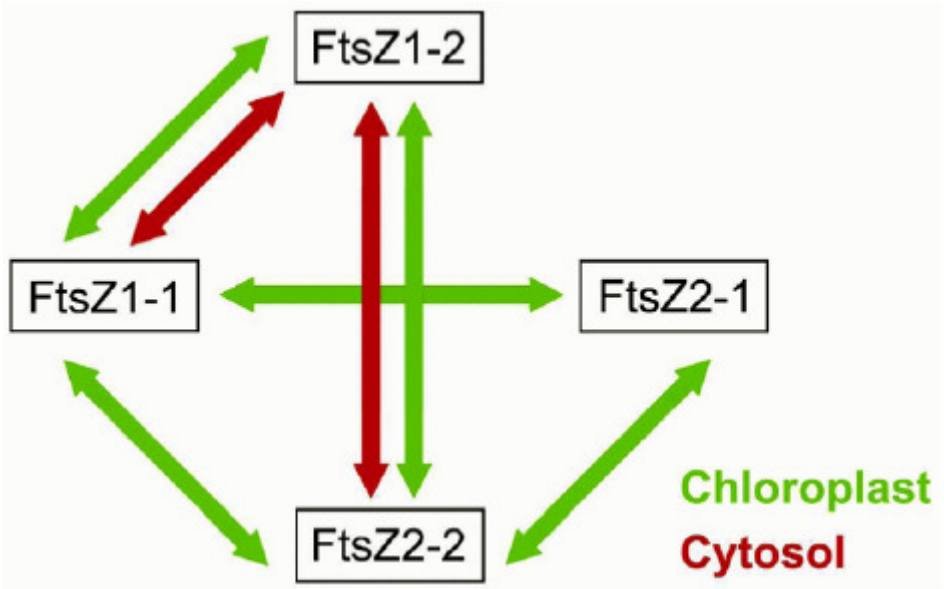

Figure 1.5.1 Model of *Pp*FtsZ interaction in their respective compartments. (Figure taken from Gremillon *et al.* 2007)

1.6. The model organism *Physcomitrella patens*

The first proof of land plants are microfossils, spores of relatives to bryophytes found in rocks of mid-Ordovician age some 475 million years ago (Wellman *et al.* 2003). The discovery of those fossils places bryophytes at the beginning of land-plant evolution and explains some of their importance to evolutionary research. Research on bryophytes closes an important gap in our understanding of land plant development.
Physcomitrella, a member of the bryophytes, has several advantages for developmental studies. Like ferns and other mosses *Physcomitrella* undergoes alteration of generation. A haploid spore reacts to the presence of light and water with the development of a green filamentous protonema. The chloronema, as it is called because of its high number of round chloroplasts, is the first juvenile gametophyte state and shows typical tip growth. Its cells have cross walls perpendicular to the filament axis. Chloronema cells divide every 10 to 12 hours (Schumaker and Dietrich 1997). Protonemal tissue can be arrested in the chloronema state by low light, addition of ammonium tartrate to the medium and low pH (Hohe and Reski 2005). Increased light and auxin induce the apical cell to differentiate into the second juvenile cell type, the caulonema. This cell type also grows filamentous, with oblique cross walls. Caulonema cells are up to 400 µm long and thinner than chloronema cells. They have less and smaller chloroplasts and divide about every 5 to 6 hours (Schumaker and Dietrich 1997). The change of cell wall orientation is brought about by microtubules (Reski 1998). When side branches form, first, a swelling arises at the apical end of the second subapical cell. The nucleus of the subapical cell moves then to the apical cell pole, where it divides. One of the daughter nuclei moves into the swelling that expands further, and is sealed off from the mother cell through the formation of a new longitudinal cell wall. Those swellings or caulonema initials can adopt two distinct developmental fates. In the absence of cytokinin, the initials continue filamentous growth. Under the influence of cytokinin a new developmental stage, that is bud formation, is initiated. Bud formation marks the transition from filamentous tip growth to three dimensional growth via a three faced apical cell (Schumaker and Dietrich 1997).The fate of the bud initial can be changed back to filamentous growth by abscisic acid treatment (Christianson 2000). On the leafy

adult gametophyte, archegonia and antheridia arise, which contain spermatozoids and egg cells. The spermatozoids need water to reach the archegonia. Inside the archegonia, fertilization takes place and from the Zygote a diploid sporophyte arises.

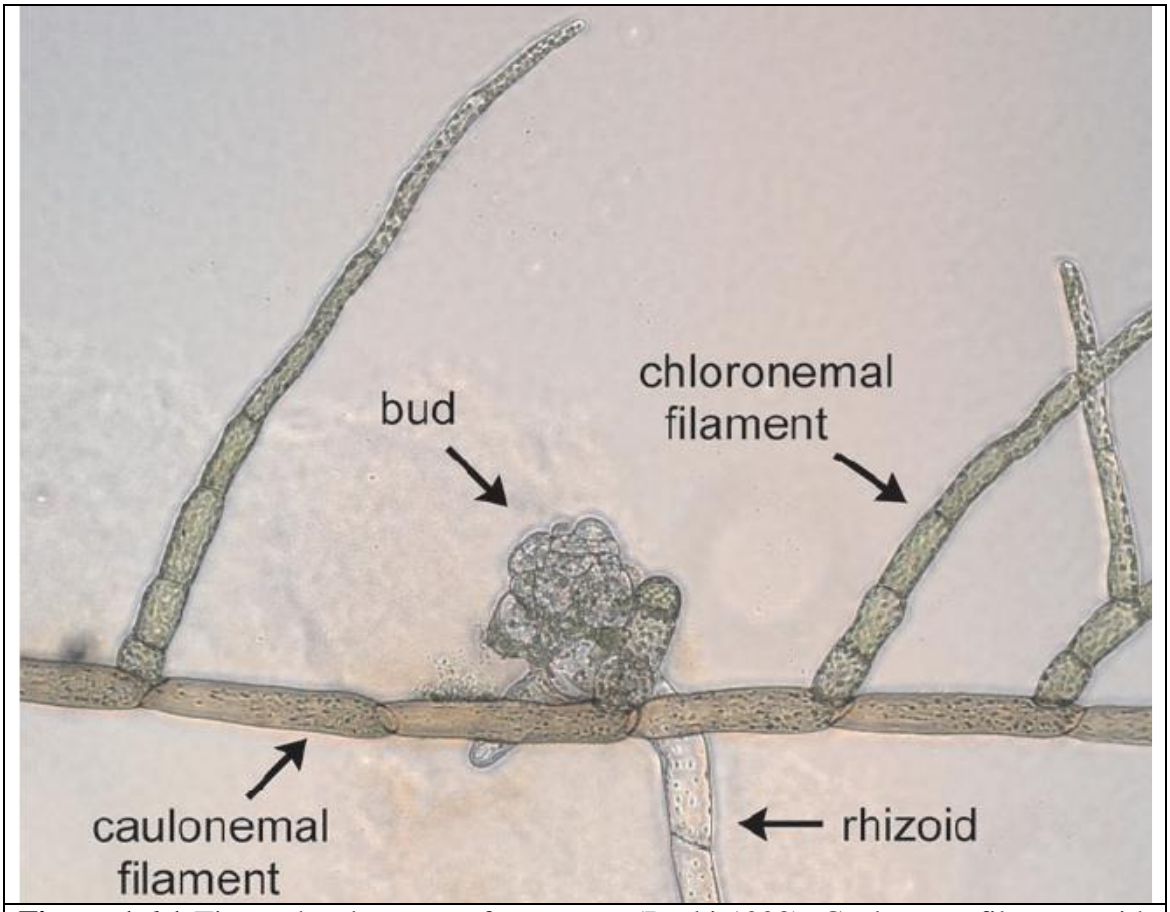

Figure 1.6.1 Tissue development of *P. patens* (Reski 1998). Caulonema filament with small chloroplasts and dark pigmentation, producing a bud and secondary chloronema above oblique cell-walls. At the base of the bud rhizoids are developed. (Figure taken from Thelander *et al*. (2005))

The sporophyte is nurtured by the gametophyte and when separated is not viable on its own. Meiosis leads to the production of haploid spores, and the cycle begins anew.
Each differentiation step is tightly controlled and brought about by a few known factors like hormones, temperature, gravity and light. This makes differentiation easy to follow and predictable. Of the filamentous growing moss protonema cells, only the tip cells divide. This provides a powerful tool for analysis of polarity. The tissues are simple and easy to cultivate.
Physcomitrella is also a powerful tool for targeted genetic manipulation, since *P. patens* is the only known land plant with an efficient mechanism for homologues recombination of foreign DNA into the nuclear genome (Schaefer and Zryd 1997).
Hohe and Reski (2005) described the regenerational potential of *P. patens* under hormone-free conditions, which makes vegetative propagation under controlled conditions easily possible.

1.7. Aim of this study

To synchronize cell- and chloroplast division, a signal is needed, that is understood by the chloroplast, initiates chloroplast division and also tells the cell what state the symbiont chloroplasts are in.
The central role of FtsZ in chloroplast division implies that it is closely controlled by the host cell. FtsZ1-2 is the only FtsZ paralogue targeted to cytoplasm and the chloroplast which could imply a role in this signaling process.
It has previously been shown in overexpression and knock-out experiments that FtsZ1-2 not only affects chloroplast division but also the cell morphology and differentiation.
These three aspects of cell development are tightly controlled by hormone and light signals.
The aim of this study was to find parameters that influence FtsZ1-2 in its interaction with the living cell, and thus provide insight in its functionality and role inside the cytoplasm of *Physcomitrella patens*. For this the following questions were asked:

1. Does hormone treatment influence FtsZ1-2 filament formation or action in the cytoplasm?
   An example for such cooperation is auxin and actin microfibrils, which interact in the cytosol and determine pattern formation (Maisch and Nick 2007).

2. Is FtsZ1-2 involved in differentiation of *P. patens* cells?
   Cyanobacterial FtsZ has been shown to have a dual role in differentiation of heterocysts in the *Nostoc* / *Anabaena* strain PCC7120 (Klint *et al.* 2005).

3. Is there an interaction between the cytoskeleton and FtsZ1-2?
   Similarities in sequence, structure and behavior exist between FtsZ and tubulin.

4. Is FtsZ1-2 involved in the plants reaction to light signals?
   One of the most important growth factors in the life of a plant is light. The connection between light signals and the differentiation in the moss *P. patens* have been shown before (Imaizumi *et al.* 2002).

2. Materials and methods

2.1. Chemicals

$Ca(NO_3)_2$ x 4 H_2O; Merck

Colchicine; Sigma Aldrich

DMSO (Dimethylsulfoxid) Serva

EGTA (Ethylenglykol-bis-(2-aminoethylethyl)-tetraacidic acid) Roth (Karlsruhe)

$FeSO_4$ x 7 H_2O; Merck

GTP (Guanosin-5'-triphosphate) Roth (Karlsruhe)

indole-3-acetic acid (IAA); Sigma-Aldrich

KCl; Merck

KH_2PO_4; Merck

LatrunculinB; Sigma Aldrich

$MgSO_4$ heptahydrat, Merck

N^6- Δ^2- isopentenyladenine, 2iP; Sigma Aldrich

1-*N*-naphthylphthalamic acid (NPA); Duchefa

Oryzalin; Sigma Aldrich

PIPES (Piperazin-N,N'-bis(2-ethansulfonic acid)) Roth (Karlsruhe)

Sanguinarine chloride hydrate; Sigma Aldrich

Verapamil; Sigma Aldrich

Z1: 4-chloro-2,6-bis(5-chloro-2-hydroxybenzyl) phenol ; ChemBridge, Hit2Lead.com

Z3: N'-{2-[2-(4-chlorophenyl)vinyl]benzo[g]quinazolin-4-yl}-N,N-diethyl-1,2-ethanediamine; ChemBridge, Hit2Lead.com

2.2. Culture medium

Knop medium:

1g $Ca(NO_3)_2$ x 4 H_2O

250 mg KCl

250 mg KH_2PO_4

250 mg $MgSO_4$ x 7 H_2O

12,5 mg $FeSO_4$ x 7 H_2O

ad 1 l H2O

pH was adjusted to 5.8 with 1 M KOH.

For Knop solid medium 12 g/l purified sugar free Koobe agar (Roth Karlsruhe) was added.

2.3. Plant material and growth conditions

2.3.1. Plant material

Wild type of *Physcomitrella patens* (Hedw.) B.S.G. (classification: Bryophyta; Funariales; Funariaceae) is a subculture of strain 16/14 which was collected in Gransden Wood, Huntingdonshire, UK, by H.L.K. Whitehouse and was propagated by Engel (1968) by a single spore. It has been characterized previously (Reski *et al.*, 1994).

FtsZ1-2:GFP ox cell line strain 97 was kindly provided by Dr. Anja Martin (Plant Biotechnology, Albert-Ludwigs-Universität Freiburg im Breisgau) who co-transformed *Physcomitrella patens* with the linearized FtsZ1-2:GFP vector, which contains the full length *fts*Z1-2 cDNA fused to *gfp* under the control of the 35S promoter, and circular pRT101neo, whose *npt*II cassette for antibiotic selection (Martin 2007).

ΔFtsZ1-2 line 114 was kindly provided by Dr. Anja Martin (Plant Biotechnology, Albert-Ludwigs-Universität Freiburg im Breisgau) who generated the knock out cell line with a construct previously cloned by Dr. Justine Kiessling (Martin 2007).

2.3.2. Growth conditions

P. patens was grown in 300 ml *Erlenmeyer* flasks containing liquid Knop medium, and was placed on orbital shakers (150 rpm, IKA KS 260 basic, IKA Labortechnik, Staufen, Germany) in a growth chamber with controlled conditions (25 ± 1°C; light-dark regime of 16:8 h).

Light was given from above from 5 fluorescent tubes, Philips TLD 15W/25 light flux of 25 µmol s^{-1} m^{-2}.
Subcultivation was carried out in 10-day intervals, protonema cultures were blended for 3 min at 26000 rpm with a Heidolph *silent crusher* M after transfer to fresh Knop medium.

Adult gametophytes were axenicaly grown in petridishes, on solid Knop medium which was placed in a growth chamber with controlled conditions (see above). Light was given from above from 5 fluorescent tubes, Osram L 18W/25 light flux of 55 µmol s^{-1} m^{-2}.
Subcultivation was carried out every 8 weeks by transferring the adult gametophytes to fresh solid Knop medium.

2.4. Microscopy and cell measurements

For microscopic examination an AxioImagerZ.1 microscope (Zeiss) with an ApoTome slider for the generation of optical sections was used. For documentation, pictures were taken with the digital AxioCam MRm, which is a cooled digital CCD camera.

Rhodamine fluorescence was observed with the CY3, 43 HE filter set (exitation wavelength 550 nm, emission wavelength 605 nm).
GFP fluorescence was observed with the 43 HE filter set (exitation wavelength 500 nm, emission wavelength 535 nm).

For analysis of cell morphology differential interference contrast illumination was used.
Measurements of cell length were conducted with the AxioVision software.
If not stated otherwise, random pictures of 100 protonemata were taken and the cell length of 200 cells per sample measured. Cell division in the samples was not synchronized, so that all apical cells were not measured, because they were the only ones growing.

Counting of side branches:
Starting at the apical cell and proceeding to the tenth cell in basal direction, all side branches and side branch initials of 100 protonemata were counted. The average number is presented in [%]

Images were adapted in respect to brightness and contrast with the AxioVision software and Photoshop software (Adobe Systems, San Jose, CA, USA).

2.5. Hormone treatment

If not otherwise stated, 5 ml of 14 day old cultures of wild type, FtsZ1-2:GFP ox cell line and ΔFtsZ1-2 line were transferred to 100 ml Erlenmeyer flasks containing 45 ml of fresh sterile Knop medium with the addition of the appropriate concentration of hormone. Control samples were treated likewise with the addition of the corresponding amount of solvent instead of hormone. The samples were incubated under the appropriate light conditions for 6 days. For quantification random pictures were taken and 200 protonema cells were measured for cell length.

2.5.1. Treatment with 2iP

Samples were treated as above with the addition of 20 µM 2iP. Control samples were treated likewise with the addition of the corresponding amount of Ethanol instead of 2iP.

2.5.2. Treatment with IAA

Samples were treated as above with the addition of 20 µM of IAA. Control samples were treated likewise with the addition of the corresponding amount of DMSO (water free) instead of IAA.

2.5.3. Treatment with NPA

Samples were treated as above with the addition of 10 µM of NPA. Control samples were treated likewise with the addition of the corresponding amount of DMSO (water free) instead of NPA.

2.5.4. Treatment with ABA

Samples were treated as above with the addition of 20 µM of ABA. Control samples were treated likewise with the addition of the corresponding amount of 100% Ethanol instead of ABA.

2.6. Light treatment

Culture conditions:

2 ml samples of 14 day old cultures of wild type, FtsZ1-2:GFP ox cell line and ΔFtsZ1-2 line were plated on solid Knop medium. The samples were incubated under the appropriate light conditions for four days.

Light conditions:

Strong light was provided from above with a sodium high pressure tube from Phillips Master Son T, Pia Green Power 400 W, light flux 100 µmol s^{-1} m^{-2}.

Blue light was provided from above with a light field containing light emitting diodes TLDR 5800 (Vishay) with a wave length peak at 650 nm. Light flux was adjusted to 100 µmol s^{-1} m^{-2}.

Red light was provided from above with a light field containing light emitting diodes HLmP- HB57- LP000 (Avago Technologies) with a wave length peak at 470 nm. Light flux was adjusted to 100 µmol s^{-1} m^{-2}.

2.7. Incubation under calcium stress

14 day old samples of all three *P. patens* cell lines were incubated in Knop medium without Ca^{2+} with the addition of 5 mM EGTA (pH 5,8 adjusted with 1 M KOH) for four days under low light conditions.

Influence of intracellular Ca^{2+} transport was determined by incubating 14 day old samples of all three cell lines in Knop medium with the addition of 50 µM Verapamil, a Ca^{2+} channel blocker, for four days under low light conditions.

As a control 14 day old samples of all three cell lines were grown for four days under low light conditions in standard Knop medium.

2.8. Cytoskeleton inhibition drug treatment

2.8.1. Latrunculin B treatment for fluorescence measurement

10 days old *P. patens* FtsZ1-2:GFP overexpression cell line grown under low light conditions was treated with Latrunculin B at a final concentration of 1 µM and incubated under strong light conditions in 100 ml Erlenmeyer flasks for 3 days. The control was also treated with Latrunculin B and incubated for 3 days under low light conditions.
Of those cultures, samples were taken and 200 protonemata checked for fluorescence.

2.8.2. Cold treatment for fluorescence measurement

To test if cold treatment had an effect on FtsZ1-2:GFP filament stability, 1 ml protonemal tissue from liquid cultures of the FtsZ1-2:GFP overexpression line was incubated for 15 and 30 minutes on ice. Prior to incubation 200 protonema were checked for fluorescent cytoplasmic bundles. After the appropriate time the counting was repeated with the treated cells.

2.8.3. Oryzalin treatment for fluorescence measurement

To test if longer incubation of *P. patens* FtsZ1-2:GFP overexpression lines with Oryzalin had an effect on FtsZ filament stability, agitated liquid cultures were treated with 10 µM Oryzalin (final concentration), incubated for 6 hours under low light conditions and then checked for fluorescence.
Prior to incubation 200 protonema were checked for fluorescent cytoplasmic bundles. After six hours the counting was repeated with the treated cells.

2.9. FtsZ inhibitor treatment

2.9.1. Zantrin Z1 treatment for fluorescence measurement

14 day old samples of the Ftsz1-2:GFP ox cell line were incubated in agitated liquid culture in the presence of 10 µM of Z1 (5mM stock solution in DMSO, sterile filtered) for 15, 30, 45 and 60 minutes and then 200 Protonema were checked for fluorescence.
Control samples were treated likewise but with a corresponding amount of DMSO (2 µl DMSO to 1 ml Knop medium).

2.9.2. Zantrin Z3 treatment for cell length measurements

Samples of 10 day old *P. patens* cell lines grown in liquid cultures on orbital shakers were transferred to fresh Knop medium and treated with 5 µM of Z3 (5 mM stock solution in DMSO, sterile filtered) for 72 h under low light conditions.
Control cells were treated with a corresponding amount of DMSO (50 µl per 50 ml Knop medium) and also incubated for 72 h under the same conditions. 200 cells per sample were measured for cell length.

2.9.3. Sanguinarine treatment for cell length measurements

Samples of 10 day old *P. patens* cell lines grown in agitated liquid cultures were transferred to fresh Knop medium and treated with 10 µM of Sanguinarine (10 mM stock solution in DMSO, sterile filtered) for 72 h under low light conditions.
Control cells were treated with a corresponding amount of DMSO (50 µl per 50 ml Knop medium) and also incubated for 72 h under the same conditions. 200 cells per sample were measured for cell length.

2.10. Microtubule polymerization coverslip nucleation assay

Neurotubulin from pig brain, 50 µl aliquots à 5 µg/µl

Rhodamin labled tubulin, 3 µl Aliquots

PME buffer:

0,1 M Pipes,

1 mM $MgSO_4$,

1 mM EGTA,

pH 6,9 (with KOH)

GTP–Stock: 25 mM GTP in PME

The protocol for microtubule coverslip nucleation assay (Zienicke 2007 Diploma thesis) was adapted for inhibitor study.

0.5 µl Rhodamin–tubulin were mixed with 50 µl unlabled tubulin.
Prior to polymerization the tubulin was incubated for 15 minutes on ice in the presence of the inhibitors, to allow binding, then polymerization was started by adding 15 mM GTP. After addition of GTP the samples were incubated for 30 minutes at 37°C.

At the same time, microscope slides, PME and coverslips were pre-warmed (at 37°C) to forestall microtubule depolymerization in the cold.

After incubation, the samples were diluted (1:25) with PME and the mounted samples observed with the Z1 imager and the Cy3 filter set (see above).

.

3. Results

Description of the cell lines

Kiessling (2004) showed that transiently transformed protonema of *P. patens* overexpressing FtsZ1-2:GFP were handicapped in chloroplast and cell division. Annular and filamentous structures were observed inside chloroplasts and the cytoplasm. Stable transformants also showed filamentous structures that spanned the whole cell in protonemata and leaflet cells (Figure 3.1.). Also ring-like structures inside of chloroplasts were observed.

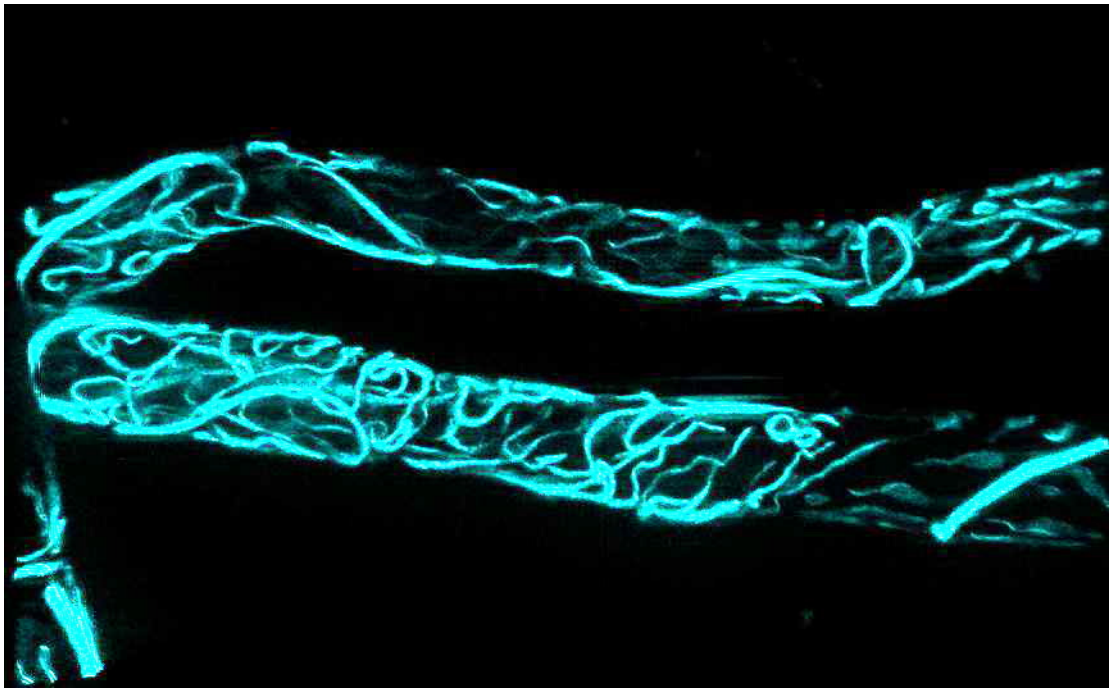

Figure 3.1 Renderimage of Z-stack of caulonema cells expressing filamentous FtsZ1-2:GFP inside the cytoplasm

FtsZ1-2:GFP ox cell line shows the formation of bell-shaped macrochloroplasts, chloroplasts with finger like protrusions, noodle-shaped chloroplasts, wild-type-like chloroplasts and minichloroplasts *in vivo* and often in the same protonema. Since they showed no different phenotype than wild type cells under standard growth conditions (white light, 55µM/sec/m^2 standard condition e.g. Martin 2007) except for chloroplast shape, all cultures were grown under low intensity light stress, to be able to perceive the maximal difference between the cell lines.

ΔFtsZ1-2 cell line was also kindly donated by Dr. Anja Martin. For this study, strain 114 has been used. Cell morphology of the knock out cell line was altered compared to wild type as has been described before (Martin 2007). Under standard growth conditions the cell width is reduced to13 µm instead of 25 µm in wild type. The cell walls are less thick and often the cross walls are not completed, so that long cells are formed. The chloroplasts do not divide as they normally do but are usually long and noodle-shaped and divided by the constricting cell wall. Since the ΔFtsZ1-2 line grew slower than the other two and subcultivation with successive blending of the protonemal

tissue led to the abundant formation of bloated cells instead of filamentous growth, the subcultivation interval was adjusted to ten days for standard growth. To be able to see differentiation in the sample cultures, 14-day-old cultures were used and transferred to fresh medium without blending for the experiments.

General impact of differentiation state on growth curve

In the following distribution of cell length is described. Cell length has been measured and then sorted into intervals of 10 µm. The "mode" interval is defined as the interval containing the highest number of cells.
To understand the result presented below, it is necessary to correlate the different populations of protonema with their appearance in the growth-curves.
Inside the test samples three differentiation stages were present: caulonema, chloronema and brachycytes. During normal growth all three cell types were present in varying numbers. One of the main properties of these three cell-types is their different cell length. Brachycytes were shortest with usually 10 to 25 µm, chloronema-cells were usually between 20 µm and 90 µm long and caulonema-cells were found to be between 70 µm and 300 µm long. These are no absolute values. The cell lengths overlap, since the transition between differentiation states is gradual (Bopp (2000)). This means the different cell lengths also change gradually. The mode interval shows the favored cell length and thus indicates the favored differentiation state of the cells in the test samples. This also means that when conditions induced e.g. caulonema development, the mode interval is shifted to the right of the curve, resulting in an approximate Poison distribution. Conditions favoring chloronema development would shift the mode interval to the middle of the growth curve, resulting in an approximate normal distribution. Transition between two differentiation states will result in the appearance of at least one other peak in the growth-curve until a "steady state" is reached, where all three cell types are again formed in a more or less constant ratio, depending on age of the culture, nutrition and other factors.

3.1. Influence of hormones on protonemal cell growth of *P. patens* cell lines

Hormones tightly regulate growth and morphology during moss development. Auxin has been reported to induce caulonema formation and has at least to be present for differentiation into buds. Cytokinin favors the growth of chloronema and together with auxin induces bud formation. Abscisic acid is important for reactions to light draught and salt stress and induces the formation of brachycytes and tmema cells, which are a form of vegetative propagation (Tintelnot (2006)).

3.1.1. Influence of high auxin concentration and FtsZ1-2 expression on cell growth

Since previous examination of ΔFtsZ1-2 cell lines showed that caulonema development was impaired under standard conditions (Martin 2007) and this development is thought

to be auxin dependent (Schumaker, Dietrich 1998), the influence of exogenous auxin, namely the cell-inherent IAA was tested on 14-day-old samples of all three cell lines.
To test the importance of functional Auxin transport, samples of the same cultures were treated with NPA, an Auxin efflux blocker. Control samples were treated as above, but with the addition of the corresponding amount of DMSO (water free) instead of hormones.

Under low light conditions, the cell lines showed different morphologies. For all three lines the predominant developmental state was chloronema, but the overexpression line showed early stages of caulonema development after 6 days with DMSO, which were rare in both other cell lines. Wild type cells produced short or rounded cells or clusters of cells with highly irregular cross walls, which might be brachycytes, in addition to wavy filamentous protonema (Figure 3.1.1.2). The knock out line grew either as round, bloated cells, as short, rounded cells or as thin knobbly filaments (width 13 µm compared to 25 µm in wild type and FtsZ1-2 ox) with mostly correct vertical cross walls, but a much higher inclination to form branches, than the other two cell lines (Figure 3.1.1.7, Figure 3.1.1.8).

Addition of 20 µM IAA to the cultures and incubation for six days led to the formation of shorter, barrel-shaped cells in both, wild type and overexpression line (Figure 3.1.1.3, Figure 3.1.1.4). Caulonema formation was not observed. ΔFtsZ1-2 protonema cells mainly grew big and bloated or small and round (Figure 3.1.1.10). The protonema had smooth cell walls and compared with control samples, branching was decreased. (Figure 3.1.1.9)

	Branching under IAA conditions		
	K.O.	WT	OX
IAA	31%	22%	16%
Control	33%	25%	21%

Table 3.1.1.1 Branches and side- branch- initials in [%]

Addition of 10 µM NPA to the cultures and incubation for six days increased the formation of short cells in both, wild type and overexpression line (Figure. 3.1.1.5, Figure 3.1.1.6.) Caulonema formation again was not observed. ΔFtsZ1-2 protonema cells grew in very irregular bunches caused by a strong increase of branching (Figure 3.1.1.11). The dominant form of cell growth was filamentous. Cell walls showed irregularly placed branch initials, giving the walls a bumpy appearance. Round cells or bloated cells were also observed, yet less often than in the control samples (Figure 3.1.1.10. Data not quantified).

	Branching under NPA conditions		
	K.O.	WT	OX
NPA	53%	24%	16%
Control	43%	27%	18%

Table 3.1.1.2 Branches and side- branch- initials in [%]

Comparison of the average cell length of the three cell lines under control conditions showed that FtsZ1-2 ox cells were longest with 54.7 µm with a standard deviation of 14.9 µm. Wild type cells had an average length of 48.2 µm (± 16.9 µm), and cells of the ΔFtsZ1-2 cell line grew on average 37.8 µm long (± 16.5 µm).

Treatment with NPA leads to a reduction of the average cell length of all three cell lines. This was most apparent in cells of the overexpression line which were on average 38.5 µm long with a standard deviation of 15.7 µm, followed by wild type cells which grew on average 37.25 µm long (± 13.6 µm). Cells of the ΔFtsZ1-2 cell line grew on average 36.9 µm long with a standard deviation of 13.9 µm.

Treatment with IAA reduced the average cell length even more. Again the highest average cell length was observed in samples of overexpression lines, with 36.7 µm (± 12.1 µm). The lowest average cell length was observed in wild type samples, 32.1 µm (± 9.9 µm). Cells of the ΔFtsZ1-2 cell line grew on average 38.8 µm long (± 14.6 µm) (Diagram 3.1.1.1). That means that treatment with exogenous IAA and an IAA efflux blocker compared with the control samples had the least effect on the average cell length of FtsZ1-2 knock out cell lines.

Since the standard deviation was rather high in all three cell lines, the distribution of the cell lengths was tested. It was revealed, that under control conditions the distribution of overexpression line and wild type cells was close to normal distributed. The mode interval for wild type was at [45- 55 µm], for the FtsZ1-2 ox line [55- 65 µm] The ΔFtsZ1-2 cell line expressed an approximate Poisson distribution with the mode interval at [25- 35 µm] and a heavy tail region up to 105 µm. This means, that the shortest as well as the longest cells were found in the knock out cell line samples (Diagram 3.1.1.2.).

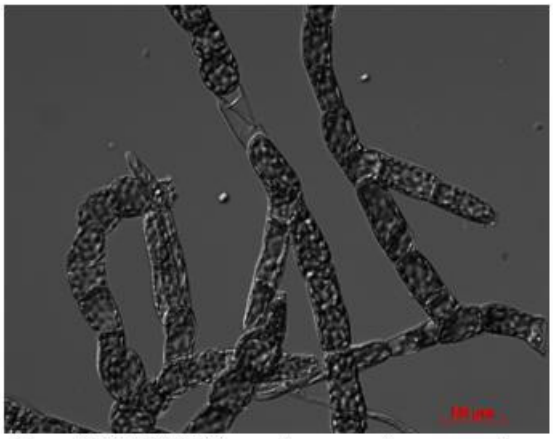

Figure 3.1.1.1 FtsZ1-2 ox protonema cells grown under Weak light conditions for 6 days

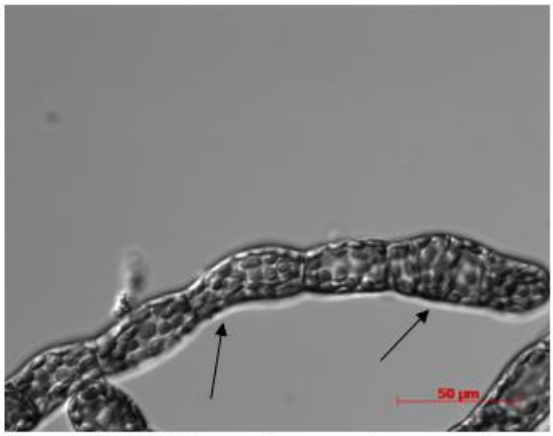

Figure 3.1.1.2 Wild type protonema cells grown under weak light conditions for 6 days showing short cells (right arrow) and wavey growth (left arrow)

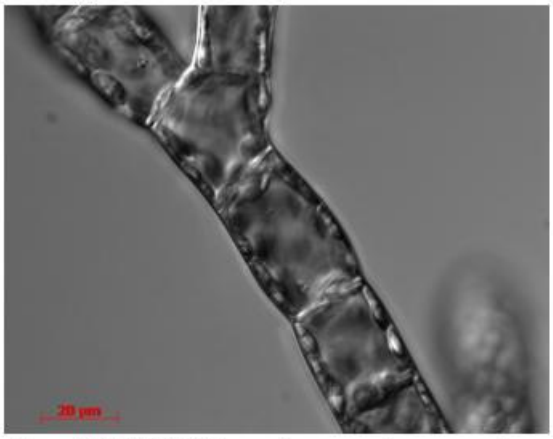

Figure 3.1.1.3 FtsZ1-2 ox protonema cells grown under weak light conditions with 20 µM IAA, showing short cells

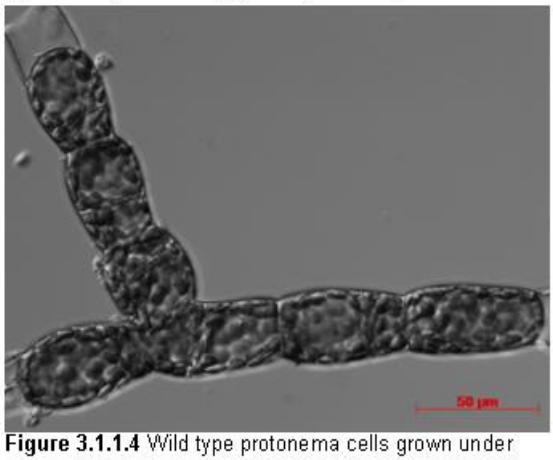

Figure 3.1.1.4 Wild type protonema cells grown under weak light conditions with 20 µM IAA, showing short cells

Figure 3.1.1.5 FtsZ1-2 ox protonema cells under weak light conditions with 10 µM NPA, showing rounded short cells

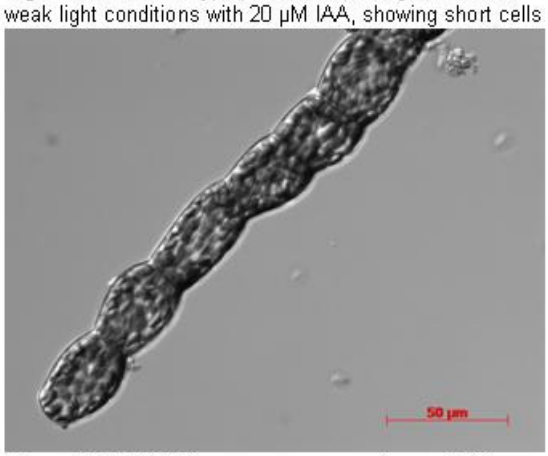

Figure 3.1.1.6 Wild type protonema under weak light conditions with 10 µM NPA, showing rounded short cells

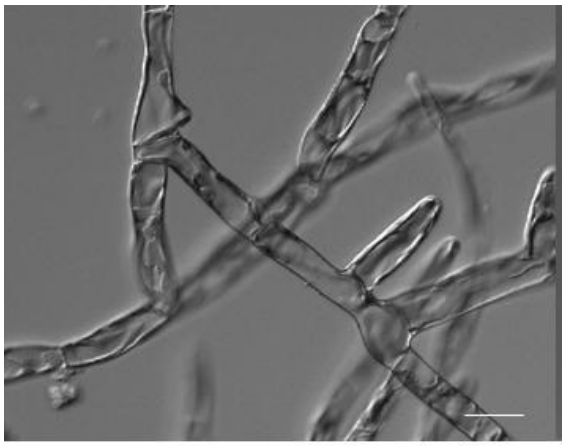

Figure 3.1.1.7 ΔFtsZ1-2 control cells showing filamentous growth. Grown for 6 days under low light conditions. Scale bar indicates 20 µm

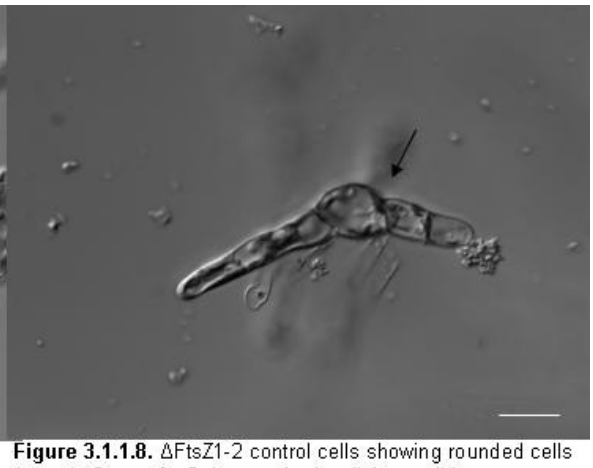

Figure 3.1.1.8. ΔFtsZ1-2 control cells showing rounded cells (arrow). Grown for 6 days under low light conditions. Scale bar indicates 20 µm

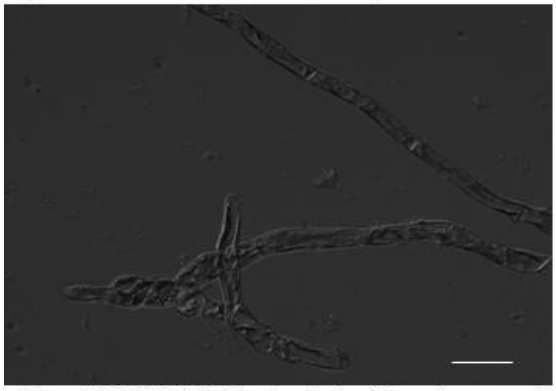

Figure 3.1.1.9 ΔFtsZ1-2 cells showing filamentous growth. Grown under low light conditions, treated with 20 µM IAA. Scale bar indicates 50 µm

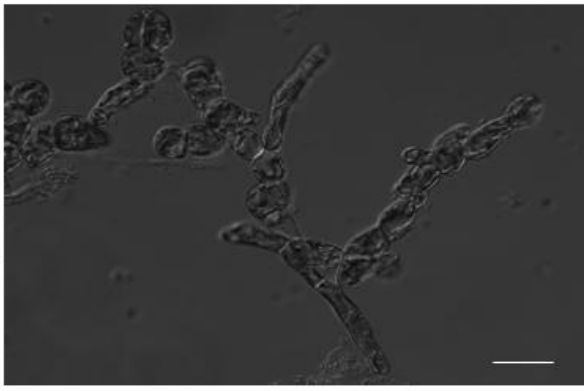

Figure 3.1.1.10 ΔFtsZ1-2 cells showing rounded cells. Grown under low light conditions treated with 20 µM IAA. Scale bar indicates 50 µm

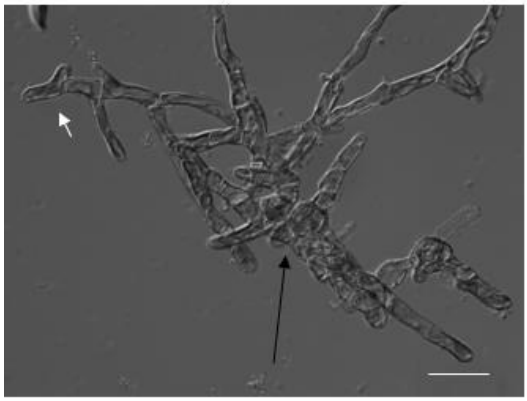

Figure 3.1.1.11 ΔFtsZ1-2 cells showing clustered growth, irregular cell shape (black arrow) and irregular branching (white arrow), treated with 10 µM NPA. Scale bar indicates 50 µm

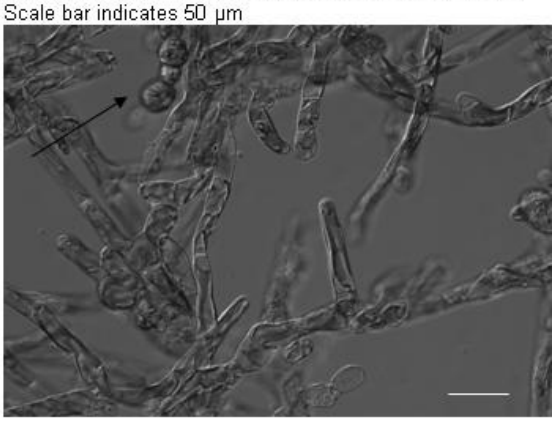

Figure 3.1.1.12 ΔFtsZ1-2 cells showing irregular cell shape and rounded cells (arrow). Grown under low light conditions, treated with 10 µM NPA. Scale bar indicates 20 µm

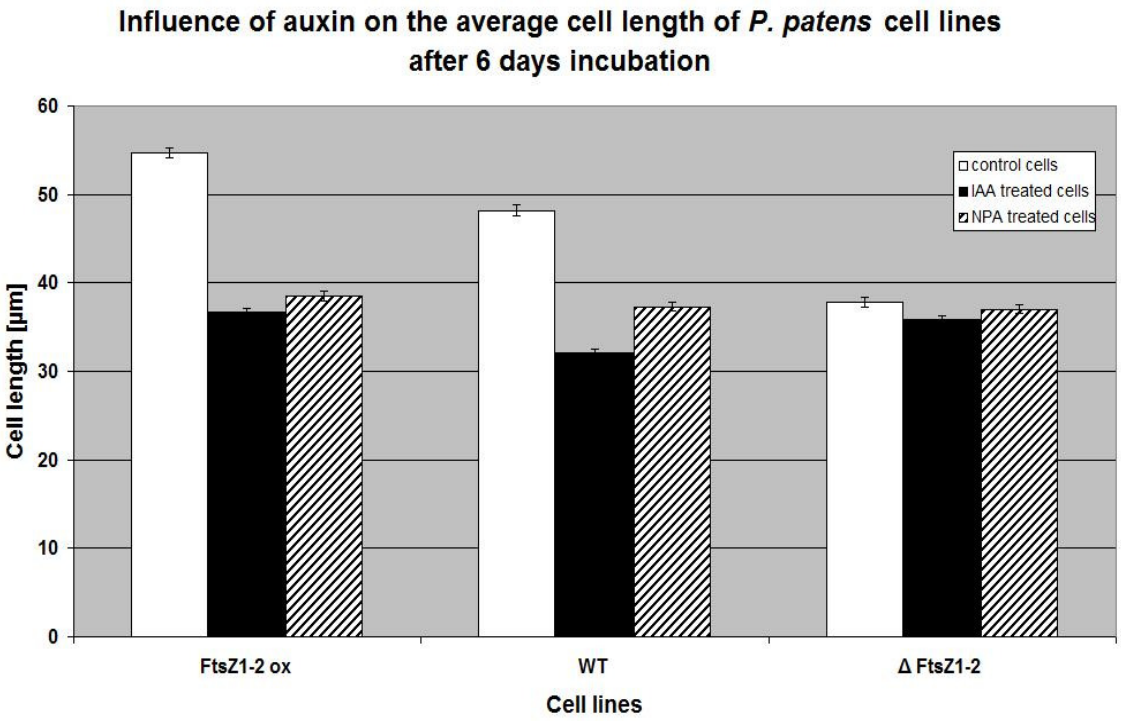

Diagram 3.1.1.1. Average cell length on *P. patens* cell lines expressing different levels of FtsZ1-2. Error bars indicate standard error for corresponding samples (n = 200).

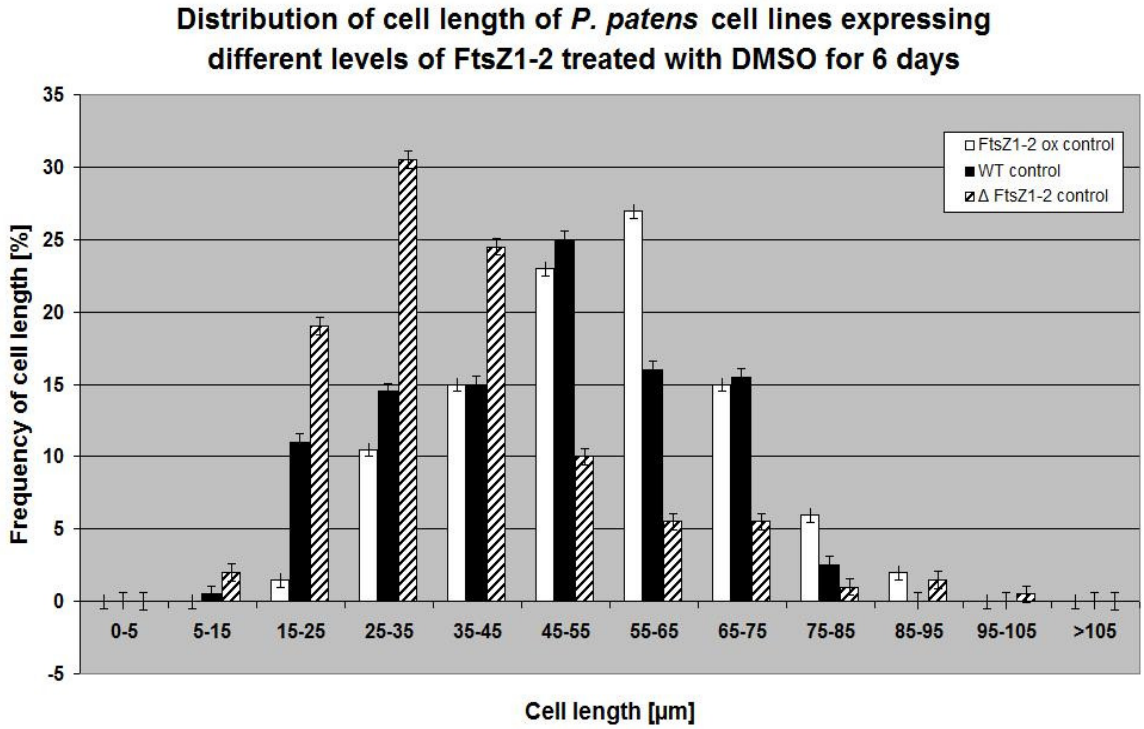

Diagram 3.1.1.2. Distribution of cell length of *P. patens* cell lines expressing different levels of FtsZ1-2 after control treatment with DMSO (water-free) for 6 days Error bars indicate standard error for corresponding samples.

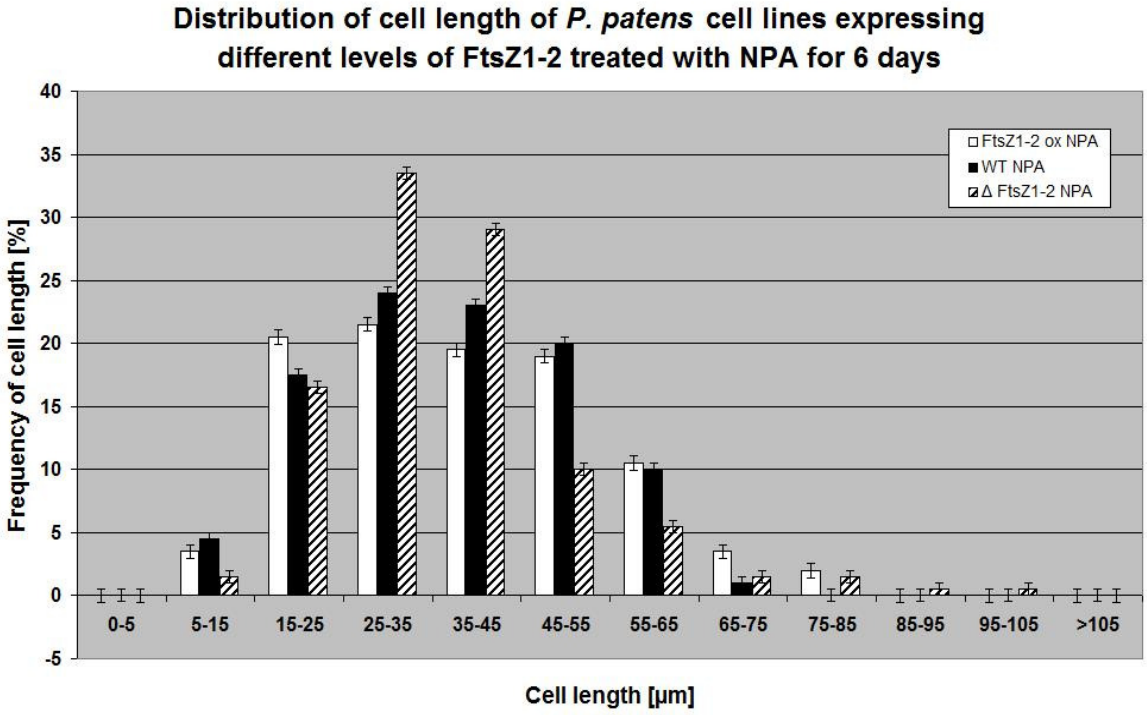

Diagram 3.1.1.3. Distribution of cell length of *P. patens* cell lines expressing different levels of FtsZ1-2 after control treatment with 10 µM NPA for 6 days. Error bars indicate standard error for corresponding samples (n = 200).

Treatment with NPA changed the pattern significantly, since now the mode interval was the same for all three cell lines, namely [25- 35 µm] indicate favored growth as chloronema. The height of the mode interval differed strongly from 33.5% for the knock out line to 24% for wild type and 21.5% for the overexpression line. Also, even though the wild type and overexpression line showed approximately normal distribution, the knock out cell line retained its Poisson distribution, including the mode interval, greatest cell length and heavy tail (Diagram 3.1.1.3.).

After treatment with IAA cell length of all three cell lines was approximately Poisson distributed. The interval containing most cells was [25- 35 µm]. The greatest difference was the maximal cell length, which was again found in the ΔFtsZ1-2 cell line, and the weight of the tail region of the curves, which was biggest in the ΔFtsZ1-2 cell line and smallest in the wild type. The range of the distribution was reduced in all three cases, so that it can be said that under low light intensity IAA promotes the formation of short cells.

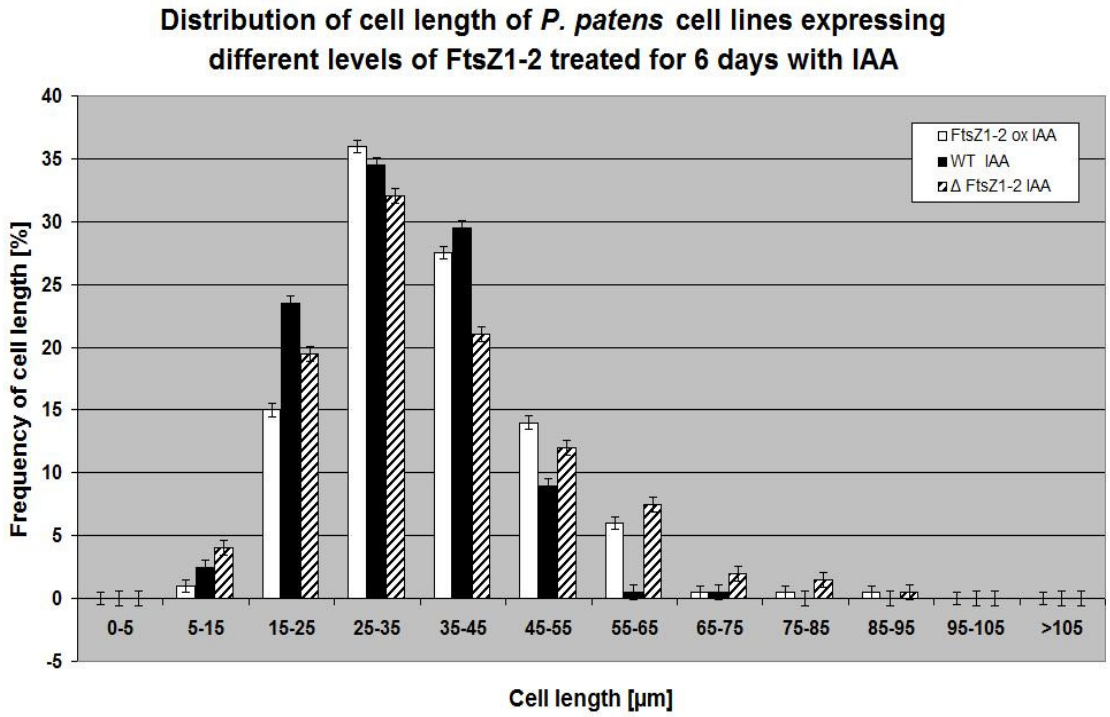

Diagram 3.1.1.4. Distribution of cell length of *P. patens* cell lines expressing different levels of FtsZ1-2 after control treatment with 20 µM IAA for 6 days. Error bars indicate standard error for corresponding samples (n = 200).

The above observations can be summarized as follows:

Under low light conditions the reduction of FtsZ1-2 concentration led to a decrease of chloronema cell length and the abundant production of brachycytes. The morphology of the knockout line was not visibly changed by treatment with auxin. Differentiation to caulonema was blocked in the presence of high amounts of exogenous auxin. Blocked auxin efflux additionally increased branch initial formation.

3.1.2. Influence of cytokinin and FtsZ1-2 expression on cell growth

Cytokinin is considered to posses antagonistic effects on auxin mediated moss plant development. Schumaker and Dietrich (1998) described its effect on moss protonema as inducing chloronema development, and bud formation in the presence of auxin.

To determine whether cytokinin has a differential effect on protonema expressing different levels of FtsZ1-2, the influence of extracellular cytokinin, namely the cell inherent 2iP was tested on 14-day-old samples of all three cell lines. In comparison with control cells, FtsZ1-2 ox cell line developed smooth chloronema cells under weak light conditions. Also early stages of caulonema were developed, yet less often than in control samples (Figure 3.1.2.1).

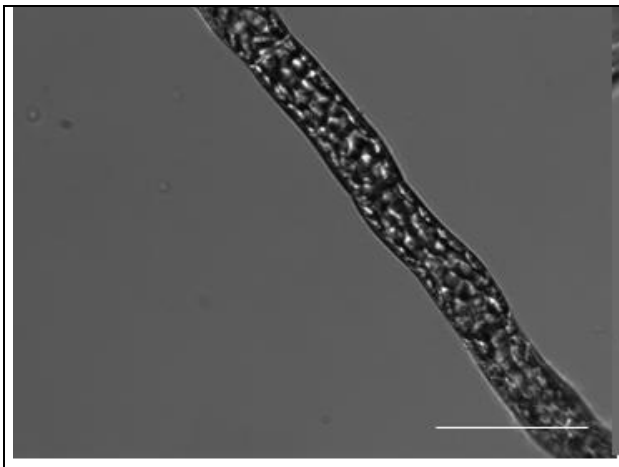

Figure 3.1.2.1 Chloronema of Ftsz1-2 ox line treated with 20 µM 2iP for 6 days. Scale bar indicates 50 µm

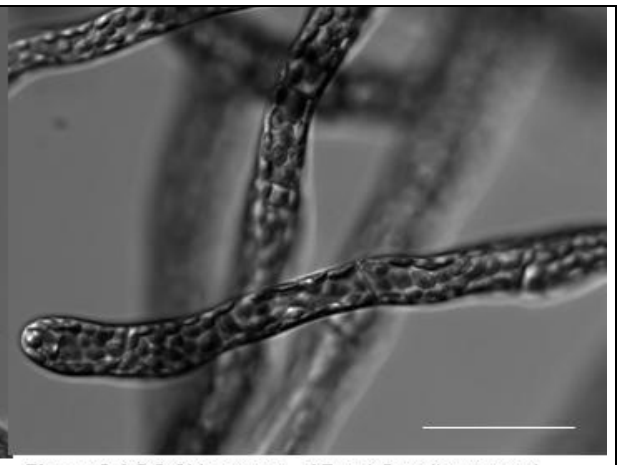

Figure 3.1.2.2 Chloronema of Ftsz1-2 ox line treated with 200 µl Ethanol for 6 days. Scale bar indicates 50 µm

Figure 3.1.2.3 Protonema of Ftsz1-2 ox line treated with 20 µM 2iP for 6 days Apical bud (left arrow), early Caulonema (right arrow). Scale bar indicates 50 µm

Figure 3.1.2.4 Protonema of Ftsz1-2 ox line treated with 20 µM 2iP for 6 days, early stage of bud developement. Scale bar indicates 50 µm

Figure 3.1.2.5 Protonema of wild type treated with 20 µM 2iP for 6 days, short cells (left arrow), early Caulonema (right arrow). Scale bar indicates 50 µm

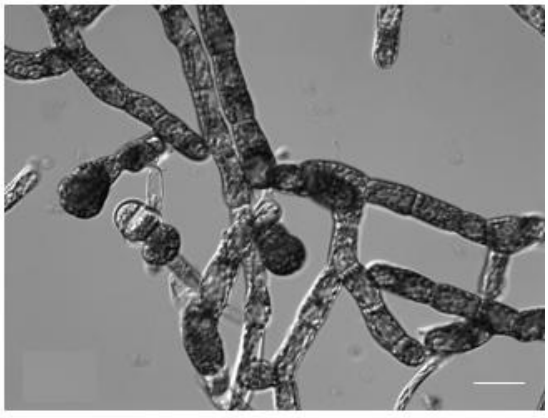

Figure 3.1.2.6 Chloronema of wild type treated with 200 µl Ethanol for 6 days. Scale bar indicates 50 µm

Bud formation became apparent two days after addition of 2iP (Figure 3.1.2.3). After six days several stages of bud development were observed. 18 % of protonemata were bearing shoot buds.

Wild type cells also developed early stages of caulonema (Figure 3.1.2.5.). Bud formation was first observed four days after treatment with 2iP and stayed rare. Only 7% of protonemata were bearing buds after six days. Short cells and brachycytes were present in the sample.

Figure 3.1.2.7 Protonema of Δ FtsZ1-2 line treated with 20 µM 2iP for 6 days showing irregular branching. Scale bar indicates 50 µm

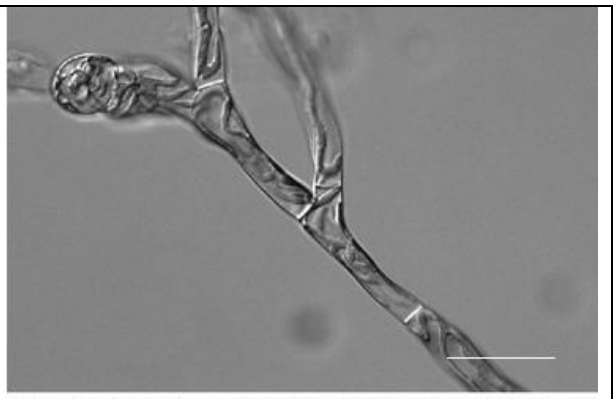

Figure 3.1.2.8 Protonema of Δ FtsZ1-2 line treated with 20 µM 2iP for 6 days showing branching. Scale bar indicates 50 µm

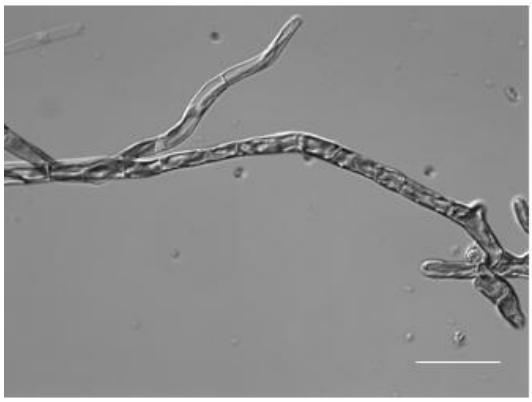

Figure 3.1.2.9 Protonema of Δ FtsZ1-2 line treated with 20 µM 2iP for 6 days showing filamentous growth. Scale bar indicates 50 µm

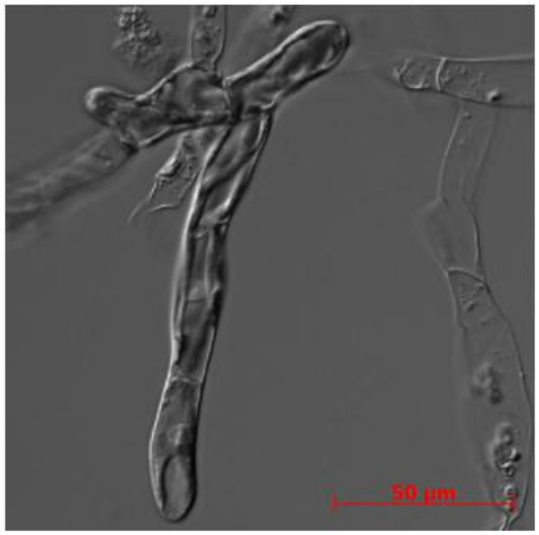

Figure 3.1.2.10 Protonema of Δ FtsZ1-2 line treated with 200 µl ethanol per 50 ml Knop's medium for 6 days showing filamentous growth. Scale bar indicates 50 µm

Figure 3.1.2.9 Protonema of Δ FtsZ1-2 line treated with 20 µM 2iP for 6 days showing rounded (right arrow) and bloated cells (left arrow).Scale bar indicates 50 µm

Figure 3.1.2.12 Protonema of Δ FtsZ1-2 line treated with 200 µl ethanol per 50 ml Knop's medium for 6 days showing rounded cells. Scale bar indicates 50 µm

ΔFtsZ1-2 protonema cells mainly grew as long smooth filaments (Figure 3.1.2.9) Branching seemed to be reduced (Data not quantified) compared to control cells. Regular and irregular branching was observed (Figure 3.1.2.7, Figure 3.1.2.8). Bloated cells and cell files of short rounded cells were also produced, yet less than in control cells (Figure 3.1.2.11.). Bud development was never observed.

Comparison of the average cell length showed, that FtsZ1-2 ox cells grew longest in the control samples with 61.3 µm and a standard deviation of 15.6 µm and that cell length was reduced by roughly 10 µm to 51.9 µm (±17.6 µm).

Wild type cells also grew longer without 2iP with an average of 45.4 µm, (± 15.5 µm), and an average cell length of 41.5 µm (± 14.8 µm) in the 2iP treated samples.
ΔFtsZ1-2 protonema cells grew 48.1 µm long, (± 21.4 µm) in control samples and contrary to the behavior of the other two cell lines elongated in 2iP treated samples to 58.2 µm with the highest standard deviation of 22.9 µm (Diagram 3.1.2.1).

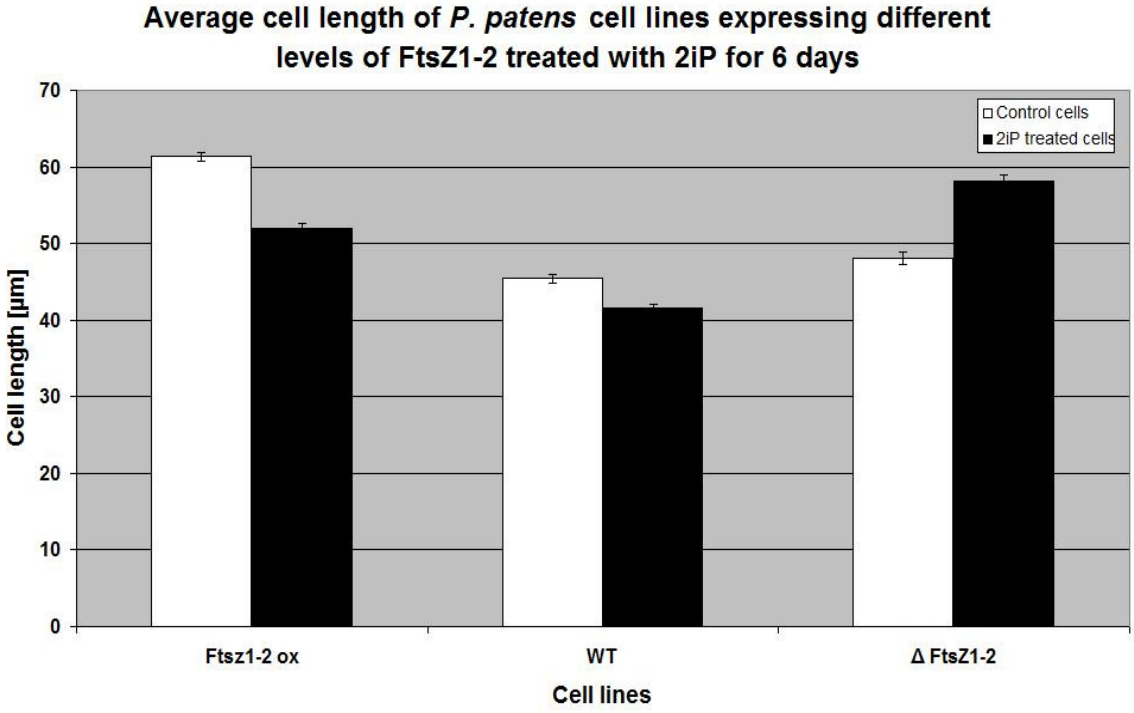

Diagram 3.1.2.1. Average cell length of *P. patens* cell lines expressing different levels of FtsZ1-2 after treatment with 20 µM 2iP. Error bars indicate standard error for corresponding samples (n = 200).

Analysis of the growth curve of the control samples showed that the length of wild type cells was approximately normally distributed. The mode interval was [35- 45 µm].
Cell length distribution of ΔFtsZ1-2 cells shows a strange pattern with three peaks at [25- 35µm] (highest), [55- 65µm] (middle) and [85- 95 µm] (lowest). This indicates ongoing differentiation of the protonema cells.

	Branching under 2iP influence		
	K.O.	WT	OX
2iP	37%	22%	20%
Control	40%	26%	24%

Table 3.1.2.1 Side branches and side branch initials in [%]

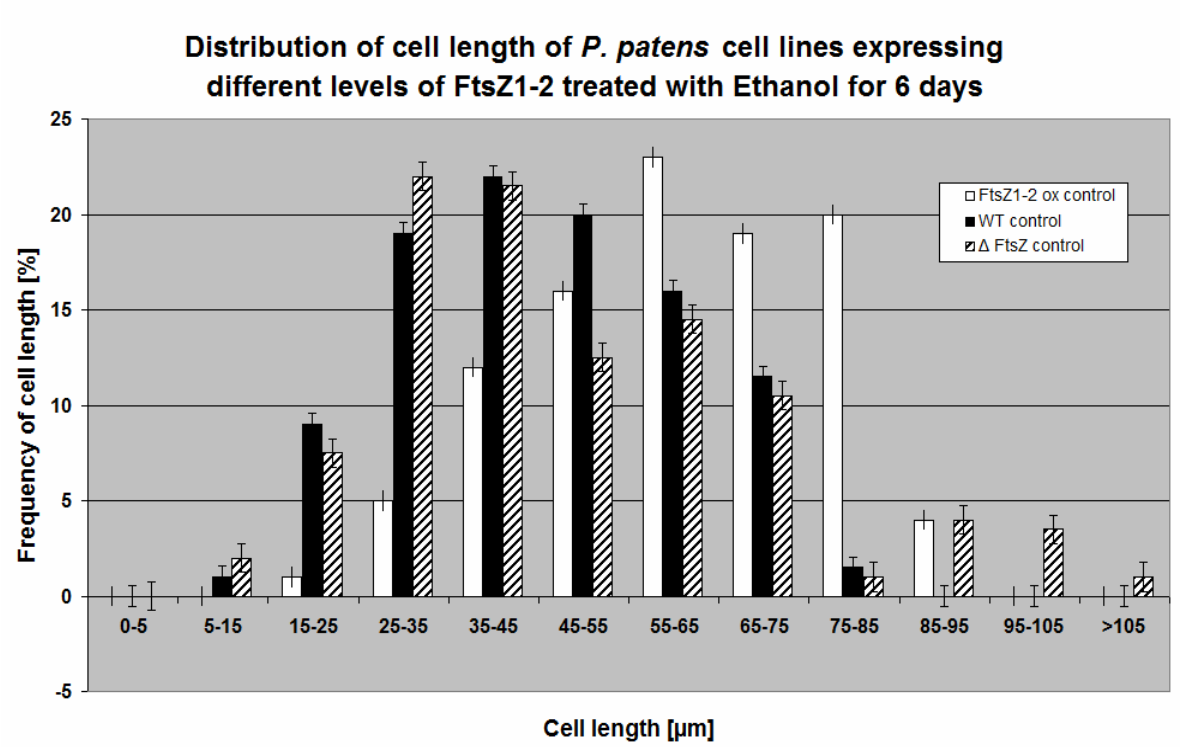

Diagram 3.1.2.2. Distribution of cell length of *P. patens* cell lines expressing different levels of FtsZ1-2 after control treatment with 200 µl EtOH per 50 ml Knop medium for 6 days and low light intensity. Error bars indicate standard error for corresponding samples (n = 200).

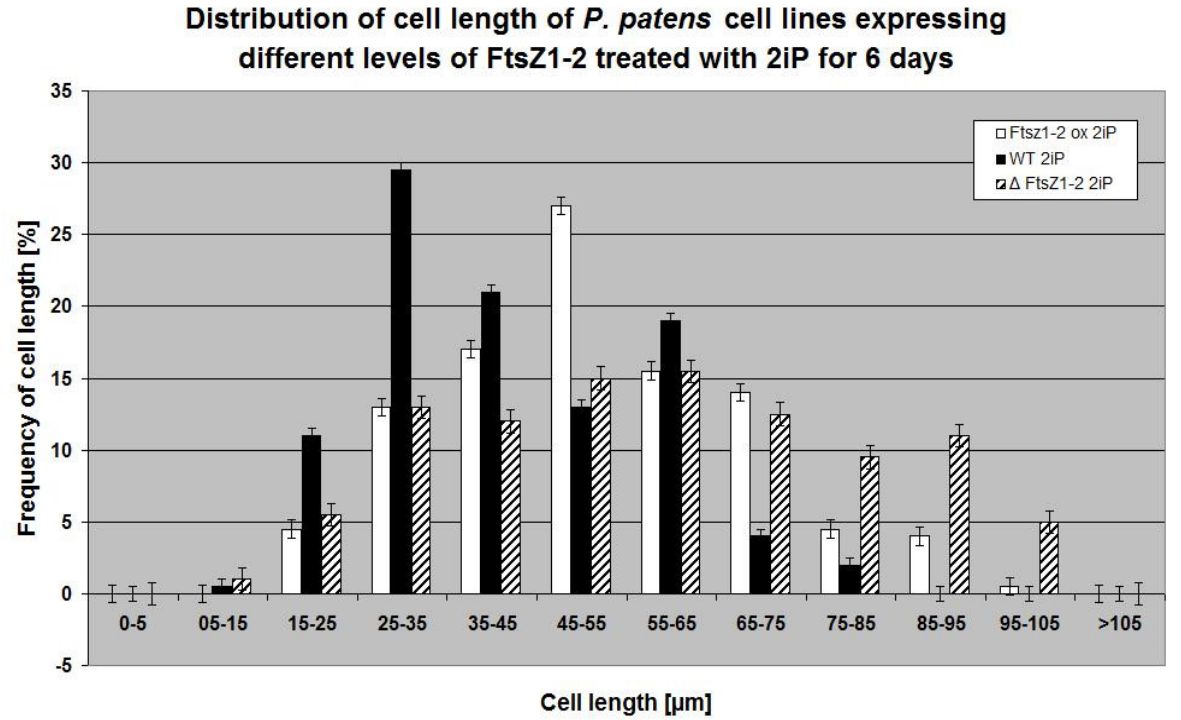

Diagram 3.1.2.3. Distribution of cell length of *P. patens* cell lines expressing different levels of FtsZ1-2 after control treatment with 20 µM 2iP for 6 days. Error bars indicate standard error for corresponding samples (n = 200).

FtsZ1-2 ox protonema cells show a mirrored Poisson distribution with the mode interval at [55- 65 µm], but show a second peak at [75- 85 µm] which points to beginning caulonema formation.

Treatment with 2iP did change the Poisson distribution of the FtsZ1-2 overexpression cell line to an approximately normal distribution. The mode interval was shifted to [45-55 µm] and the second peak disappeared, possibly because of reduced caulonema growth in favor of bud development.
Wild type cells seemed to be Poisson distributed, with the mode interval at [25 to 35µm]. This indicates that increase of cell length is inhibited. A second peak at [55-65µm] and a heavy tail region up to 85 µm, indicates caulonema development.
The growth curve of the knock out cell line developed an asymmetric flat appearance, with mass shifting to the right. The mode interval was at [55-65 µm] and the heavy tail region increased in mass. This is consistent with the above made observation that the main growth occurs as long, smooth filaments.

To summarize the results shown above :

In FtsZ1-2 over-expressing protonema cytokinin treatment reduced caulonema development when grown under low light intensity. In wild type protonema grown under low light intensity, cytokinin increased caulonema development slightly
Exogenous cytokinin did not induce bud formation in the FtsZ1-2 knock out cell line after 6 days of incubation but reduced the amount of branching and increased cell length.
Exogenous Cytokinin decreased cell length in the protonema of the FtsZ1-2 overexpression line and wild type.

3.1.3. Influence of abscisic acid and FtsZ1-2 expression on cell growth

Growth of *P. patens* wild type under influence of abscisic acid has been previously described (e.g. Tintelnot (2006)).
Under low light conditions the cytoplasm of wild type cells treated with 20 µM ABA for 6 days appeared to be denser than in control cells. The positioning of chloroplasts was changed insofar as they were mostly oriented with the edge outward (Figure 3.1.3.5). The average cell length was strongly reduced in comparison with control cells, chloronema cells were broader or bloated and cross wall positioning was disturbed (Figure 3.1.3.4). Brachycytes and tmema cells were readily formed (Figure 3.1.3.6), even to an extent where only cell clusters with oddly positioned cross walls were formed (Figure 3.1.3.5).
FtsZ1-2 overexpression cell line also showed a higher density of cytoplasm than the control cells. In cells containing normal or slightly bigger than normal chloroplasts the chloroplasts-orientation changed in the same way as in wild type cells. In the presence of macrochloroplasts, the cells appear to be filled with chloroplasts from edge to edge (Figure 3.1.3.1 and Figure 3.1.3.3). Elongation of the tip cells seemed not to be impaired by ABA treatment. The structure of the cell walls appeared less regular and started developing bumps that might develop into side branch initials. This additionally increased the irregular appearance of the outer walls. In cells with smaller, deformed or

normal chloroplasts the formation of stromules, which are tube-like extensions of chloroplasts (Waters 2004), became apparent (Figure 3.1.3.2). This was not readily observed in wild type at this stage, since the much denser positioning of the chloroplasts concealed the stromules from view. In the FtsZ1-2 over expression cell line a reversal of the polar growth of the apical cells could be observed on rare occasions. A marked increase in side branch formation could not be detected

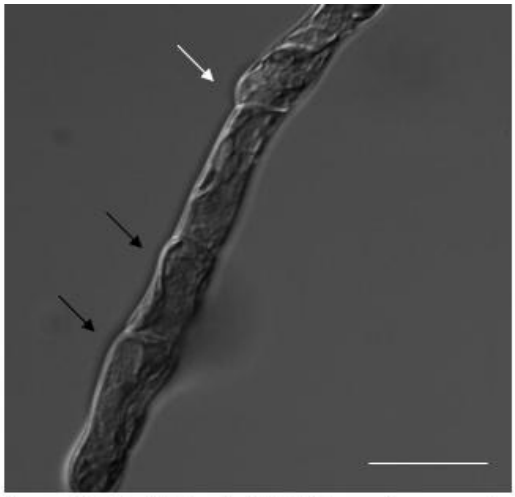

Figure 3.1.3.1 ABA treated FtsZ1-2 ox protonema cells with deformed chloroplasts showing cell wall deformation (black arrows) akin to early side branch initials (white arrow). Scale bar indicates 50 µm

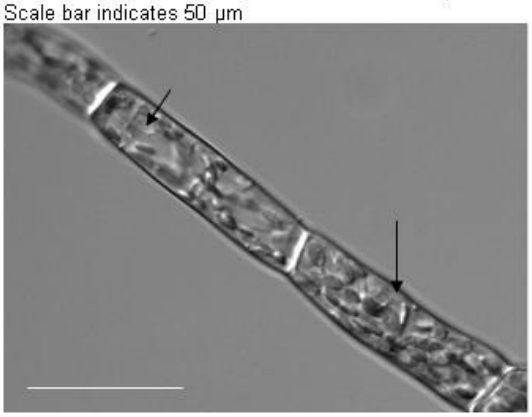

Figure 3.1.3.2 ABA treated FtsZ1-2 ox protonema cells with dividing chloroplasts showing stromules (black arrows) inside dens cytoplasm. Scale bar indicates 50 µm

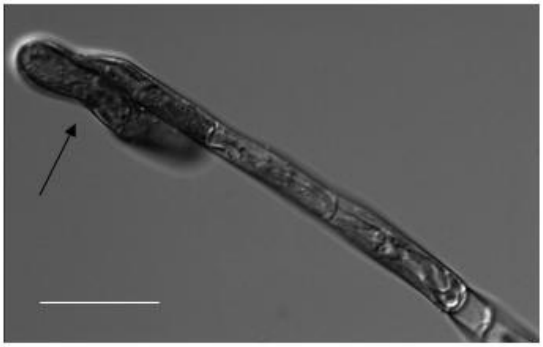

Figure 3.1.3.3 ABA treated FtsZ1-2 ox protonema cells with deformed chloroplasts showing reversed polarity and unconvetional branching (arrow). Scale bar indicates 50 µm

Figure 3.1.3.4 ABA treated wild type chloronema cells showing irregular division with obliquely placed cell walls (arrow). Scale bar indicates 50 µm

Figure 3.1.3.5 ABA treated wild typebrood body. Cells are short, dens brachycites with obliquely placed cell walls (arrow). Scale bar indicates 50 µm

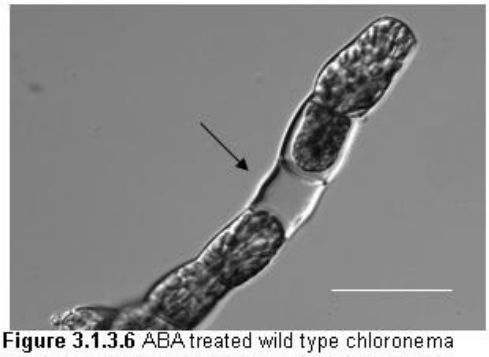

Figure 3.1.3.6 ABA treated wild type chloronema cells with dens cytoplasm and tmema cell (arrow).

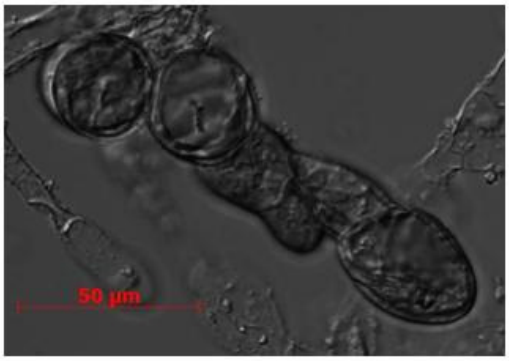

Figure 3.1.3.7 ABA treated ΔFtsZ1-2 knock out cells showing bloated, dense brachycites with deformed chloroplasts. Scale bares cindicate 50 µm

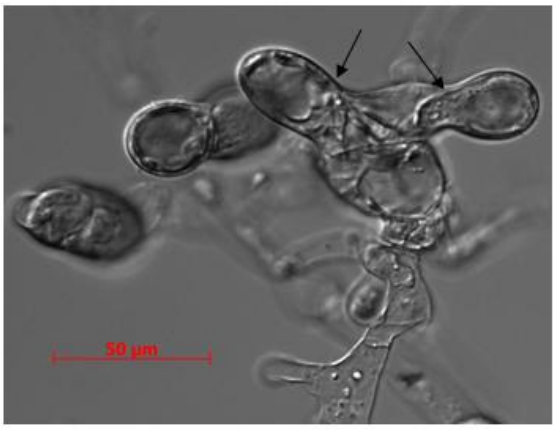

Figure 3.1.3.8 ABA treated ΔFtsZ1-2 knock out cells showing bloated, dense cells with deformed chloroplasts and irregular branching (black arrow).

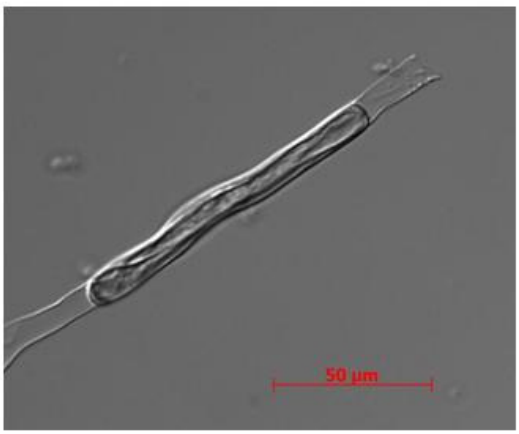

Figure 3.1.3.9 ABA treated single ΔFtsZ1-2 knock out cell showing dense cytoplasm and deformed chloroplasts.

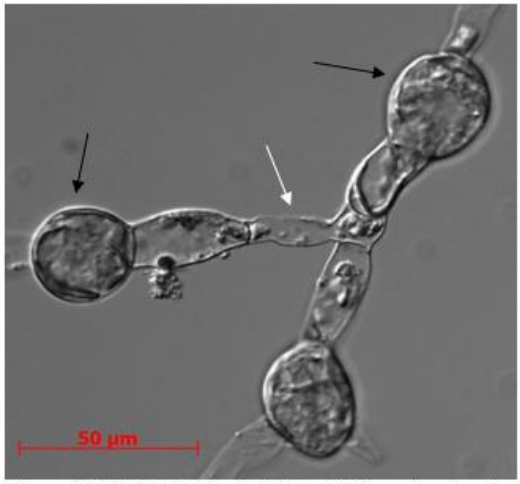

Figure 3.1.3.10 ABA treated ΔFtsZ1-2 knock out cells showing bloating (black arrow) and tmema (white arrow).

Figure 3.1.3.11 ABA treated ΔFtsZ1-2 knock out cell with two branch initials (arrows).

Figure 3.1.3.12 ABA treated ΔFtsZ1-2 knock out cell short bloated cells and tmema cells resembling normal cell shape (arrows).

ΔFtsZ1-2 knock out line showed growth in favor of bloated or rounded and clustered cell shapes (Figure 3.1.3.8). Growth of long cell files was not favored. Tmema formation was increased markedly to an extent where cell files consisted of only two cells or even only one cell (Figure3.1.3.9) per file. The knock out cell line also showed the increase in cytoplasmic density, and repositioning of chloroplasts, so that individual plastid shapes were mostly indiscernible (Figure 3.1.3.7 to 3.1.3.12). Since cell files are generally short, a marked increase in branching was not readily observed, but many cells were irregularly shaped with knobbly protrusions that might be side branch initials (Figure 3.1.3.7, Figure 3.1.3.8, and Figure 3.1.3.11). Since there were mostly two or

more of these initials instead of the normal one, an outgrowth of these would lead to the whirl of side branches that has been noted above.

	Branching under ABA influence		
	K.O.	WT	OX
ABA	48%	37%	26%
Control	39%	32%	24%

Table 3.1.3.1 Side branches and side branch initials in [%]

Analysis of cell length of the three cell lines shows that treatment with ABA led to a decrease of cell length in wild type and knock out line, yet no effect on the FtsZ1-2 ox line became apparent. Average cell length of the overexpression line is 54.25 µm in control samples (± 16.24 µm) and 54.15 µm in ABA-treated samples (± 12.67 µm). Wild type cells showed the greatest difference in cell length. When treated with ABA the average cell length was 31.37 µm (standard deviation 12.18 µm) and 44.24 µm in the control samples (± 15.92 µm). ΔFtsZ1-2 line grew to an average of 37.02 µm in the control (standard deviation 14.85 µm) and was reduced to 33.35 µm (± 13.86 µm) in the ABA-treated samples (Diagram 3.1.3.1).

Under control conditions the cell length distribution of the three cell lines shows a great difference in the mode intervals yet not in the range of distribution (all distributed over 8 intervals). The distribution of the overexpression line is approximately normal with the mode interval at 35- 45 µm and median at 55.95 µm. This cell line contained the longest cells, but none were shorter than 15 µm.

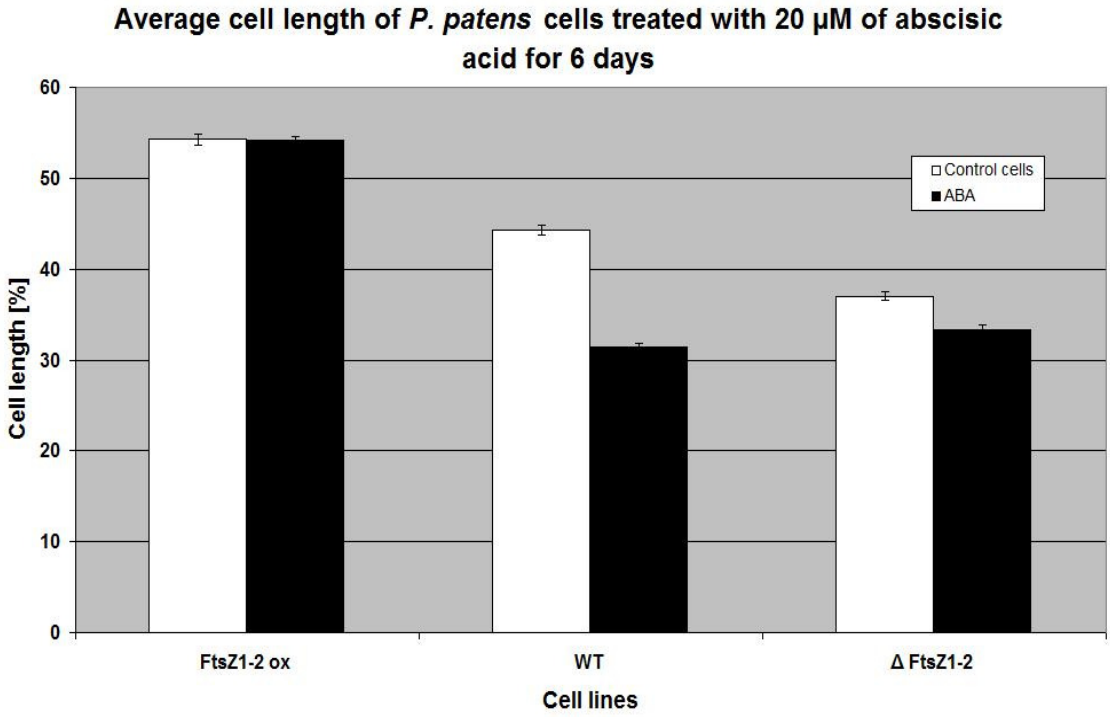

Diagram 3.1.3.1 Average cell length on *P. patens* cell lines expressing different levels of FtsZ1-2 after treatment with 20 µM ABA. Error bars indicate standard error for corresponding samples (n = 200).

Under control conditions the cell length distribution of the knock out cell line was asymmetrical, but it can be surmised, that a Poisson distribution was present from interval [5-15 µm] to interval [55-65µm] with the mode interval at [25- 35 µm] and a second normal distribution attached as a tail around a peak at [65- 75 µm].
The length of the wild type cells was very asymmetrically distributed. The mode interval was at [45- 55 µm]. This fits the median which was at 45.97 µm and the average cell length which was 44.24 µm. The intervals next to the mode interval contained nearly the same mass as the mode interval (between 15 to 20 % of the sample). Thus the cell length distribution of the wild type cells could be interpreted as a slightly flattened and perturbed normal distribution with a mode interval shifted to the right.

Treatment with ABA led to a shift of the distribution of FtsZ1-2 ox cell line. The mode interval was shifted to [55-65 µm] and the distribution resembled approximately a mirrored Poisson distribution. This points out a slight increase in cell length of the overexpression cell line, when treated with ABA.
Wild type cells treated with ABA were approximately normally distributed around the mode interval of [25- 35 µm] which had shifted to the left. The range of the distribution was also reduced. This decrease of the average cell length indicates that wild type cells showed the strongest reaction to ABA treatment.
Distribution of ΔFtsZ1-2 line showed the least difference between ABA treated cells and control samples. The distribution again resembled an approximate normal distribution yet mass from the tail region was shifted in front of the mode interval. The mode interval as well as the weight of said interval stayed the same. Even though the average cell length showed a slight decrease in length under ABA treatment, the median was only reduced to 31.02 µm, which is a reduction of only 2,65 µm. This means that the knock out cell line showed the least reaction to ABA treatment.

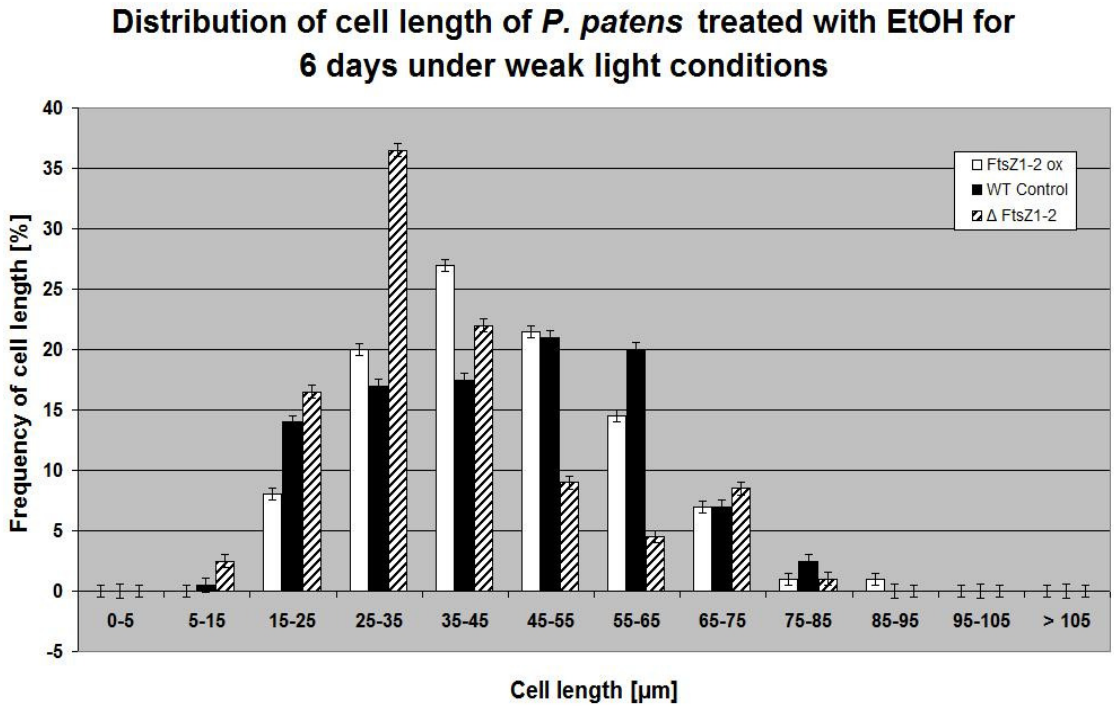

Diagram 3.1.3.2 Distribution of cell length of *P. patens* cell lines expressing different levels of FtsZ1-2 after control treatment with 20 µl EtOH per 50 ml Knop medium for 6 days. Error bars indicate standard error for corresponding samples (n = 200).

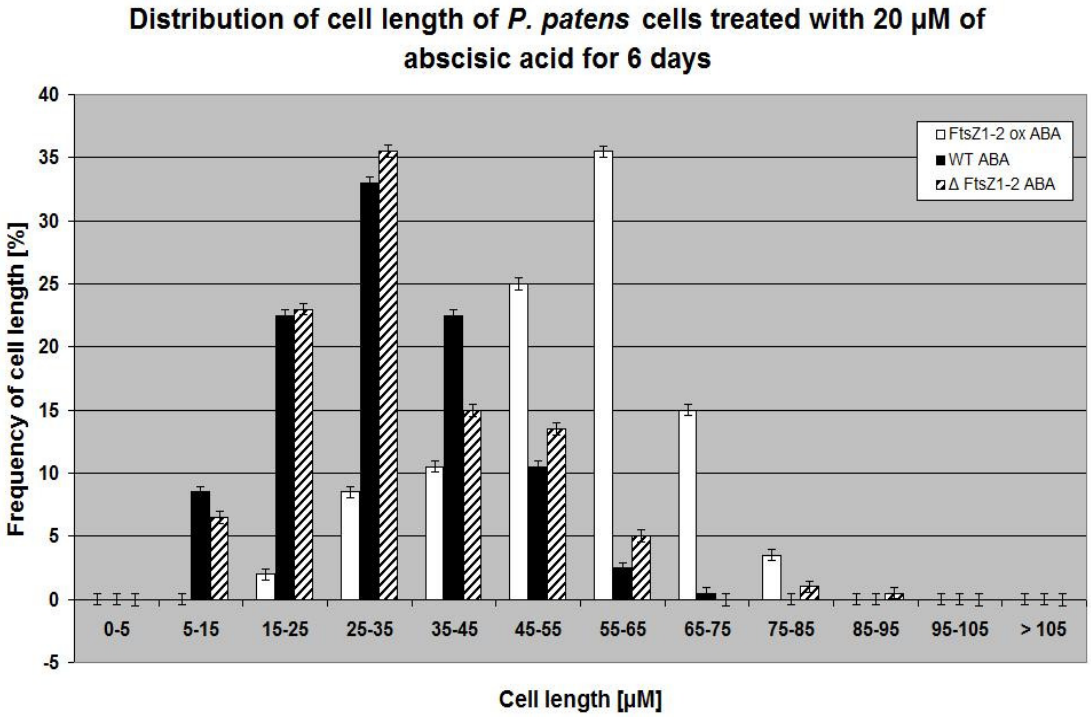

Diagram 3.1.3.3. Cell length distribution of *P. patens* cell lines expressing different levels of FtsZ1-2 after treatment with 20 µM ABA. Error bars indicate standard error (n = 200).

The results shown above can be summerized as follows:

Morphology of the ftsZ1-2 knock out cell line was not changed further by ABA treatment, except for increased branch initial and strong increased tmema formation. Overexpression of FtsZ1-2 hindered ABA induced short cell formation.

3.2. Influence of hormone treatment on GFP fluorescence in FtsZ1-2:GFP ox cell line

PpFtsZ1-2 has been shown to possess a peptide transport sequence addressing the protein not only to the chloroplast but also to the cytoplasm (Kiessling *et al.* 2004), where it forms annular and filamentous branching structures.
Under low light conditions these structures slowly disappear with every subcultivation step. New structures are rarely formed and their appearance could not be linked to any developmental stage by simple observation, because of their disappearing nature. This means it could not be discerned if the observed structures had been newly formed or if cells containing FtsZ1-2:GFP filaments retained them prior to subcultivation.

3.2.1. Influence of auxin on GFP fluorescence in FtsZ1-2:GFP ox cell line

To test for the influence of Auxin on GFP fluorescence, 14 day old cultures of FtsZ1-2:GFP ox cell lines were transferred into fresh Knop medium containing 20 µM of IAA and were incubated under low light conditions for 6 days in a shaking culture. To test the influence of functional Auxin transport, samples from the same culture were transferred to fresh medium containing 10 µM of NPA, an Auxin transport blocker. Control cells were samples of the same cultures transferred to fresh Knop medium.

Control cells showed a total of 25% of fluorescing protonema. Of those 17% contained fluorescent structures on chloroplasts, 10% showed cytoplasmic FtsZ1-2 filaments and 8% showed a diffuse fluorescence inside the cytoplasm. Treatment with NPA increased the total fluorescence to 33%. Also there was an increase of the amount of fluorescent chloroplasts (32%) but a decrease in the number of filaments (1%) as well as a reduced amount of diffuse cytoplasmic fluorescence (5%).

Treatment with IAA led to a total amount of 42% fluorescent protonema. A strong increase in diffuse fluorescence inside the cytoplasm (19% of the counted protonema) could be noted. Of the protonema, 28% showed fluorescent chloroplasts. A decrease in fluorescent cytoplasmic filaments to 4% was detected (Diagram 3.2.1.1).

Figure 3.2.1.1 FtsZ1-2:GFP ox protonema cells showing diffuse green fluorescence inside the cytoplasm

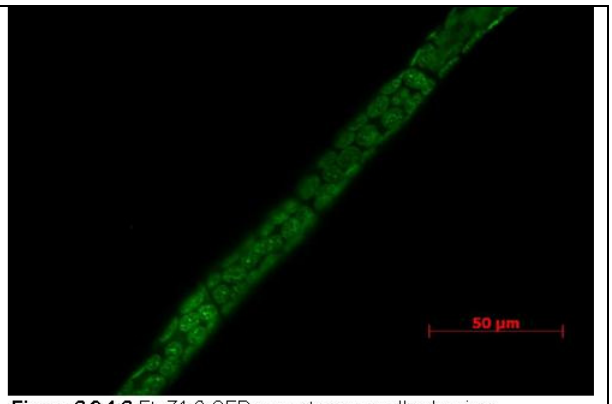

Figure 3.2.1.3 FtsZ1-2:GFP ox protonema cells showing green fluorescence inside the chloroplasts

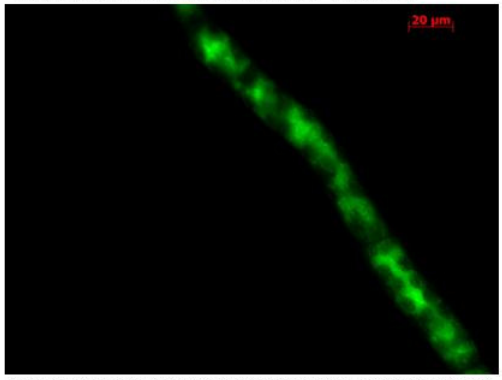

Figure 3.2.1.2 FtsZ1-2:GFP ox protonema cells showing diffuse green fluorescence inside the cytoplasm

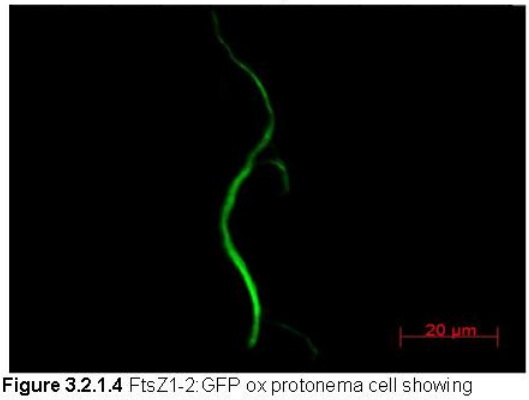

Figure 3.2.1.4 FtsZ1-2:GFP ox protonema cell showing green fluorescent filaments inside the chloroplasts

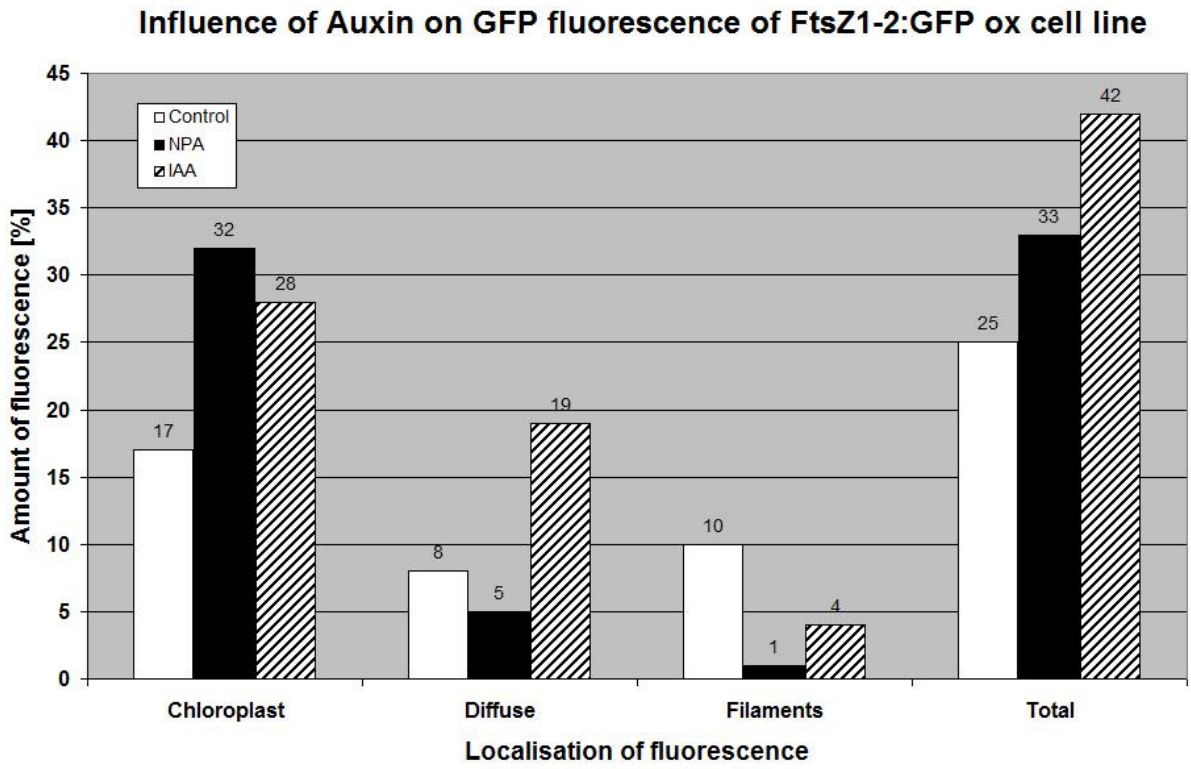

Diagram 3.2.1.1 Amount of fluorescence per protonema depending on Auxin level after 6 days of incubation under low light conditions.

3.2.2. Influence of cytokinin on GFP fluorescence in FtsZ1-2:GFP ox cell line

To test for the influence of cytokinin on GFP fluorescence, 14-day-old cultures of FtsZ1-2:GFP ox cell lines were transferred into fresh Knop medium containing 20 µM of 2iP and were incubated under weak light conditions for 6 days in a shaking culture. Control cells were samples of the same cultures transferred to fresh Knop medium.

Control cells showed a total of 27% of fluorescent protonema. Most fluorescence was found in chloroplasts, about half of the fluorescing protonema contained cytoplasmic FtsZ1-2:GFP filaments and only 5% of the tested protonema showed a diffuse cytoplasmic fluorescence.

Treatment with 2iP leads to a slight increase in fluorescence of chloroplasts after 2 days of incubation. After 3 days, an increase in cytoplasmic filaments could be measured from 12% on day two to 17% on day three.
After six days, a total amount of fluorescent protonema of 42% could be counted. The amount of protonema containing filaments had increased to 36%. 41% of the protonema showed fluorescent chloroplasts and 6% of the observed protonema showed diffuse cytoplasmic fluorescence. (Diagram 3.2.2.1)

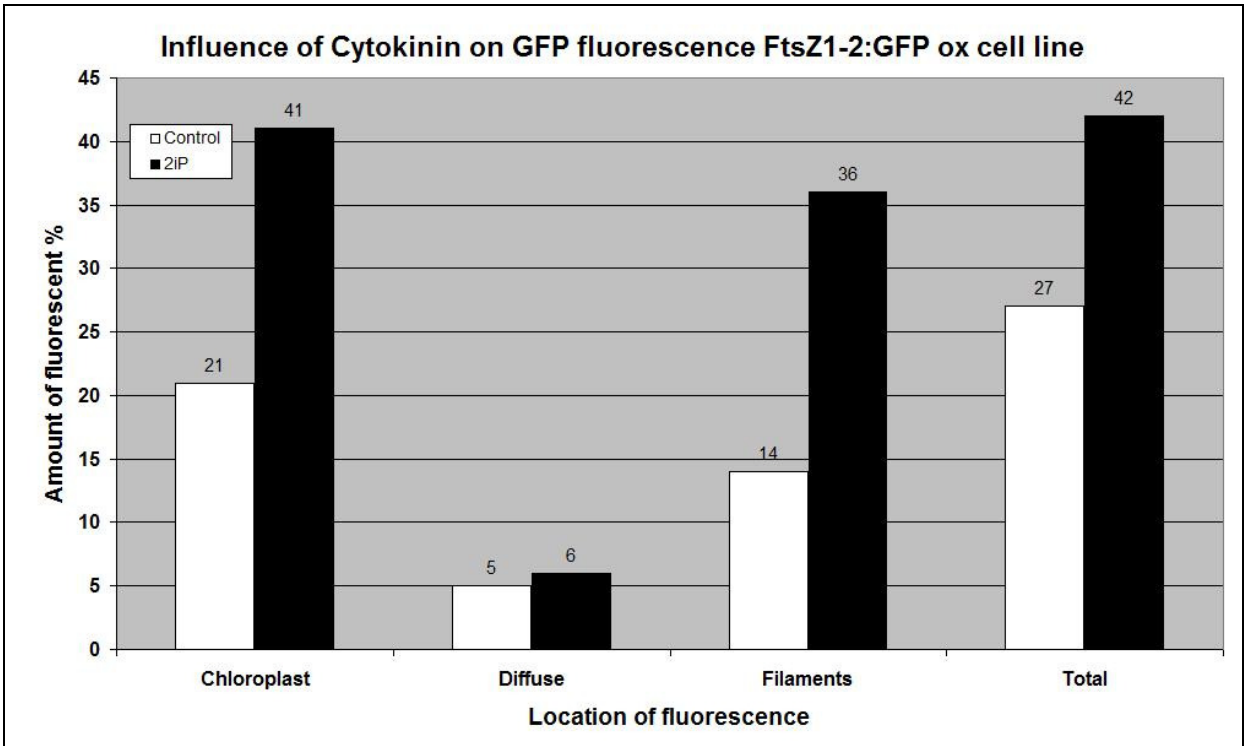

Diagram 3.2.2.1 Amount of fluorescence in the presence of 20 µM cytokinin after 6 days of incubation under low light conditions.

3.2.3. Influence of abscisic acid on GFP fluorescence in FtsZ1-2:GFP ox cell line

To test for the influence of abscisic acid on GFP fluorescence, 14 day old cultures of FtsZ1-2:GFP ox cell lines were transferred into fresh Knop medium containing 20 µM of ABA and were incubated under low light conditions for 6 days in a shaking culture. Control cells were samples of the same cultures transferred to fresh Knop medium.

Control cells showed a total of 31% of fluorescent protonema. Most fluorescence was found in chloroplasts (21%), 15% of the observed protonema contained cytoplasmic FtsZ1-2:GFP filaments and only 9% of the tested protonema showed a diffuse cytoplasmic fluorescence.

Treatment with ABA led to a slight decrease of the amount of fluorescence of chloroplasts (19%) after 6 days of incubation.
A total amount of fluorescent protonema of 29% could be counted, which represents also a slight decrease compared to control samples. Of those, 23% contained diffuse fluorescence. The amount of protonema containing FtsZ1-2:GFP filaments decreased to 5%. (Diagram 3.2.3.1)
Since ABA leads to a strong relocation of organelles and changes in the cell compartment, these values have to be treated carefully. This is because the shifted position of the chloroplasts may have hidden chloroplast-born and cytoplasmic GFP structures from view.

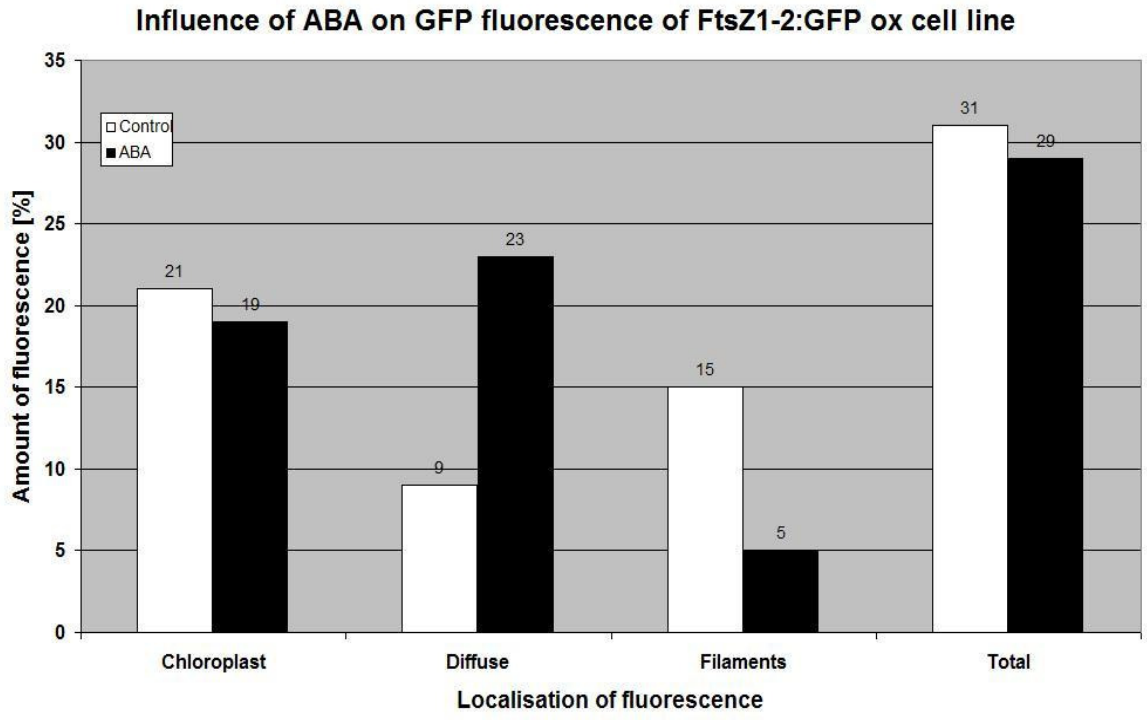

Diagram 3.2.3.1 Amount of fluorescence in the presence of 20 µM abscisic acid after 6 days of incubation under low light conditions.

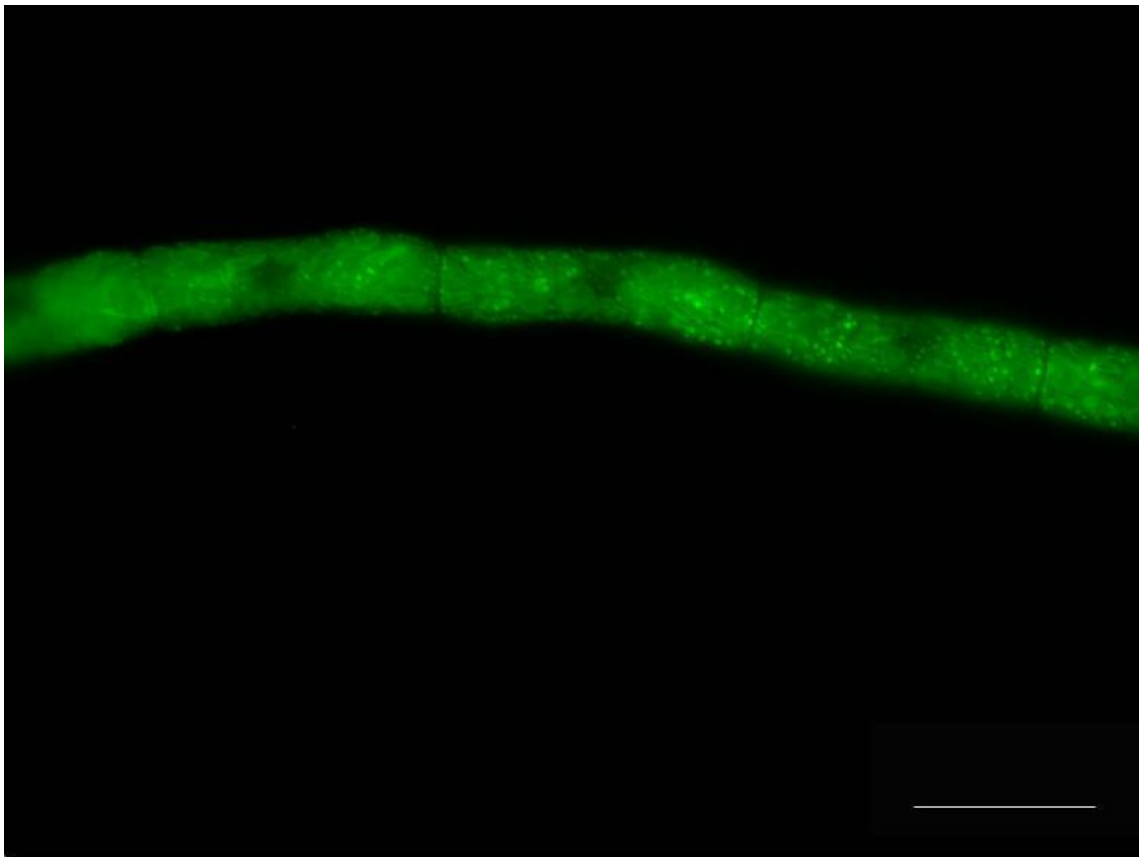

Figure 3.2.3.1 FtsZ1-2 ox cell line with diffuse fluorescence in the presence of 20 µM ABA after 6 days of incubation under low light conditions. Scale bar equals 20 µm

The effect of hormone treatment on fluorescence compared with control samples is summarized in Table 3.2.3.1:

	Location of fluorescence			
	Chloroplast	Diffuse cytoplasm	Filaments cytoplasm	Protonema expressing fluorescence
NPA	**++**	**-**	**-**	**+**
IAA	**+**	**++**	**+**	**++**
2iP	**++**	**+**	**++**	**++**
ABA	**(-)**	**++**	**-**	**-**

Table 3.2.3.1. Location of fluorescence under the influence of different hormones. (+ = increase, ++ = strong increase, - = decrease, (-) values not clear.

3.3. Influence of light quality and quantity on protonema cell growth of *P. patens* cell lines

3.3.1. Wild type cells under different light conditions

The predominant developmental stage of wild type protonema under weak light conditions is chloronema. Caulonema are rarely induced and only in small amounts, even 20 days after blending. The cells are mostly cylindrical, yet show a slight swelling at the apically-oriented pole. The protonemata grow with few branches, except when brachycytes are formed. Brachycytes branch off in every direction. Average cell length is between 35 to 45 µm. Brachycytes and tmema cells are readily formed to a point where only two cells remain per cell file. Chloroplasts are in close proximity to each other and appear to fill the complete cytoplasm. This appearance is enhanced, because the chloroplasts are oriented with their broad sides towards the cell wall so that they can collect maximum light. Generally wild type cells show strong symptoms of abscisic acid induction, like short cells, dense cytoplasm and small vacuoles as a light stress response.

Under strong light conditions those weak-light-induced abscisic acid effects disappear within four days. Caulonema development is induced, chloroplasts become smaller and fewer and the swelling at the apically-oriented cell poles disappears. Branching also increases.

After discerning a phenotypical difference between wild type cultures grown under weak light conditions (25 µM*sec^{-1}*m^{-2}) and then placed under the influence of about the double amount of light (55 µM*sec^{-1}*m^{-2} standard condition according to Schumaker and Dietrich 1990), it was deemed necessary to test for morphological differences under strong light conditions (100µM*sec^{-1}*m^{-2}). Also a hypothetical interaction of FtsZ1-2 with a photoreceptorsystem could not be excluded and needed to be examined. For this the influence of light quality on growth and development of *P. patens* cell lines was tested.

3.3.2. Influence of white light on differentiation and protonema growth of *P. patens* cell lines

To test the influence of strong white light on cell growth, samples of liquide cultures of 14 day old protonemal tissue of all three cell lines which had been grown under low light conditions, were transferred to fresh Knop medium without blending and incubated for 6 days under strong light conditions.

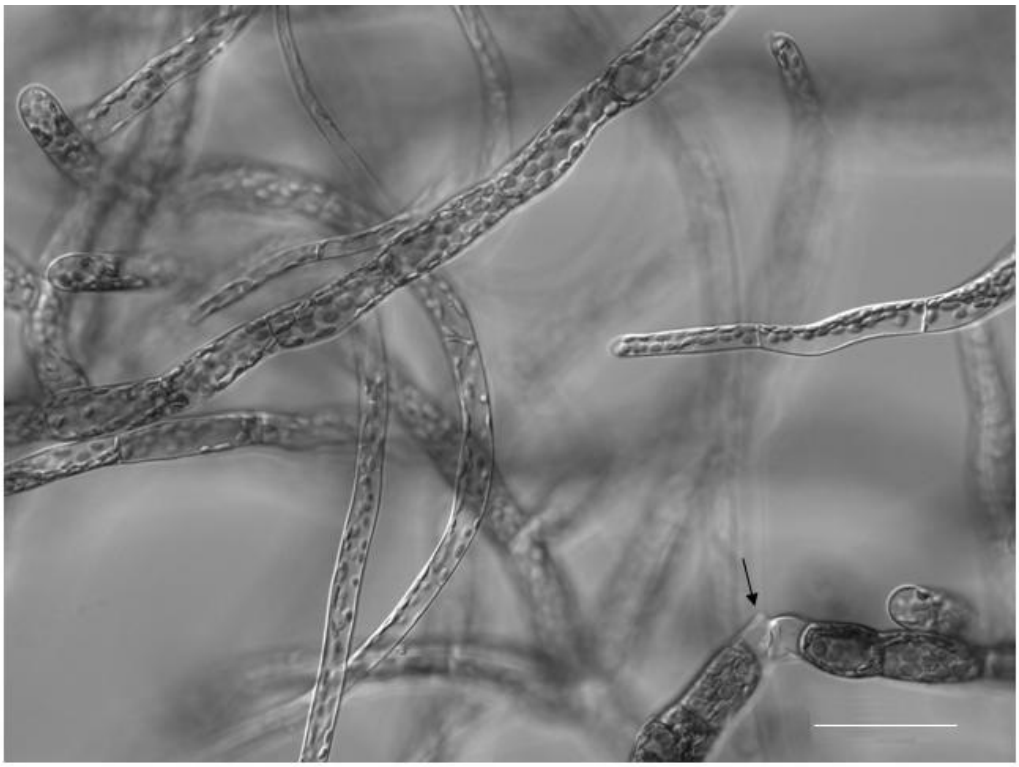

Figure 3.3.1.1. Protonema of wild type grown under strong light conditions for 6 days,showing caulonema, chloronema brachycytes and tmema (arrow) Scale bar indicates 50 µm

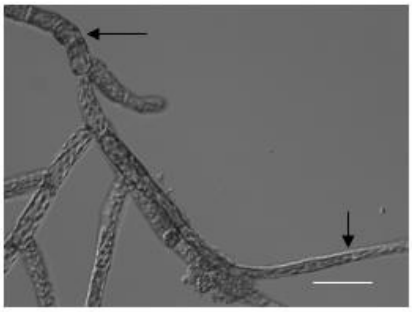

Figure 3.3.1.2.
FtsZ1-2 ox, protonema cells grown under strong light conditions for 6 days. Arrows indicating early caulonema (right) and short cells (left), Scale bar indicates 50 µm.

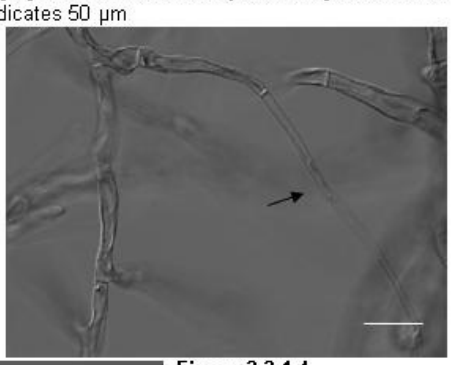

Figure 3.3.1.4.
Δ FtsZ1-2 cell line, grown under strong light conditions for 6 days. Arrow indicating long thin caulonema like cell. Scale bar indicates 50 µm

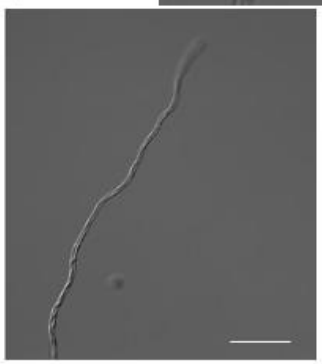

Figure 3.3.1.3.
FtsZ1-2 ox, late stage caulonema grown under strong light conditions for 6 days. Scale bar indicates 50 µm

Control samples were also transferred to fresh Knop medium without blending and incubated under low light intensity. After this, cell length was measured as above.

Morphological changes were observed to be strongest in the FtsZ1-2 ox cell line. Caulonema development was first observed on the second day after incubation. It progressed fast to late caulonema stages, which were very long (90 to 400 µm) and very thin (13 to 5µm) with few and pale spindly chloroplasts (Figure 3.3.2.3). These cells were excluded from the measurements below because of measurability. They were simply too long to fit on the pictures completely, in most cases. This has a direct influence on the average cell length of FtsZ1-2 ox in Diagram 3.3.2.1., which appears to

be shorter than it would otherwise be. Brachycytes were present but rare. Branching was increased (Figure 3.3.1.2).

Wild type cells were also released from weak light symptoms, but more slowly than in the overexpression cell line, which means that there were more early stages of caulonema development (Figure 3.3.2.1). Late stages of caulonema could also be found, but were fewer in number than in overexpression line samples. Brachycytes were formed, but not as abundantly as before. Branching was reduced.

The knock out cell line also showed an increase in cell length. Growth of rounded and bloated cells was reduced and could rarely be observed in the strong light samples. Filaments were long and slightly bumpy in appearance. This was caused by numerous branch initials. Growth of long thin late stage caulonema-like filaments was strongly enhanced, compared with weak light conditions (Figure 3.3.2.4).

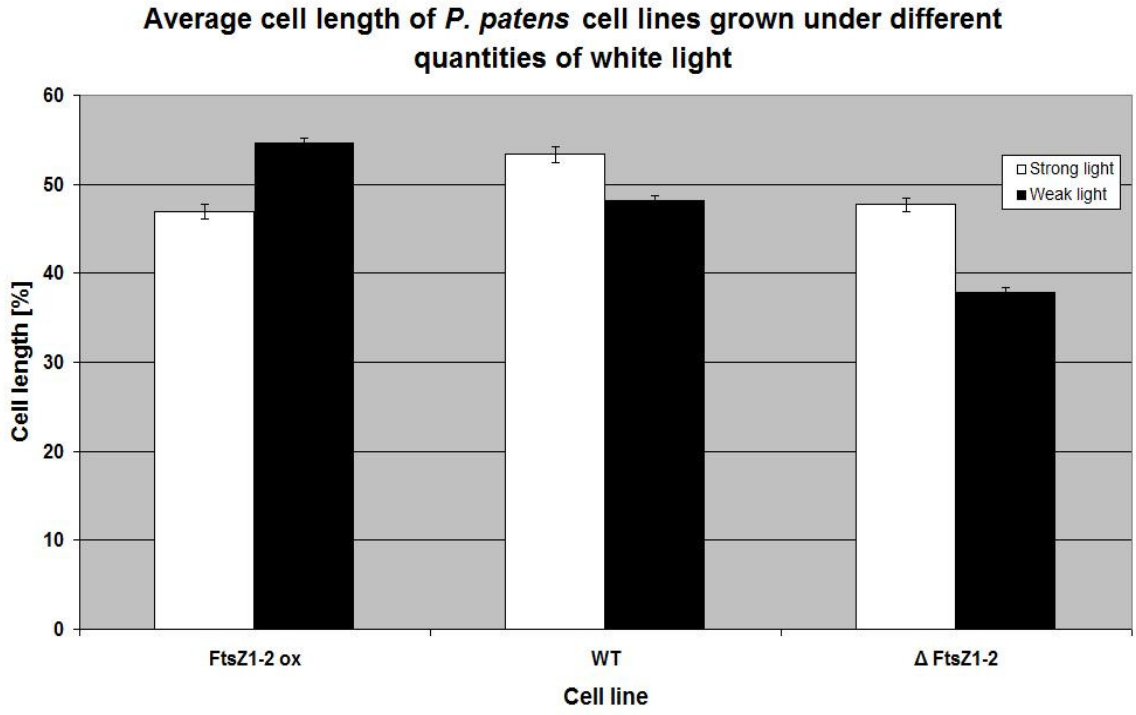

Diagram 3.3.2.1 Average cell length of cell lines expressing different levels of FtsZ1-2 grown under different light conditions. Low light (25 µM*sec^{-1}*m$^{-2)}$, strong light (55 µM*sec^{-1}*m$^{-2)}$. Error bars indicate standard error (n = 200).

Comparison of average cell length (Diagram 3.3.2.1) showed that the amount of chloronema cells and early stage caulonema were strongly reduced (7% to weak light sample: 46.9 µm, standard deviation of 23.9 µm) in FtsZ1-2 ox strong light samples, due to the exclusion of late stage caulonema from the measurement mentioned before.
Weak light samples of overexpression cell lines showed the highest average length (54.7 µm, ± 14.9 µm), followed by the wild type, where the average cell length increased under strong light conditions to 53.5 µm (± 24.9 µm), compared to samples grown under weak light conditions with an average cell length of 48.2 µm (± 16.9 µm).
The length of ΔFtsZ1-2 cells was increased under strong light conditions (47.7 µm, ± 20.2 µm) compared to samples grown under weak light conditions (37.8 µm, ± 16.5 µm)

The distribution of cell length showed that wild type cells and FtsZ1-2 ox cells grown under weak light conditions grew with approximately normal distribution with the mode interval at 45- 55 µm for wild type and a shifted mode interval for FtsZ1-2 ox cell line at 55- 65 µm.

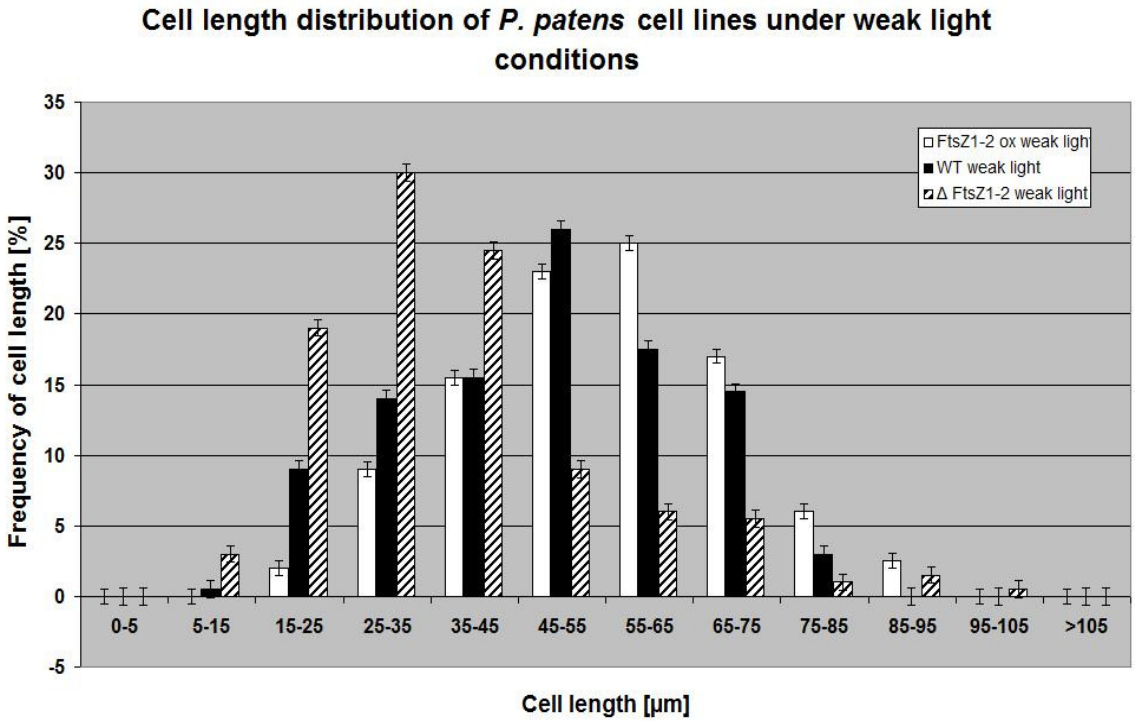

Diagram 3.3.2.2 Distribution of cell length of cell lines expressing different levels of FtsZ1-2 grown under low light conditions. Error bars indicate standard error (n = 200).

ΔFtsZ1-2 cells were approximately Poisson-distributed under control conditions, with the mode interval at [25- 35] µm and a slight plateau at [65- 75 µm] (Diagram 3.3.2.2).

Under strong light conditions ΔFtsZ1-2 cells showed a disrupted Poisson distribution with the mode interval at [25- 35 µm], a mass shift towards the tail region and a second peak at [45- 55 µm]. The plateau at 65- 75 µm remained but now contained nearly a fifth of all measured cells in comparison with weak light samples, where it contained only a tenth.
The distribution of wild type cells was completely broken up under strong light conditions. Even though the mode interval was retained at [45- 55 µm], a new peak developed at [25- 35 µm] and a third, if slight peak at [85- 95 µm]. Also a mass shift towards the tail region took place, which corresponds with the observation of an increased caulonema and reduced brachycyte formation.

	Branching under White light conditions		
	K.O.	WT	OX
Strong white	53%	27%	32%
Low light	45%	23%	29%

Table3.3.2.1 Branching and side branch initials in [%]

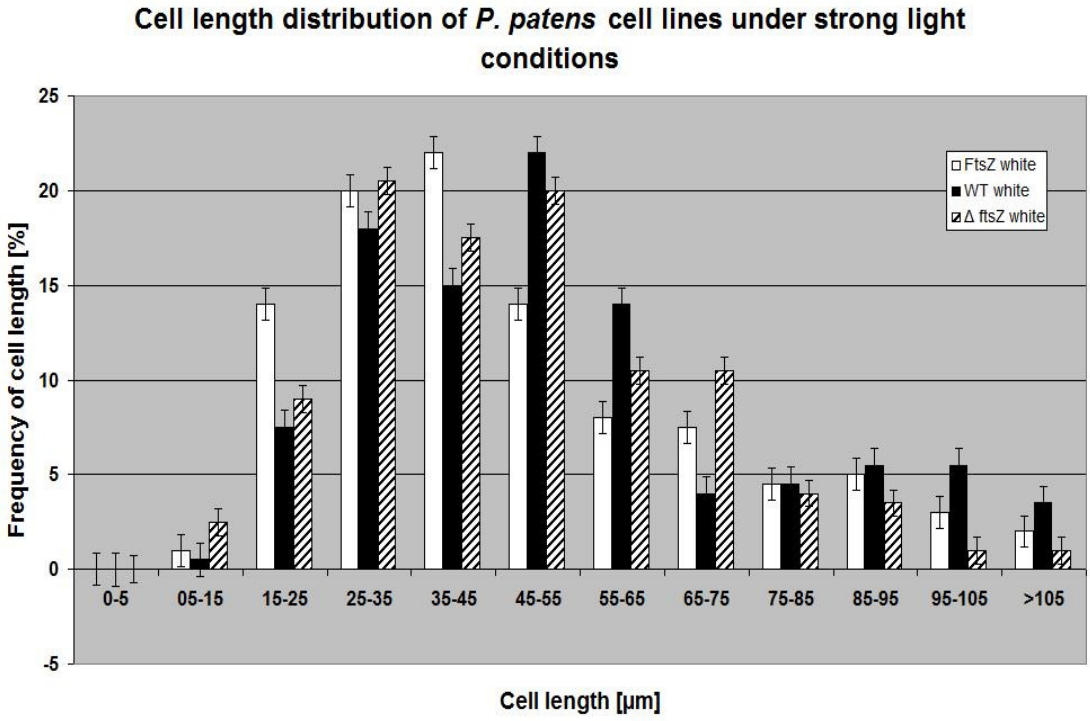

Diagram 3.3.2.3 Distribution of cell length of protonema cells of *P. patens* cell lines expressing different levels of FtsZ1-2, grown under strong light conditions for 6 days. Error bars indicate standard error (n = 200).

FtsZ1-2 overexpression cell line had its mode interval at [35- 45 µm] followed by a heavy tail region and a slight second peak at]85- 95 µm]. That means that this cell line is approximately Poisson-distributed. Though at first glance cell length seems to be reduced, the findings correspond with the fact that chloronema growth is reduced and late stage caulonema cells, which have been abundantly formed, have been omitted from measurement for practical reasons.

Concluding it can be said, that:

> FtsZ1-2 overexpression led to a faster differentiation response to strong light conditions. Late stage caulonema formation was not observed in FtsZ1-2 knock out cell line

3.3.3. Influence of blue light on differentiation and protonemal cell growth of *P. patens* cell lines

To test the influence of blue light, protonemal tissue samples of all three cell lines were plated on Petri dishes containing solid Knop medium and incubated under a light intensity of 100 µM*sec^{-1}*m^{-2}. The samples were incubated for four days. Controls were treated likewise, but incubated with strong white light (likewise 100 µM/sec/m^2).

Measurements were taken as above.

The predominant growth stage after blue light treatment was chloronema, though cells appeared strongly elongated in the wild type and FtsZ1-2 ox cell line (Figure 3.3.3.3). The overexpression line was also producing short cells, reminiscent of the short brachycytes produced by the wild type under low light conditions. Branching and cell length was enhanced within the wild type (Figure3.3.3.5) and slightly so in the overexpression cell line, yet branching was slightly reduced in the FtsZ1-2 ox line.

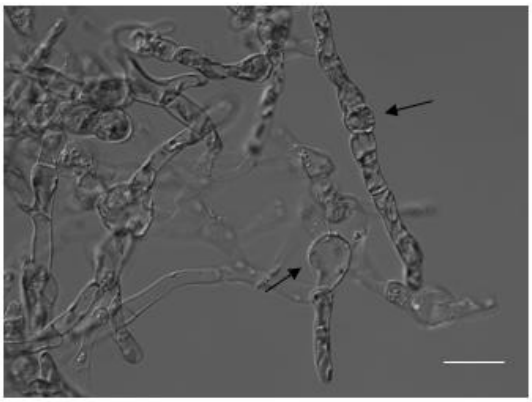

Figure 3.3.2.1 Δ FtsZ1-2 cell line, grown under strong Blue light for 3 days, showing short rounded cells (right arrow) and bloated cells (left arrow) (Scale bar 50 µm)

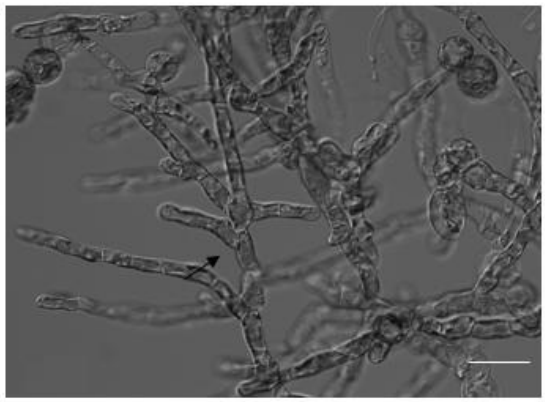

Figure 3.3.2.2. Δ FtsZ1-2 cell line, grown under strong blue light for 3 days, showing branching and cell files (Scale bar 50 µm)

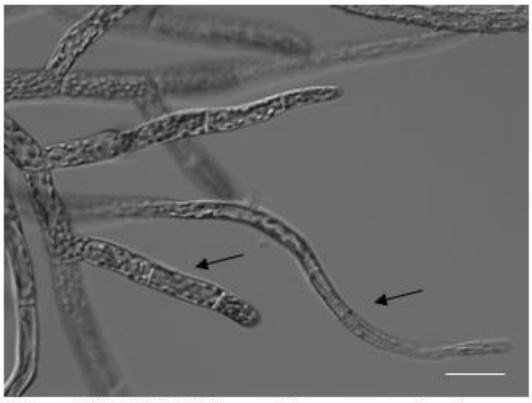

Figure 3.3.2.3 FtsZ1-2 ox cell line grown under strong blue light for 3 days showing caulonema and chloronema

Figure 3.3.2.4 FtsZ1-2 ox cell line grown under strong blue light for 3 days showing branching chloronema

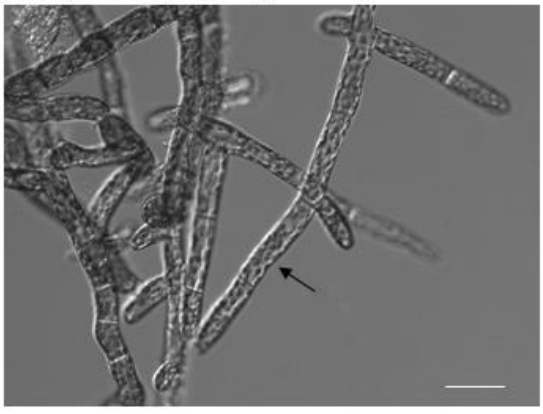

Figure 3.3.2.5 Wild type cells grown under strong blue light for 3 days showing branching elongated chloronema Cells (arrow) (Scale bars indicate 50 µm)

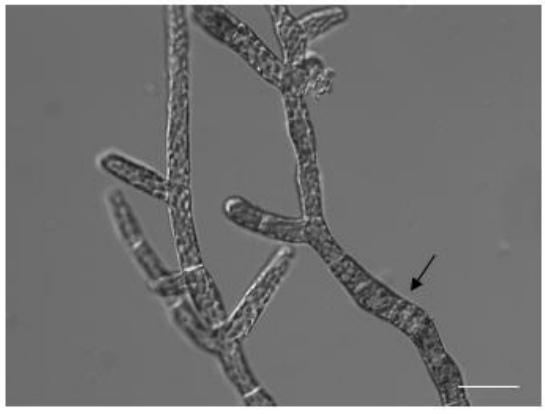

Figure 3.3.2.6 Wild type cells grown under strong blue light for 3 days, showing short cells (arrow) (Scale bars indicate 50 µm)

Early stages of caulonema were rare in all three cell lines, yet more numerous in the FtsZ1-2 ox line. Late stages of caulonema were not observed.

The knock out cell line grew mostly as files of rounded cells, with occasional interspaced bloated ones (Figure 3.3.3.1). Branching was neither enhanced nor reduced. Branch initials were not as prominent as in control samples.
Measurement of the cell length showed that blue light decreased the average cell length of wild type cells from 53.4 µm with a standard deviation of 24.9 µm for cells grown under strong white light to 42.1 µm ± 15.1 µm under blue light. FtsZ1-2 ox cell lines showed a slight increase of average cell length under blue light (47.2 µm, ± 16.8 µm compared to cells grown in white light with an average cell length of 46.9 µm (±23.9 µm).
But since the difference is so small and the standard deviation is big in both cases, this difference may not be significant.
In the case of FtsZ1-2 knock out cell lines, an increase in cell length of 5 µm was observed. Under blue light, the knock out line showed an average cell length of 53.7 µm ± 20.7 µm, while grown under white light an average of only 47.7 µm was reached (± 20.2 µm).

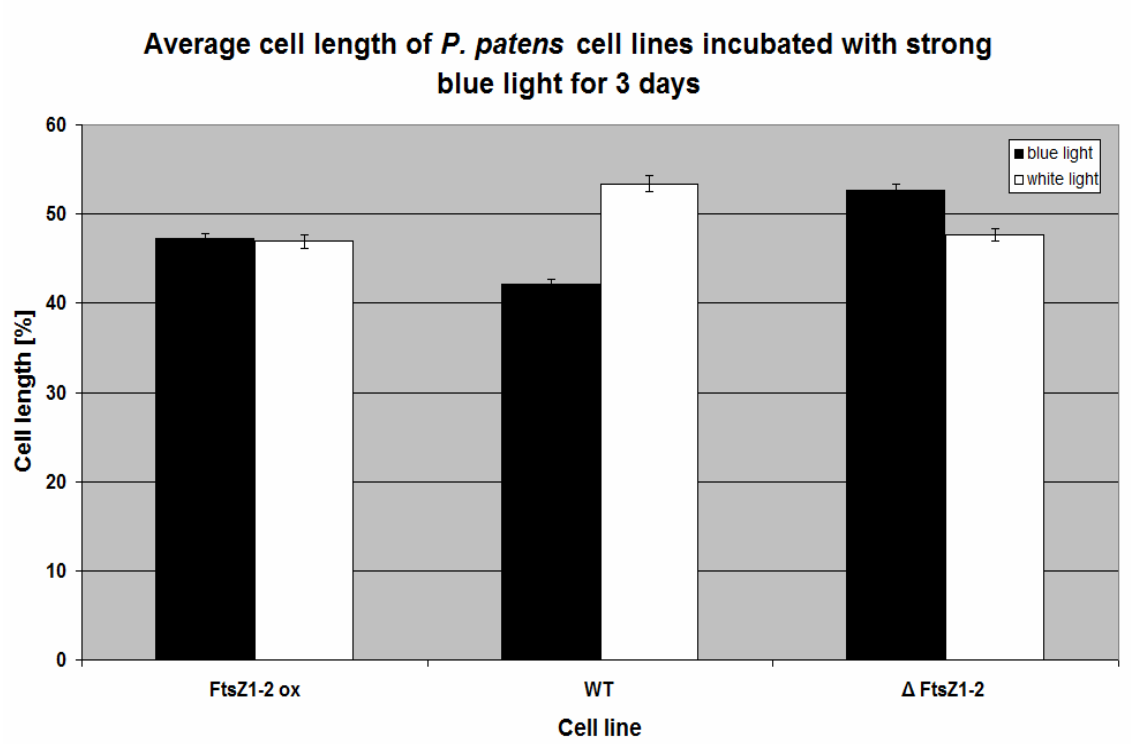

Diagram 3.3.3.1 Average cell length of *P. patens* cell lines expressing different levels of FtsZ1-2 grown under strong blue light for 3 days, compared with protonema cells grown under white light of the same intensity. Error bars indicate standard error (n = 200).

Distribution of cell length shows a strong influence of blue light on the cells of the FtsZ1-2 knock out cell line (Diagram 3.3.3.2). The cells were approximately normal distributed with the mode interval at [45- 55 µm], a second peak at [25- 35 µm] and a plateau at 75- 85 µm. This does not fit its usual Poisson distribution and might suggest differentiation processes that have not been readily observable under the microscope, since chloronema and caulonema are not discernable by their phenotype. This cell line is the only one that produced cells with a length of more than 95 µm when treated with strong blue light.
Wild type cells were also approximately normally distributed with their mode interval at [35- 45 µm], yet there is a steep rise between interval [15- 25 µm] and [25- 35 µm], on

the left flank of the growth curve, which fits the observed reduction of brachycyte formation under strong blue light.
FtsZ1-2 ox cell line distribution also approaches normal distribution with the mode interval at [55- 65 µm] mirroring the elongated chloronema cells observed in the sample, and a second peak at 25- 35 µm, corresponding to the observed short cells.
The distribution of protonema cells grown under white light shows differentiation in progress for all three cell lines (Diagram 3.3.3.3).
In the case of the ΔFtsZ1-2 cell line the mode interval is reached at [25- 35 µm]. Then a heavy tail region with a second slight peak at [85- 95 µm] follows. This describes an approximate flat Poisson distribution.

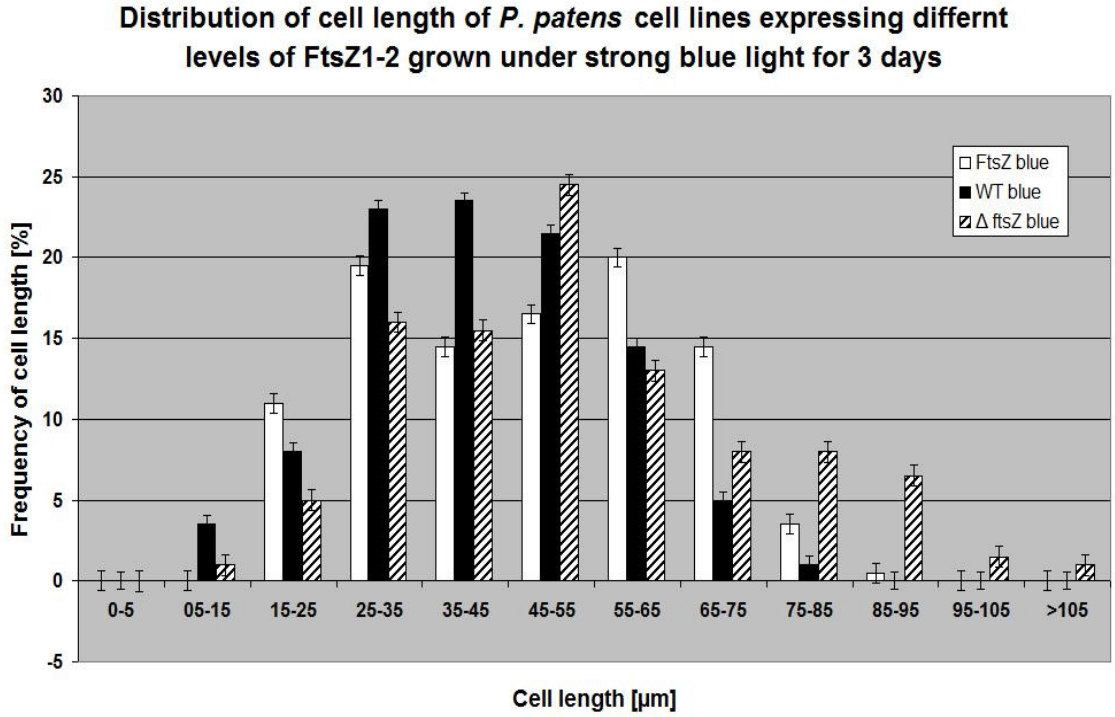

Diagram 3.3.3.2 Distribution of cell length of *P. patens* cell lines grown under strong blue light. Error bars indicate standard error (n = 200).

In the case of the overexpression cell line the mode interval is reached after a steep rise on the left flank of the growth curve at [25- 35 µm]. Then a second peak follows at [45- 55 µm], and a third at [65- 75 µm]. The tail region of the curve shows that caulonema formation has been induced, yet weakly.
Wild type mirrors the distribution of FtsZ1-2 ox line up to interval seven. After that the growth curve follows rather that of the knock out cell line. The curve looks as if it has been constructed out of three normal distribution curves that have been merged. This is indicating that the transition in differentiation has not yet reached its close, or has just been induced.

	Branching under Blue light conditions		
	K.O.	WT	OX
Blue light	42%	69%	33%
Control	39%	25%	29%

Table3.3.3.1 Branching and side branch initials in [%]

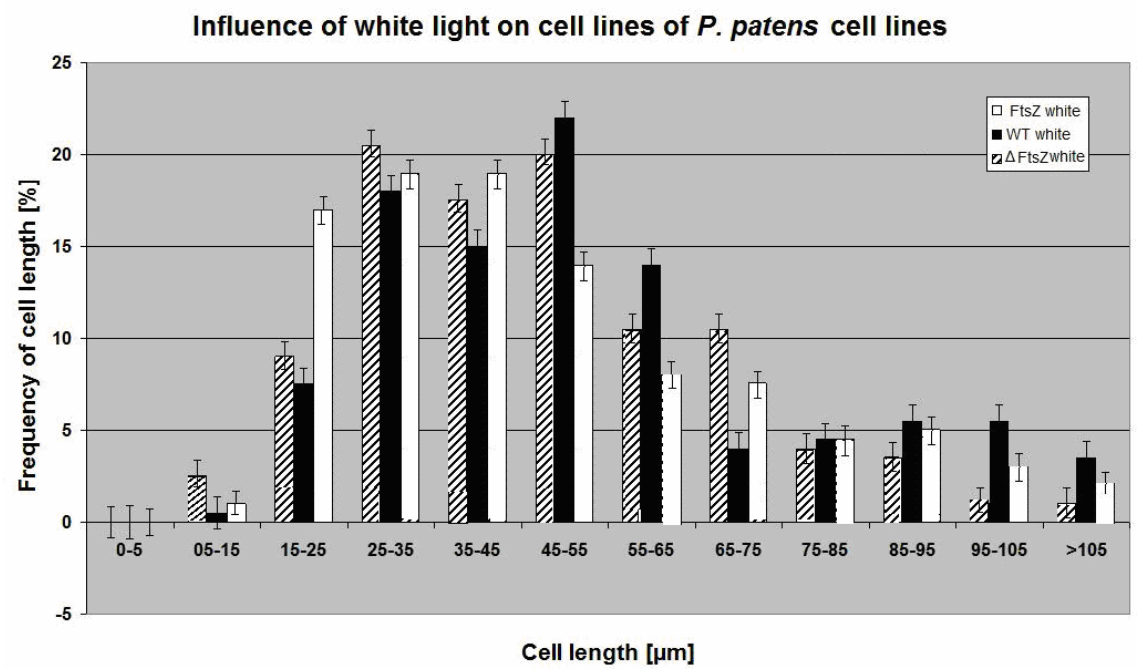

Diagram 3.3.3.3 Distribution of cell length of *P. patens* cell lines grown under strong white light for 3 days. Error bars indicate standard error (n = 200).

To summarize the above:

The results above indicate that the influence of blue light leads to a slight decrease in cell length in wild type and in the FtsZ1-2 ox cell line. Caulonema differentiation was inhibited in both cell lines. The cell length of the knock out cell line was increased and the growth curve indicated no influence of blue light on differentiation, compared with the white light control.

3.3.4. Influence of red light on differentiation and protonema growth of *P. patens* cell lines

To test the influence of red light, protonemal tissue samples of all three cell lines were plated on Petri dishes containing solid Knop medium and incubated under a light intensity of 100 µM*sec^{-1}*m^{-2}. The samples were incubated for four days. Controls were treated likewise, but incubated with strong white light (also 100 µM*sec^{-1}*m^{-2}).

Incubation with red light led to an increased amount of caulonema production in the wild type and overexpression cell line. FtsZ1-2 ox line produced more late stage caulonema (Figure 3.3.4.4, very long and thin) than the wild type. Chloronema cells elongate in both cell lines and a strong effect on chloroplast size in FtsZ1-2 ox cell line was detected. The amount of macro-chloroplasts and deformed chloroplasts increased markedly inside apical cells and the first two subapical cells (37%), compared to control cells under white light conditions (24%) (Figure 3.3.4.4 and 3.3.4.5).
Wild type cells showed an increased branching behavior. The branches mostly stem from brachycytes and short chloronema cells (Figure 3.3.4.5). The overexpression line lacked this increased branching.

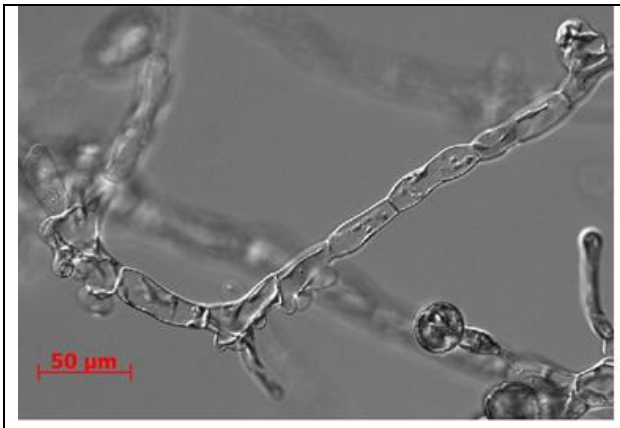

Figure 3.3.4.1 Δ FtsZ1-2 cell line, grown under strong red light for 3 days showing filamentous growth with rounded cells.

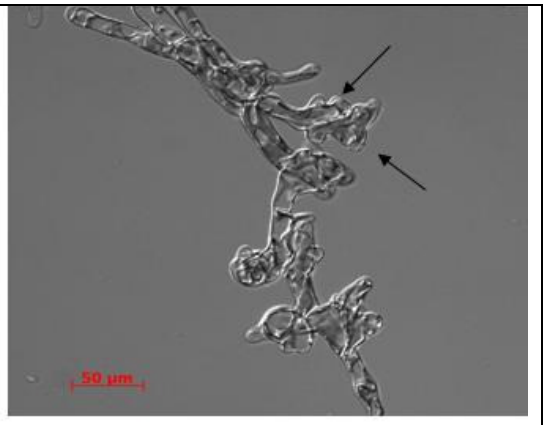

Figure 3.3.4.2 Δ FtsZ1-2 cell line, grown under strong red light showing clustered growth with irregular branch initials (arrows).

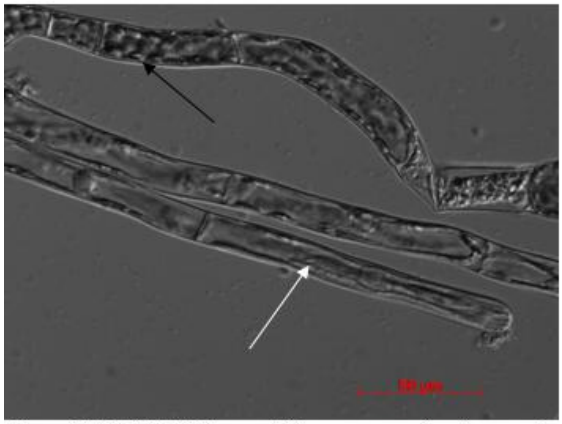

Figure 3.3.4.3 FtsZ1-2 ox cell line, grown under strong red light showing elongated protonema cells with deformed (white arrow) and normal (black arrow) chloroplasts.

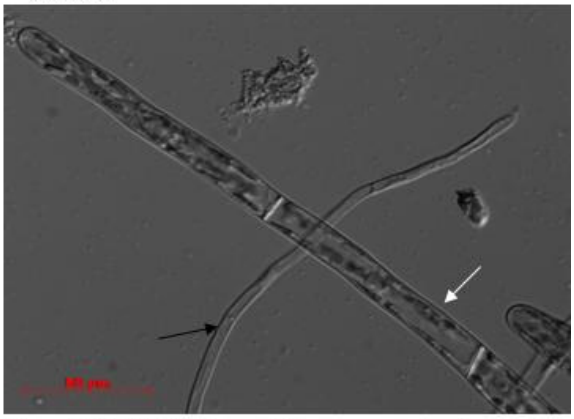

Figure 3.3.4.4 FtsZ1-2 ox cell line, grown under strong red light showing early (white arrow) and late stage caulonema cells (black arrow).

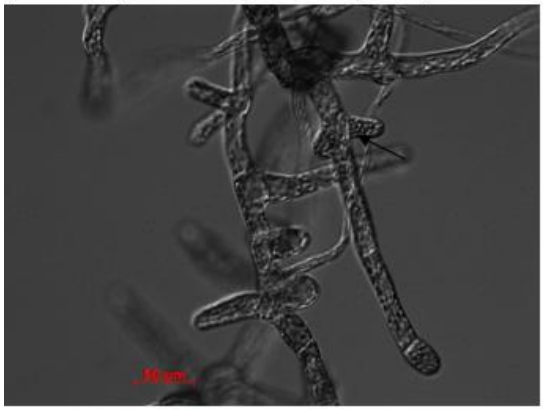

Figure 3.3.4.5 Wild type protonema, grown under strong red light showing elongated chloronema cells with increased branching (arrow).

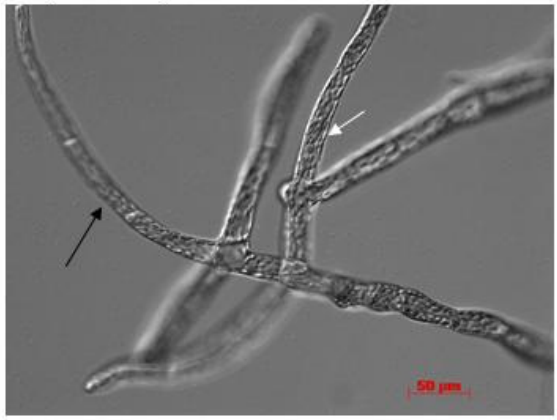

Figure 3.3.4.6 Wild type protonema, grown under strong red light showing elongated chloronema (white arrow) cells and early stage caulonema (black arrow).

Both cell lines shared the tendency to form smooth and straight outer cell walls.
In contrast to this, the knock out cell line formed filaments of rounded cells with constrictions at the cross walls (Figure 3.3.4.1). The strongest effect though was the strongly increased tendency to form numerous irregular side branch initials on one cell. This leads to clustered growth in whirls. This tendency was reduced in the control cells under strong light, yet was present under low light conditions, though not to this extent.

The average cell length of FtsZ1-2 ox cell line under strong red light is 52.6 µm with a standard deviation of 26.1 µm. Under white light the average cell length of the

overexpression line is 46.9 µm ± 23.9 µm. On average, wild type cells are shorter (45.29 µm) under red light with a smaller standard deviation of 18.74 µm. White light leads to a increased average cell length in wild type ± 24.9 µm.
The shortest cells were formed in the ΔFtsZ1-2 cell line which has an average cell length of 39.34 µm and the smallest standard deviation of 17.6 µm under strong red light. Incubated with white light the average cell length increases to 47.7 µm ± 20.2 µm.

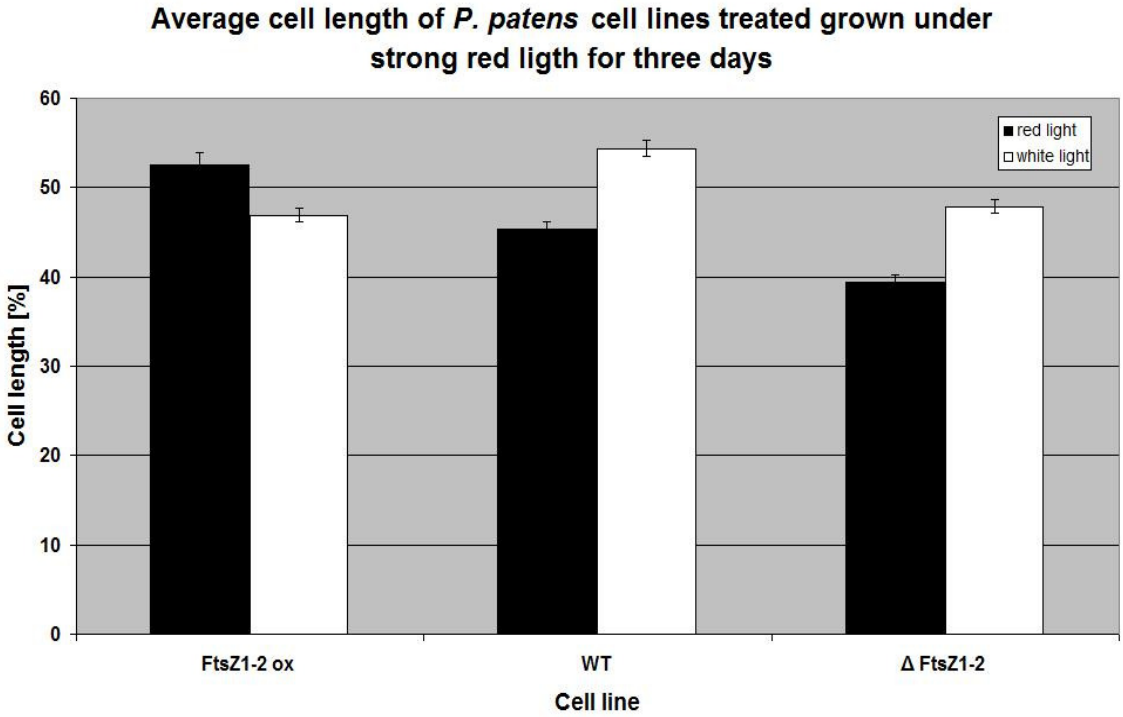

Diagram 3.3.4.1 Average cell length of *P. patens* protonema cells expressing different levels of FtsZ1-2, grown under strong red light for 3 days. Error bars indicate standard error (n=200).

The distribution of the cell lengths of the three samples is depicted in diagram 3.3.4.3.
The growth curve of wild type cells shows a normal distribution around the mode interval at 35- 45 µm. This is followed by a second peak at 55- 65 µm. The mode interval in the control samples was [45- 55 µm]. A heavy tail region is present, yet the amount of mass is reduced compared to white light treated cells. This fits the observed long chloronema cells and early caulonema stages.

	Branching under Red light conditions		
	K.O.	WT	OX
Red light	78%	32%	14%
Control	64%	22%	28%

Table 3.3.4.1 Side-branches and side- branch- initials in [%]

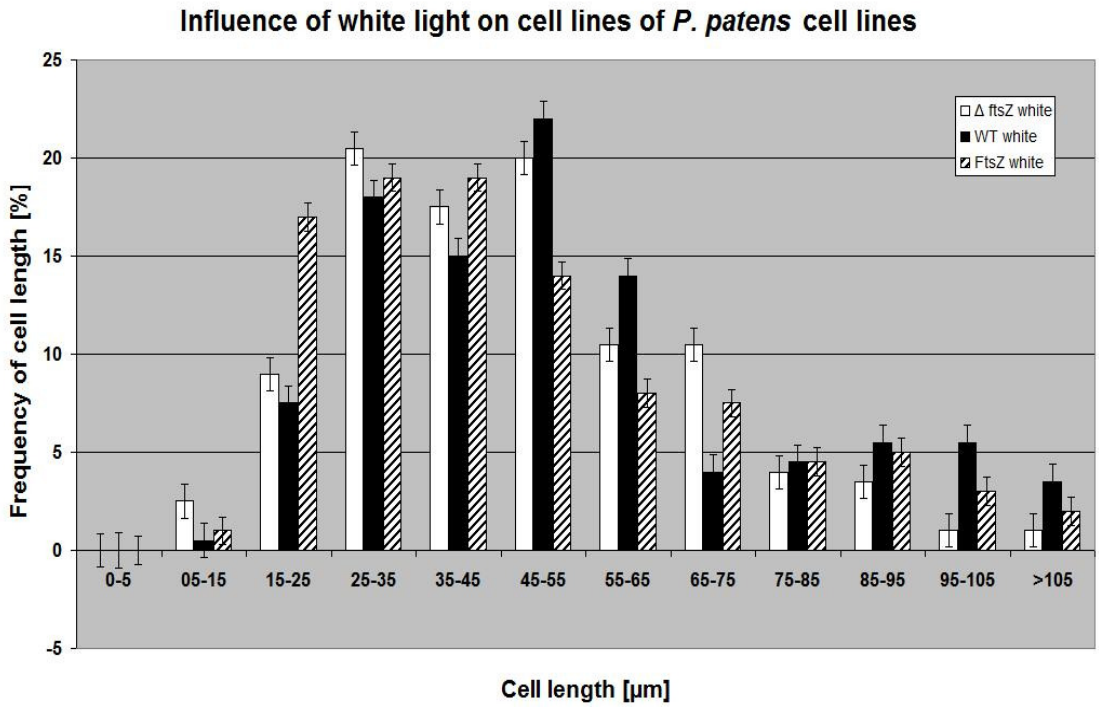

Diagram 3.3.4.2 Distribution of cell length of *P. patens* cell lines grown under strong white light for 3 days. Error bars indicate standard error (n=200).

The FtsZ1-2 overexpression cell line shows a flat normal distribution around the mode interval at 35- 45 µm, yet this interval contains only a fifth of the measured cells. Even so, this is an increase to the control samples, where less than 20% of the measured cells were [35 to 45 µm] long. The heavy tail region contains two more peaks at [65 -75 µm] and [85- 95 µm].

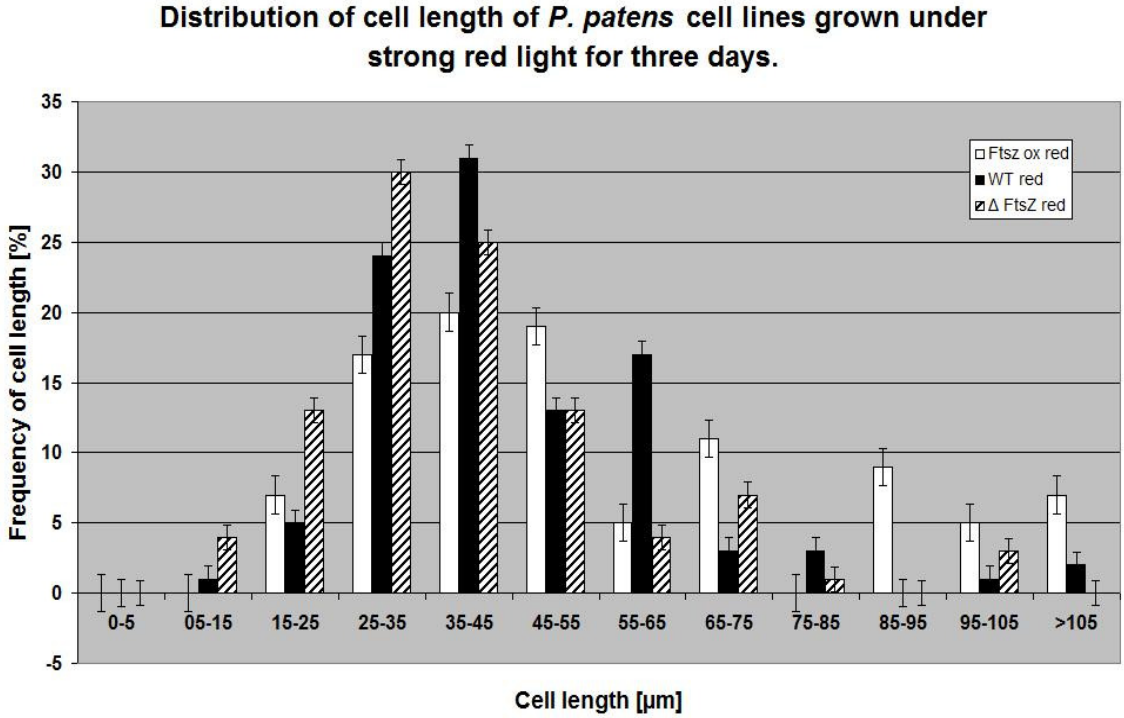

Diagram 3.3.4.3 Distribution of cell length of *P. patens* protonema cells expressing different levels of FtsZ1-2, grown under strong red light for 3 days. Error bars indicate standard error (n = 200).

Late stage caulonema cells again were not measured (see above), yet differentiation into caulonema can be surmised to be the reason for the two peaks in the tail region.

ΔFtsZ1-2 cell line has its mode interval at [25- 35 µm]. 30% of the mass of the sample are located there. This is a decided increase in mass compared to white light samples, where only 21% of the measured cells were located in the mode interval. A slight peak at 65- 75 µm and an even slighter one at [95- 105 µm] mirror the growth behavior of the other two cell lines.

As a conclusion it can be said that strong red light:

> increased cell length in the presence of FtsZ1-2 and decreased cell length in the absence of FtsZ1-2. The amount of branching in the Knock out cell line was increased. The amount of deformed chloroplasts in the presence FtsZ1-2overexpression line was also increased..

3.4. Influence of light quality on GFP fluorescence in FtsZ1-2:GFP ox cell line

To test the influence of different light qualities on GFP fluorescence, 14 day old protonemal tissue samples of the FtsZ1-2:GFP ox cell line were plated on Petri dishes containing solid Knop medium. The light fields were arranged in a way as to provide a light intensity of 100 $\mu M*sec^{-1}*m^{-2}$. The samples were incubated for four days. Controls were treated likewise, but incubated with weak white light (25 $\mu M*sec^{-1}*m^{-2}$). For quantification, 200 protonema per sample were examined for fluorescence.

Diagram 3.4.1 shows the location of fluorescence of protonema cells incubated under different light qualities.
Control cells contained a total of 27% of fluorescent protonemata. Most fluorescence was observed in chloroplasts with 21%. 6% showed a diffuse fluorescence in the cytoplasm and only 5% contained FtsZ1-2:GFP filaments.
Incubation under strong white light increased the total amount of fluorescence to 46%. 43.5% of these protonemata showed fluorescent structures on their chloroplasts, which is the highest amount for chloroplast-bound fluorescence in the examined samples. Diffuse cytoplasmic fluorescence was increased to 9.5% and FtsZ1-2:GFP filament formation was reduced to 4.5%.
Under red light conditions the total amount of fluorescent protonemata was the same as under white light (46%). FtsZ1-2 filament induction decreased further to 4 %, but the amount of diffuse fluorescence inside the cytoplasm increased to 23%. This is the highest value for this compartment in the examined samples. Fluorescence of chloroplasts was 33%.
Blue light induced the highest total fluorescence of the examined samples, reaching 52% of the samples. 36% of the tested protonema contained fluorescent structures on their chloroplasts and 16% showed diffuse fluorescence inside their cytoplasm. The number of protonema with FtsZ1-2:GFP filaments decreased to the lowest value for the tested samples, 3% of the samples.

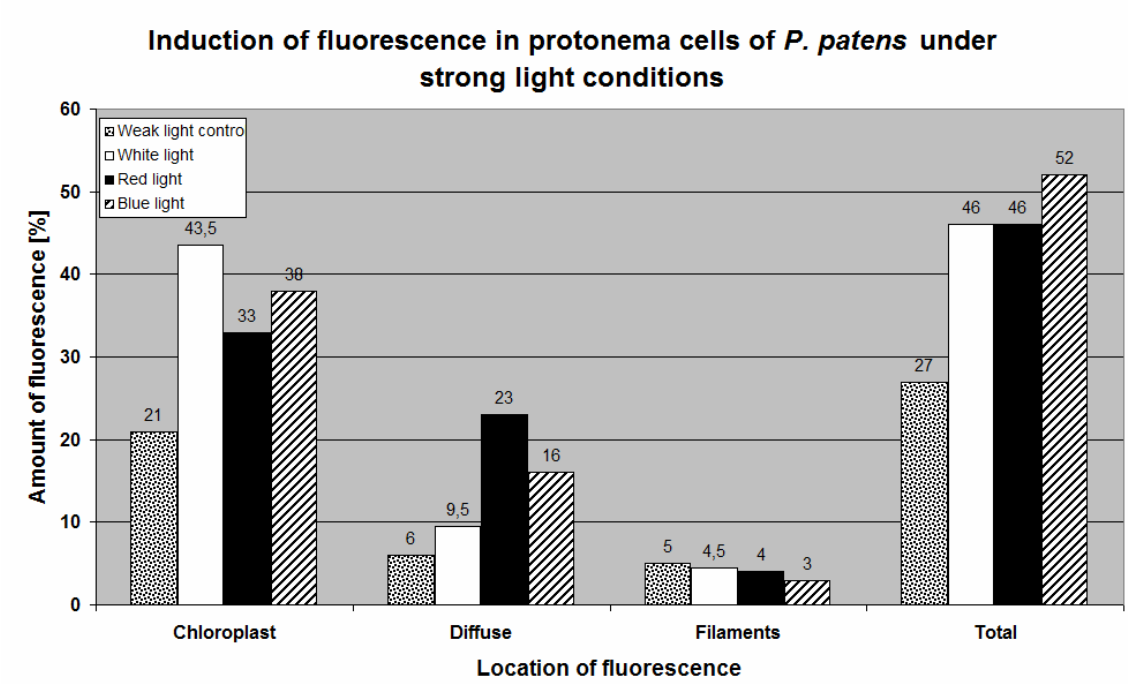

Diagram 3.4.1 Fluorescence of FtsZ1-2:GFP ox cell line grown under different light conditions for 4 days (n = 200 protonema).

Since cytokinin promoted the formation of cytoplasmic filaments the most (see chapter 3.2.2) a cross examination was made. For this, samples were treated as above, but 20 µM of 2iP was added to the fresh Knop medium.

Diagram 3.4.2 shows the location of fluorescence in protonema cells incubated under different light qualities in the presence of cytokinin.

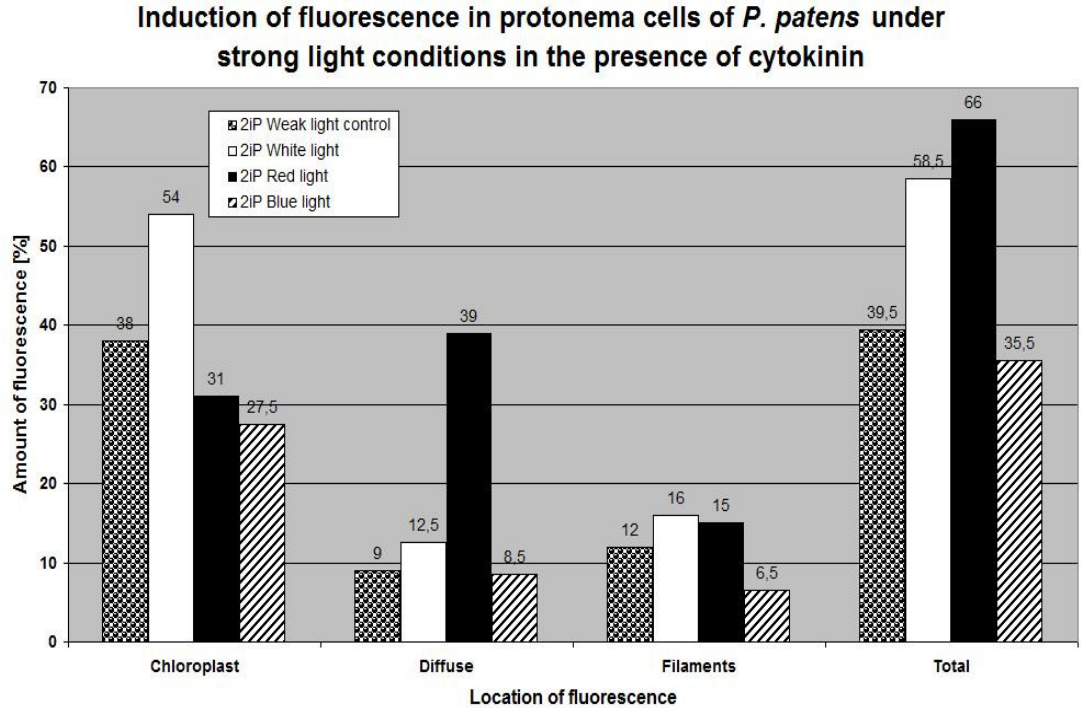

Diagram 3.4.2 Fluorescence of FtsZ1-2:GFP ox cell line grown under different light conditions for 4 days in the presence of 20 µM of 2iP. (n = 200 protonema)

The control cells contained a total of 39.5% of fluorescent protonema. Most fluorescence was observed in chloroplasts with 38%. This means that nearly all examined fluorescent protonema had fluorescent structures in their chloroplasts. 9% showed a diffuse fluorescence in the cytoplasm and only 12% contained FtsZ1-2:GFP filaments.
Incubation under strong white light increased the total amount of fluorescence to 58.5%. 54 % of these showed fluorescent structures on their chloroplasts, which is the highest amount for chloroplast bound fluorescence in the examined samples. Diffuse cytoplasmic fluorescence was increased to 12.5% and FtsZ1-2:GFP filament formation was increased to 16%, also the highest amount for the examined samples.

Under red light conditions the total amount of fluorescence was the same as under white light (66%). FtsZ1-2 filament induction increased to 15 %, but the amount of diffuse fluorescence inside the cytoplasm increased to 39%. This is the highest value for this compartment in the examined samples. Fluorescence of chloroplasts decreased to 31%.

Blue light induced the lowest fluorescence of the examined samples, which amounted to 35.5%. 27.5% of the tested protonema contained fluorescent structures on their chloroplasts and 8.5% showed diffuse fluorescence inside their cytoplasm. The number of protonema with FtsZ1-2:GFP filaments decreased to the lowest value of all tested samples, which amounted to 6,5%.

The effect of light quality on fluorescence compared with control samples is summed up in Tables 3.4.1.1 and 3.4.1.2 .

	Location of fluorescence			
	Chloroplast	Diffuse cytoplasm	Filaments cytoplasm	Total
Low light	-	-	+	-
White light	++	+	-	+
Blue light	+	++	-	+
Red light	+	++	-	++

Table 3.4.1.1 Location of fluorescence under the influence of light quality (+ = increase, ++ = strong increase, - = decrease, -- = strong decrease, (-) values not clear.)

	Location of fluorescence in the presence of 2iP			
	Chloroplast	Diffuse cytoplasm	Filaments cytoplasm	Total
Low light	-	+	+	-
White light	++	+	++	+
Blue light	-	-	-	+
Red light	+	++	++	++

Table 3.4.1.2 Location of fluorescence under the influence of light quality in the presence of 2iP (+ = increase, ++ = strong increase, - = decrease, -- = strong decrease, (-) values not clear.)

3.5. Influence of FtsZ inhibiting drugs on protonemal cell growth of *P. patens* cell lines

3.5.1. Influence of Zantrin Z3 on growth of *P. patens* cell lines

Z3 is a small molecule that inhibits bacterial cell division by stabilising the FtsZ protein in a Taxol like fashion. Moss cells treated with Z3 should show a strong effect on wild type, a somewhat muted effect on overexpression lines and either a very strong effect, or no effect at all on FtsZ1-2 knock out cell line.
Treatment with Z3 led to a strong plasmolysis effect in all three cell lines. Yet measurements indicate that cell division took place none the less. The cells looked very stressed, yet when treated with Z3.
FtsZ1-2 ox cell line produced even, smooth cells walls, without constrictions at the cross walls. Maybe caused by declining turgor pressure, a wavy shape for the overexpression cells also occurred. Plasmolysis did not bunch up the chloroplasts in a plasma tube, since the plasmolysis effect was much weaker than in wild type cells. This made it possible to observe, that the chloroplasts were no longer aligned in an orderly fashion, but lying inside the plasma as if their support was cut. Macrochloroplasts were not observed. Caulonema were neither induced nor found at all in the tested sample, even though there were early and a few late stages of caulonema in the control samples.

Wild type cells had turned a dark green color, resulting from the concentration of their chloroplasts into a shrinking plasma tube. Cell shape was mostly short and barrel shaped, but also bloated cells and clustered growth did occur, which was reminiscent of the growth pattern of the knock out cell line.

ΔFtsZ1-2 cell line often grew in short cell files of four or less cells. Bloated and clustered round cells were also abundant in the samples. The controls showed their typical filamentous growth with interspaced bloated cells and strange branching behavior. Bloated and clustered cells did not show any branch-initials, branching seemed to be inhibited.

Diagram 3.5.1.1 shows, that the average cell length of the overexpression line and wild type cells were reduced compared to control cells. In the case of FtsZ1-2 ox line by 25% from 55.4 µm with a standard deviation of 14.55 to 40.9µm ± 12.9 µm in Z3 treated samples. The average length of wild type was reduced by about a third in comparison to control cells, from 47.8 µm (standard deviation of 17.1 µm) to 31.5 µm (± 12.9 µm). Z3 treatment showed no significant effect on the average length of FtsZ1-2 knock out cells. Control cells had an average length of 44.2 µm (± 17.0 µm) and Z3 treated samples grew on average 44.5 µm long (standard deviation of 18.7 µm).

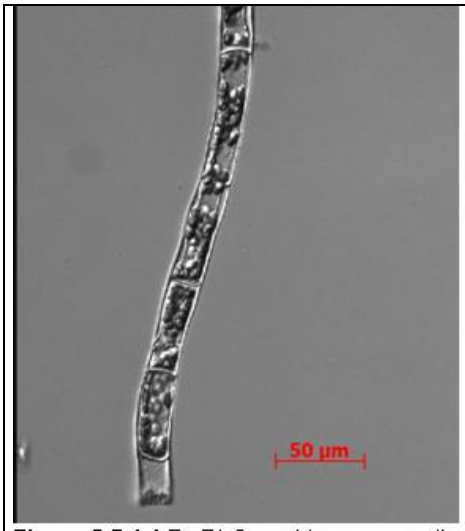

Figure 3.5.1.1 FtsZ1-2 ox chloronema cells treated with Z3 for 72h.

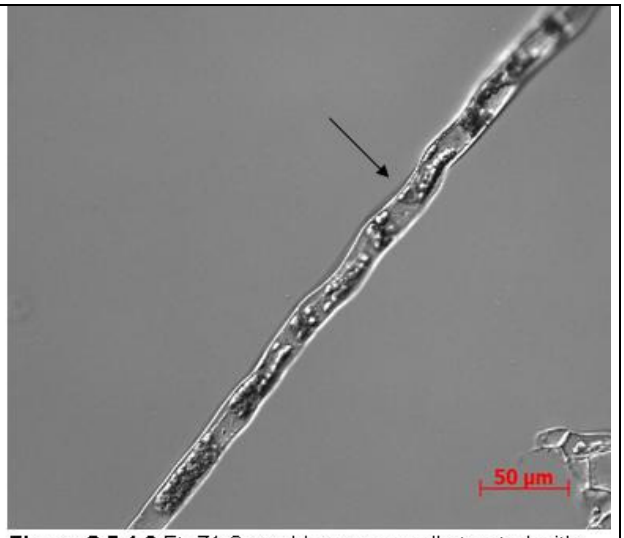

Figure 3.5.1.2 FtsZ1-2 ox chloronema cells treated with Z3 for 72h arrow indicating wavey cell wall deformation.

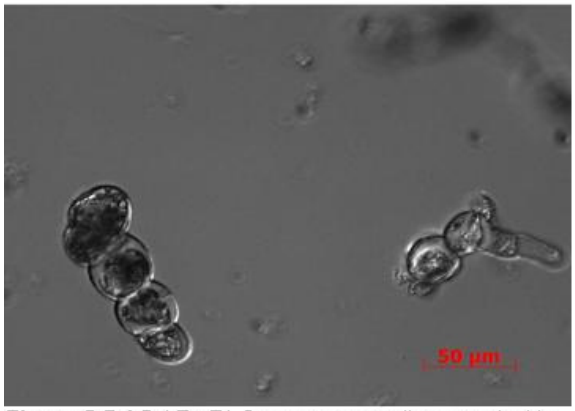

Figure 3.5.1.3 ΔFtsZ1-2 protonema cells treated with Z3 for 72h showing clustered growth of bloated cells.

Figure 3.5.1.4 ΔFtsZ1-2 protonema cells treated with Z3 for 72h showing unaffected filamentous growth.

Figure 3.5.1.5 Wild type cells treated with Z3 for 72h showing plasmolysed short cells and bloated cells.

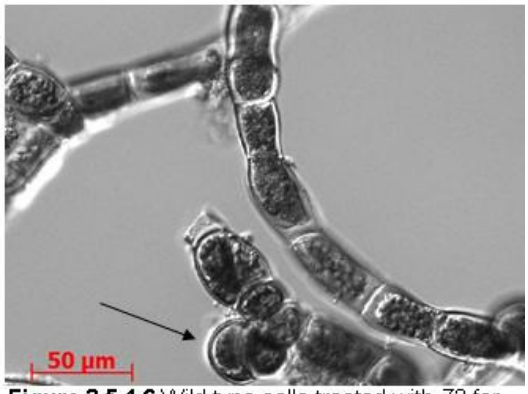

Figure 3.5.1.6 Wild type cells treated with Z3 for 72h showing plasmolysed clustered cells (arrow).

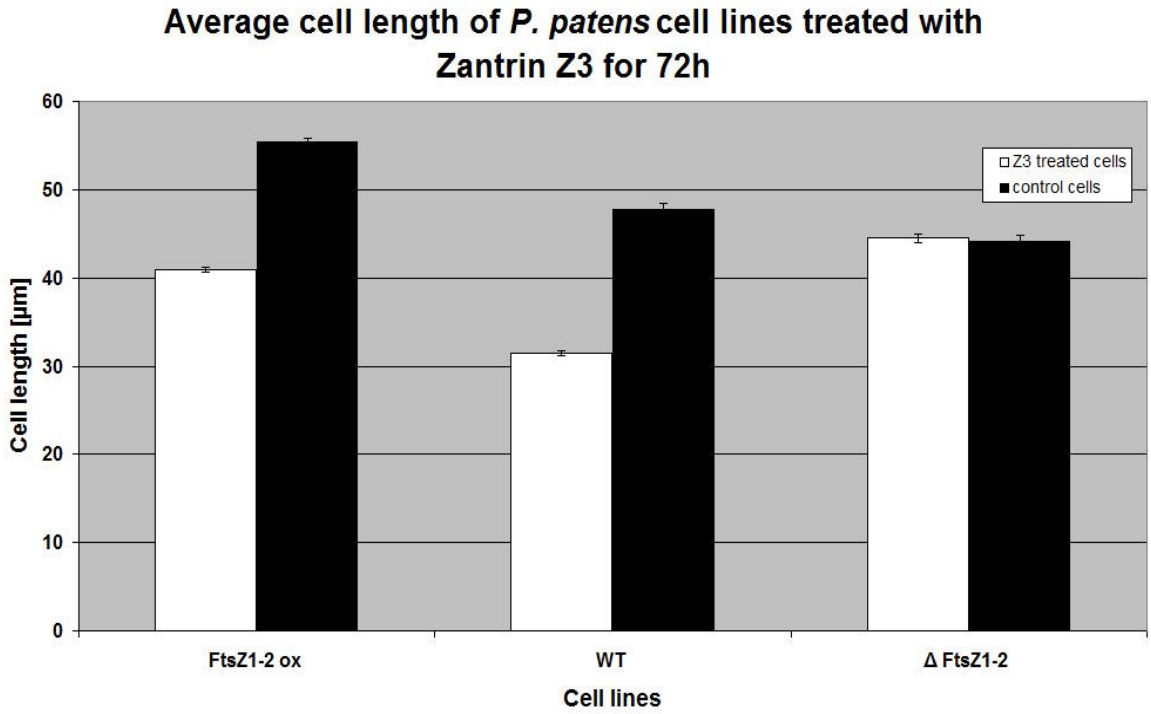

Diagram 3.5.1.1 Average cell length of *P. patens* cell lines treated with 5 µM Zantrin Z3 for 72 hours under low light conditions.

Comparison of the frequency of cell length of wild type and FtsZ1-2 ox cells treated with Z3 (Diagram 3.5.1.2) showed that in both cases the mode interval of the measured cells was [25- 35 µm]. Yet 34% of the measured wild type cells were shorter than that, when compared to FtsZ1-2 ox cells. Of this cell line only 8.5% of the measured cells were shorter than the interval containing the average. That means that the cell length of both cell lines is approximately normally distributed, but both are axially upset at the left flank, meaning that development of shorter cells is not possible.
The knock out line showed a slow increase in cell length frequency until the mode interval was reached, which was shifted by 10 µm compared with the other cell lines to [35- 45 µm], yet only 32% of the measured cells were shorter than the average. Distribution of cell length in this cell line came closest to resemble a normal distribution even so a slight tail region was also present. The observed knock out cell line also showed the longest cells when treated with Z3. 3.5% of the measured cells were longer than 85 µm, a cell length the other two lines did achieve, neither in the treated samples nor in the controls.
Diagram 3.5.1.3 shows the distribution of cell length under control conditions. The control samples of wild type showed approximately normal distribution around a mode interval at [45- 55 µm]. That means that the mode interval of the Z3 treated samples shifted about 20 µm to the left indicating decisively an inhibition in elongation and differentiation of the wild type cells.
Distribution of cell length of FtsZ1-2 ox cell lines under control conditions showed a mode interval that was shifted even more to the right (55- 65µm). This mode interval was reached through a soft slope on the left flank of the growth curve, indicating that differentiation had come to a close already. The steep decline on the right flank indicates that caulonema development was not yet fully induced in the sample. All in all the distribution resembles a slightly upset normal distribution or mirrored Poisson distribution.

The ΔFtsZ1-2 cell line mirrored the distribution of the overexpression line only the upset was positioned on the left flank instead of the right. The mode interval was at 25-35 µm, yet the slow incline on the right flank indicates only a slight hindrance in cell differentiation.

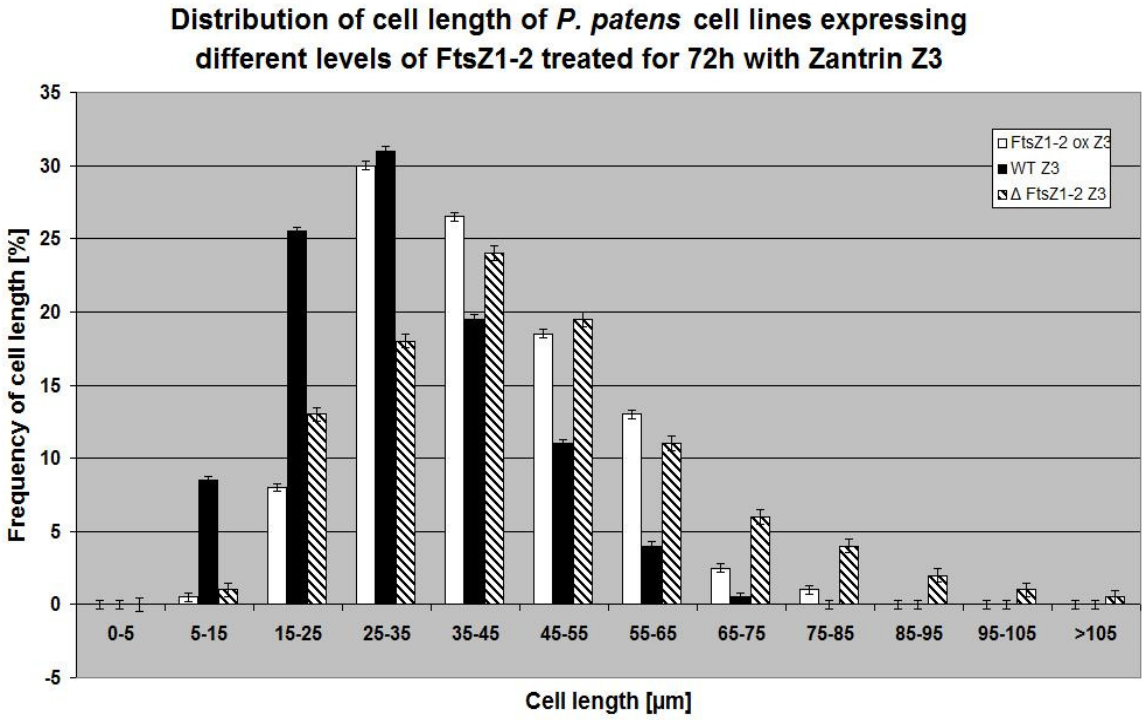

Diagram 3.5.1.2 Distribution of cell length of *P. patens* cell lines treated with 5 µM Zantrin Z3 for 72 hours under low light conditions.

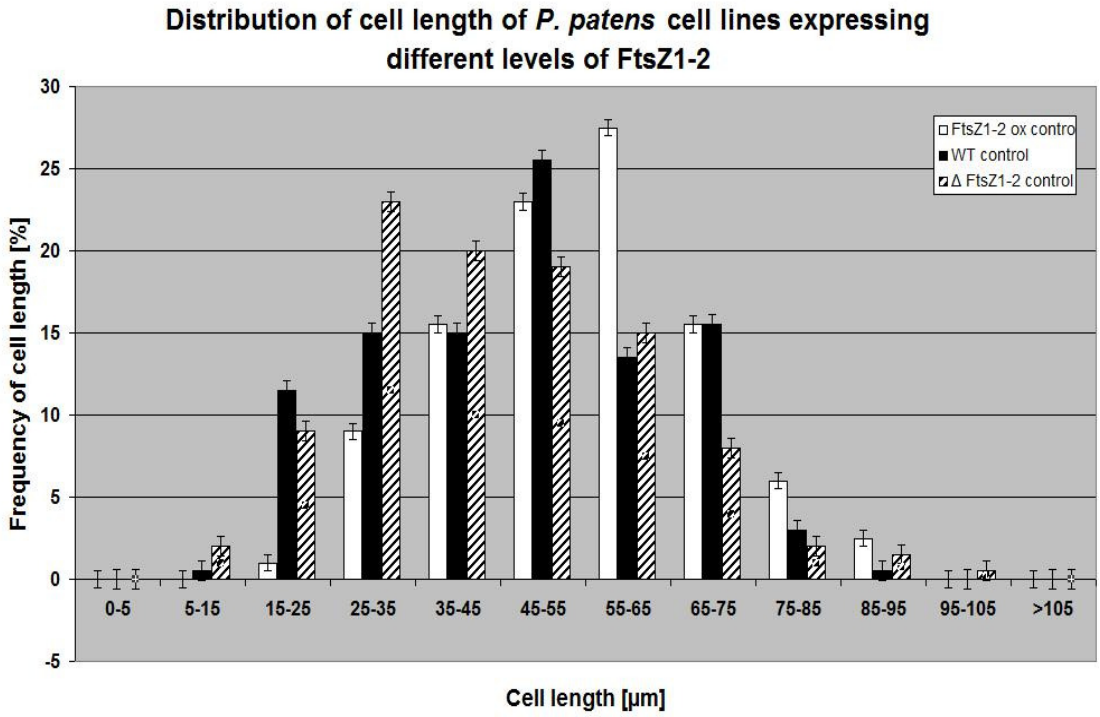

Diagram 3.5.1.3 Distribution of cell length of *P. patens* cell lines treated with DMSO for 72 hours under low light conditions.

As a conclusion it can be said that treatment with Z3 under low light conditions:

1. decreased cell length in the presence of FtsZ1-2
2. did not decrease cell length in the FtsZ1-2 knock out cell line and
3. inhibited caulonema differentiation.

3.5.2. Influence of Sanguinarine on growth of *P. patens* cell lines

Sanguinarine is the toxin of the Canadian blood root *Sanguinaria canadensis*. Its antibiotic properties are usually applied in tooth paste or mouth wash solutions. It inhibits FtsZ assembly through steric hindrance by binding in the vicinity of the GTP binding sight of the FtsZ monomer.

Cells treated with Sanguinarine for three days tended to secret a dens hyaline substance into the medium. This was especially apparent for wild type cells (Figure 3.5.2.3). The cells of the overexpression cell line and of the wild type appeared broader than normal (up to 32 µm istead of 25 µm). Apical cells were rounded and often broader at the tip than at the base (Figure 3.5.2.4).
ΔFtsZ1-2 cell line protonemata were not noticeably more deformed than usual, except for the shape of their chloroplasts (Figure 3.5.2.1). They were no longer noodle shaped but ball shaped or crumpled (Figure 3.5.2.2) and often clustered at one end of the cell.

Analysis of the average cell length showed that all three cell lines decreased in cell length. FtsZ1-2 ox cell line was reduced by about 6 µm from 61.5 µm in the control (± 15.6 µm) to 55.5 µm in the Sanguinarine treated samples (± 13.2 µm). The decline in cell length was most obvious in wild type cells, where the average cell length was reduced by 18.7 µm from an average of 45.5 µm (± 15.5 µm) to 25.8 µm (± 8.3 µm). Nearly as strong a decrease in average cell length appears with the knock out cell line. There the average cell length is reduced from 48.1 µm long control cells (standard deviation of 21.4 µm) to an average of 32.2 µm (± 14.2 µm).
The fact that all cell lines are affected by this treatment indicates a second target for Sanguinarine.
Analysis of distribution of cell length shows that the cells of the control samples of the overexpression line and wild type cells were mostly normal distributed. The mode interval of FtsZ1-2 ox cell line was at [55- 65 µm] indicating favored growth of chloronema. The left flank rises slowly and contains most of the mass of the sample. The steep decline at interval [75- 85 µm] hints at a beginning of caulonema differentiation that was not yet completed.
Wild type cells were normal distributed around the mode interval at [35- 45 µm] and with a maximal cell length of 85 µm. This fits the observation that growth was in favor of chloronema and that caulonemata were not readily observed.
Cells of the ΔFtsZ1-2 cell line again show an asymmetric growth curve. The mode interval was at [25- 35 µm]. A second peak appeared at [55- 65 µm] and a third one at 85- 95 µm. This can be explained with the fact, that the sample produced three populations of cell types. Cell files of short, straight or rounded cells were most often observed. Those cell files were interspaced with big bloated cells that were not as frequent as the short cells. On occasion long straight cells inside filaments were observed. These were comparatively rare yet present and obvious (Figure 3.5.2.7). This

implies ongoing differentiation for the growth curve and the sample in favor of chloronema and bracycytes.

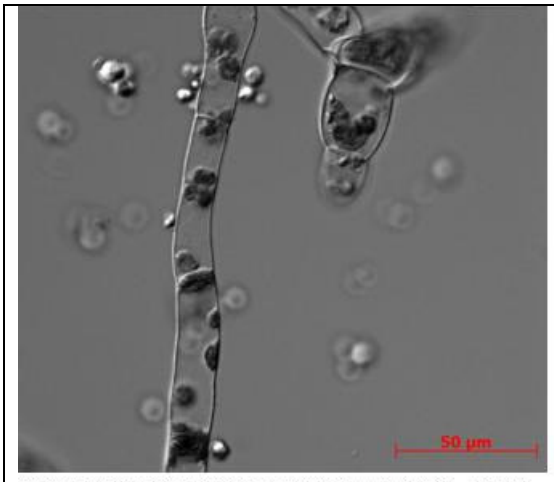

Figure 3.5.2.1 ΔFtsZ1-2 cells treated with 10 µM of Sanguinarine showing deformed chloroplasts

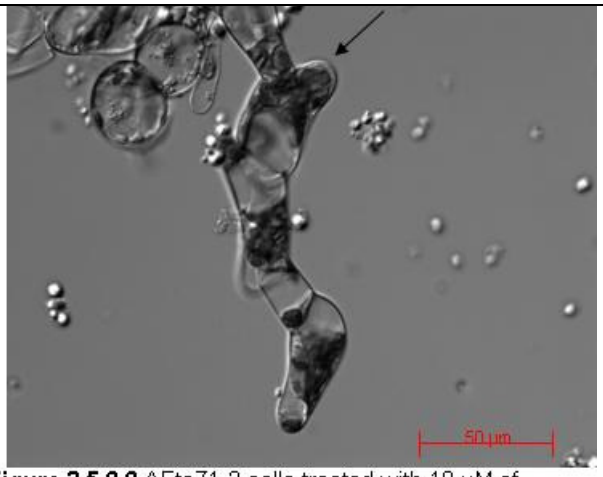

Figure 3.5.2.2 ΔFtsZ1-2 cells treated with 10 µM of Sanguinarine showing bloated and rounded cells with branch initials (arrow) Scale bar corresponds to 50µm

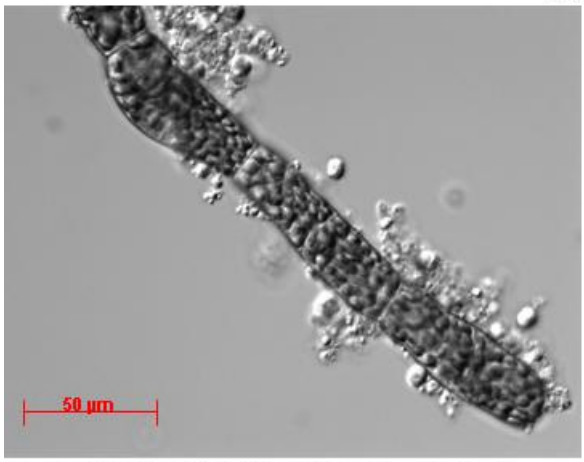

Figure 3.5.2.3 Wild type cells treated with 10 µM of Sanguinarine showing short cells and secret

Figure 3.5.2.4 Wild type cells treated with Sanguinarine showing short cells and deformed apical cells

Figure 3.5.2.5 FtsZ1-2 ox cells treated with 10 µM of Sanguinarine showing slantwise formeg cross walls and short cells. Scale bar corresponds to 50 µm

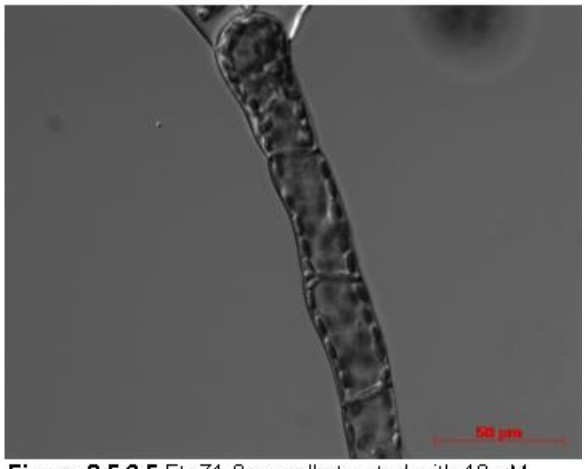

Figure 3.5.2.5 FtsZ1-2 ox cells treated with 10 µM of Sanguinarine showing slantwise formed cross walls and short cells. Scale bar corresponds to 50 µm

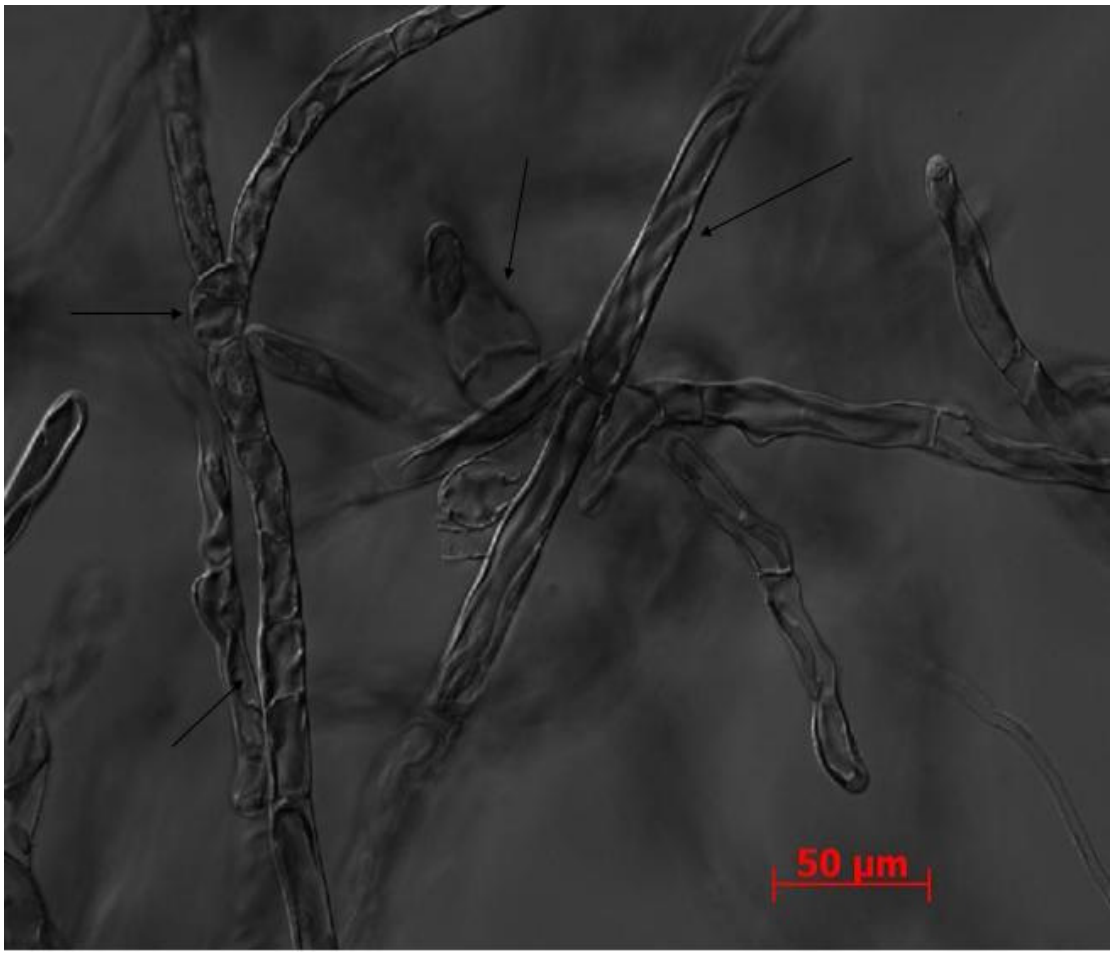

Figure 3.5.2.7 14 day old sample of ΔFtsZ1-2 cell line treated with DMSO for 3 days, showing cell files of short straight (arrow left bottom) or rounded cells (arrow top left). Big bloated cell (arrow middle) and long straight cells (right arrow).

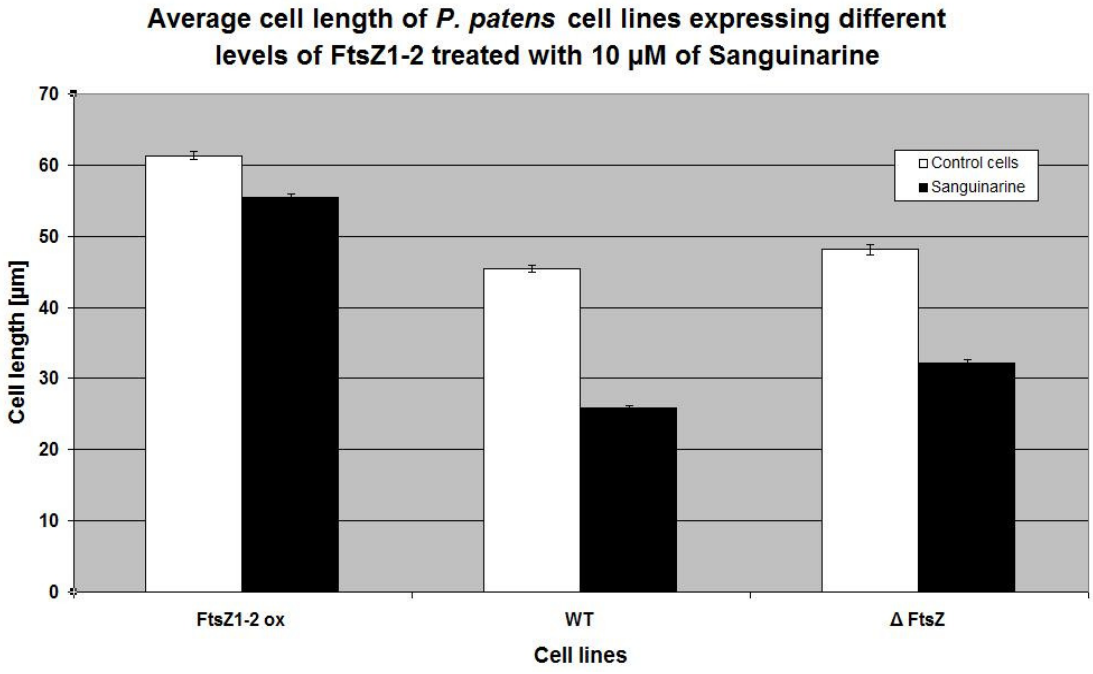

Diagram 3.5.2.1 Average cell length of three *P. patens* cell lines treated with 10 µM Sanguinarine for three days under low light conditions. Error bars indicate standard error (n =200).

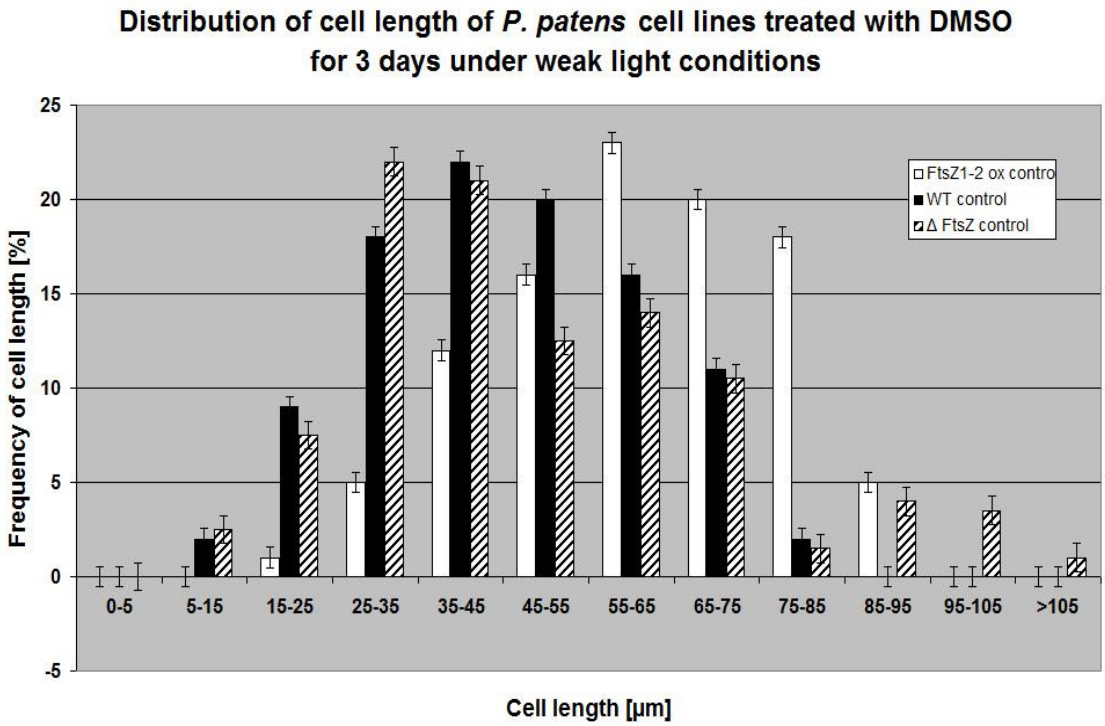

Diagram 3.5.2.2. Distribution of frequency of cell length in three *P. patens* cell lines expressing different levels of FtsZ1-2 under low light conditions, treated with 50 µl DMSO per 50 ml Knop medium for three days.

Treatment with 10 µM Sanguinarine had a strong effect on the distribution of cell length frequency of wild type cells. They were still normal distributed but the mode interval was shifted to the left (15- 35 µm). 80% of the mass of the sample is now found in the mode interval and the one adjoining the mode interval to the right. The range of the growth curve is reduced to a maximal cell length of [45- 55 µm].

ΔFtsZ1-2 cell line retains its mode interval at [25- 35 µm] after treatment with Sanguinarine but it now contains more than 25% of the measured cells. Also the second peak is reduced in mass and shifted to the left from interval [55- 65 µm] to interval [45- 55 µm]. The third peak disappears altogether. The range of the growth curve is reduced to a maximal cell length of 85 µm. This fits the observation that the long straight cells disappear from the sample. The distribution resembles now a disturbed normal distribution or a flat Poisson distribution.

FtsZ1-2 ox cell line also retained its mode interval at [55- 65 µm]. Further more the incline at the left flank and the range of the growth curve stayed the same after treatment with Sanguinarine. The difference is the loss of the shoulder at interval [75- 85 µm} and in the height of the mode interval which now contains nearly 34 % of the measured cells. This mass shift corresponds with the reduced average cell length noted earlier.

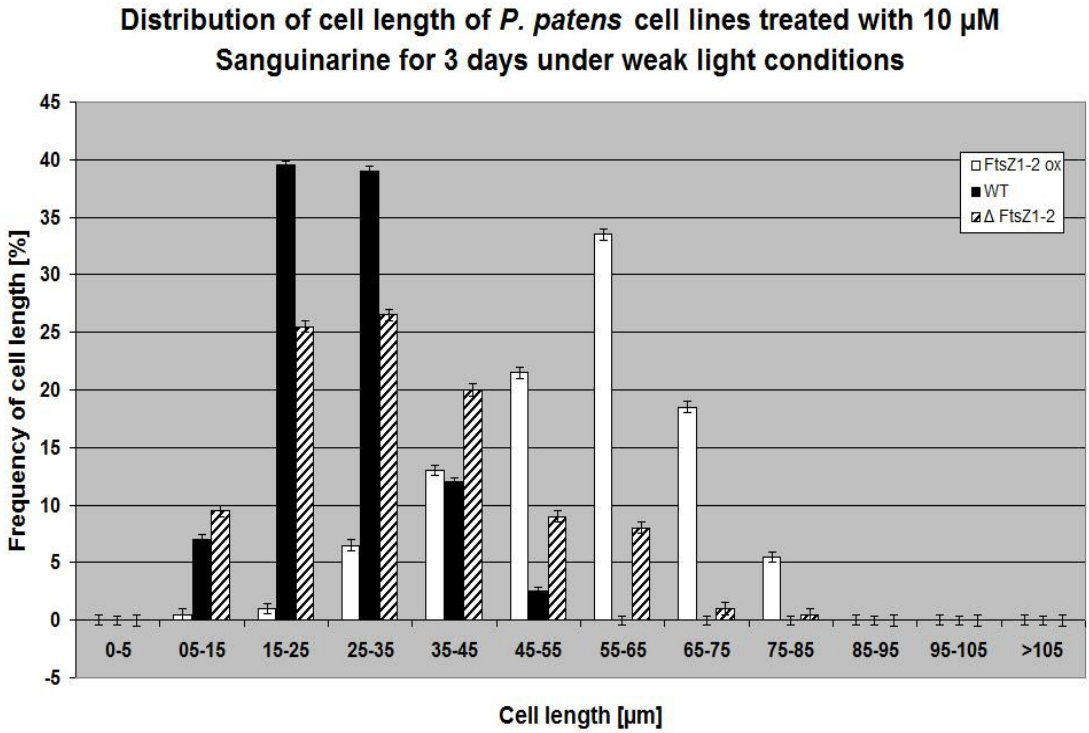

Diagram 3.5.2.3 Distribution of cell length frequency in three *P. patens* cell lines expressing different levels of FtsZ1-2 under low light conditions after 3 days of treatment with 10 µM Sanguinarine.

Concluding it can be said that treatment with Sanguinarine under low light conditions affected all three cell lines. It had a slight decreasing effect on the cell length of the overexpression cell line and a marked effect on the cell length of the knock out cell line and wild type. Caulonema development was inhibited in all three cell lines.

3.6. Influence of FtsZ inhibitors on FtsZ1-2 GFP fluorescence

3.6.1. Sanguinarine

14 day old protonema tissue samples of *P. patens* FtsZ1-2:GFP ox cell line with a FtsZ1-2:GFP filament content of 14% were incubated in an Eppendorf tube for 10 minutes in the presence of 20 µM Sanguinarine and then checked for fluorescence.
Since Sanguinarine shows a slight autofluorescence and accumulates especially at membranes, quantification in the chloroplast and cytoplasm compartments was difficult, since chloroplasts began to glow positively after 15 minutes of incubation and this fluorescence might have masked GFP fluorescence, which made quantification impossible.
Before autofluorescence started masking the GFP signal, no effect on fluorescent structures could be descerned. Of FtsZ1-2:GFP cytoplasmic filaments only strong bundles could be readily observed. This might account for the slight decrease in the observed fluorescence, which was 12% after 10 minutes. Yet another effect was observable after short term Sanguinarine treatment. The fluorescence of the cross walls

was strongly increased in nearly all observed cells of the overexpression cell line (Figure 3.6.1.1), where fluorescence had hitherto not been observable, except for rare cases, where filaments formed annular structures at the cross walls. Another observation was the distinct fluorescence of the outer wall, where slight bumps indicated emerging side branch initials (Figure 3.6.1.2).
When FtsZ1-2 knock out cells were treated with Sanguinarine for 10 minutes (as above) a strong fluorescence of the chloroplasts and the nuclei could be observed, but no cell wall fluorescence was observed (Figure 3.6.1.3). After longer incubation (30 min) fluorescence was also found at the outer walls and the cross walls.

Wild Type cells treated with Sanguinarine for 10 minutes showed a weak fluorescence of the cross walls and side branch initials (Figure 3.6.1.4) .

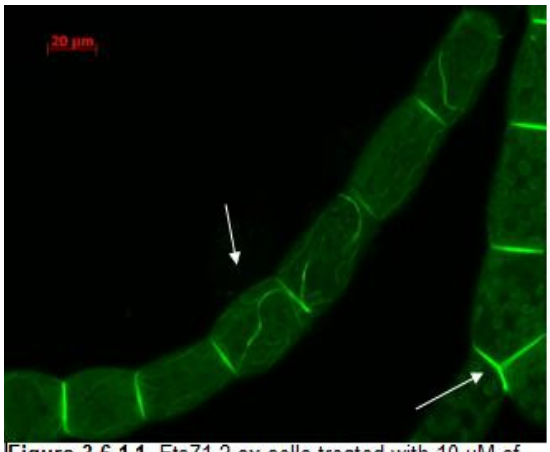

Figure 3.6.1.1 FtsZ1-2 ox cells treated with 10 µM of Sanguinarine showing FtsZ1-2 filaments (left arrow) and fluorescent cell walls (right arrow)

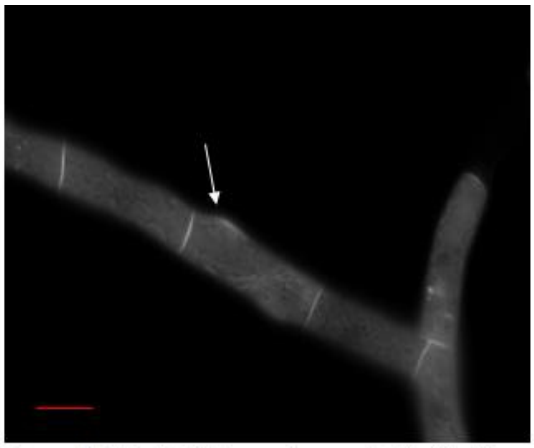

Figure 3.6.1.2 FtsZ1-2 ox cells treated with 10 µM of Sanguinarine showing early branch initials and fluorescent cross walls (white arrow) (Scale bar =20µm)

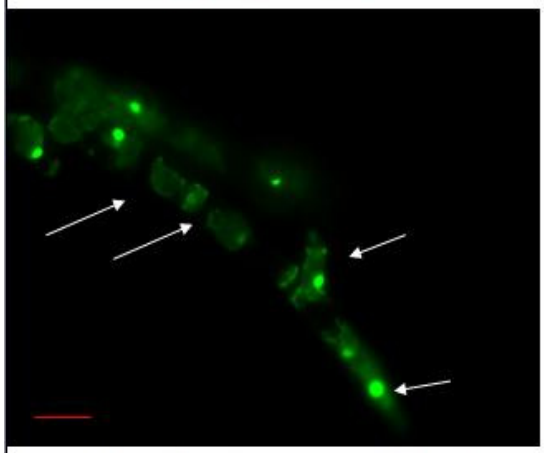

Figure 3.6.1.3 ΔFtsZ1-2 cells treated with 10 µM of Sanguinarine showing no fluorescent walls (left arrows) but strong fluorescence of nuclei and chloroplasts (right arrows)

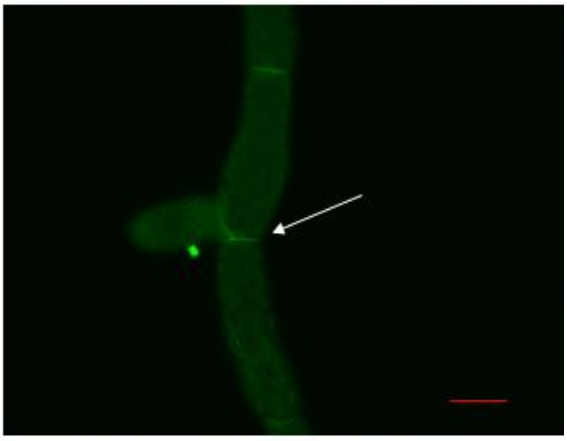

Figure 3.6.1.4 Wild type chloronema showing weak fluorescence at the cross walls after treatement with 10 µM of Sanguinarine (right arrows)

To check for an influence of Sanguinarine on FtsZ1-2 filament formation, 14 day old samples of the Ftsz1-2:GFP ox cell line were incubated in liquid culture in the presence of 10 µM Sanguinarine and with and without 20 µM 2iP for three days under strong light conditions. Control samples were treated likewise but with a corresponding amount of DMSO (50 µl DMSO to 50 ml Knop medium). 200 protonema were checked for fluorescence.

Since autofluorescence masked diffuse fluorescence, chloroplast fluorescence and thin cytoplasmic filaments, no dependable values of fluorescence development could be quantified.

Control cells showed a total of 16.5% of fluorescent filaments. Prior to incubation 14% FtsZ1-2:GFP filaments were observed. Sanguinarine treated samples showed a total of 13.5% fluorescent filaments. This would signify a slight inhibiting effect on FtsZ1-2:GFP filament formation in the absence of cytokinin. In the presence of 2iP, fluorescence increased in both samples, yet stronger in the untreated sample (22% fluorescent protonema) than in the one containing Sanguinarine (16%). This would mean Sanguinarine has a slight inhibiting effect in FtsZ1-2:GFP filament formation.

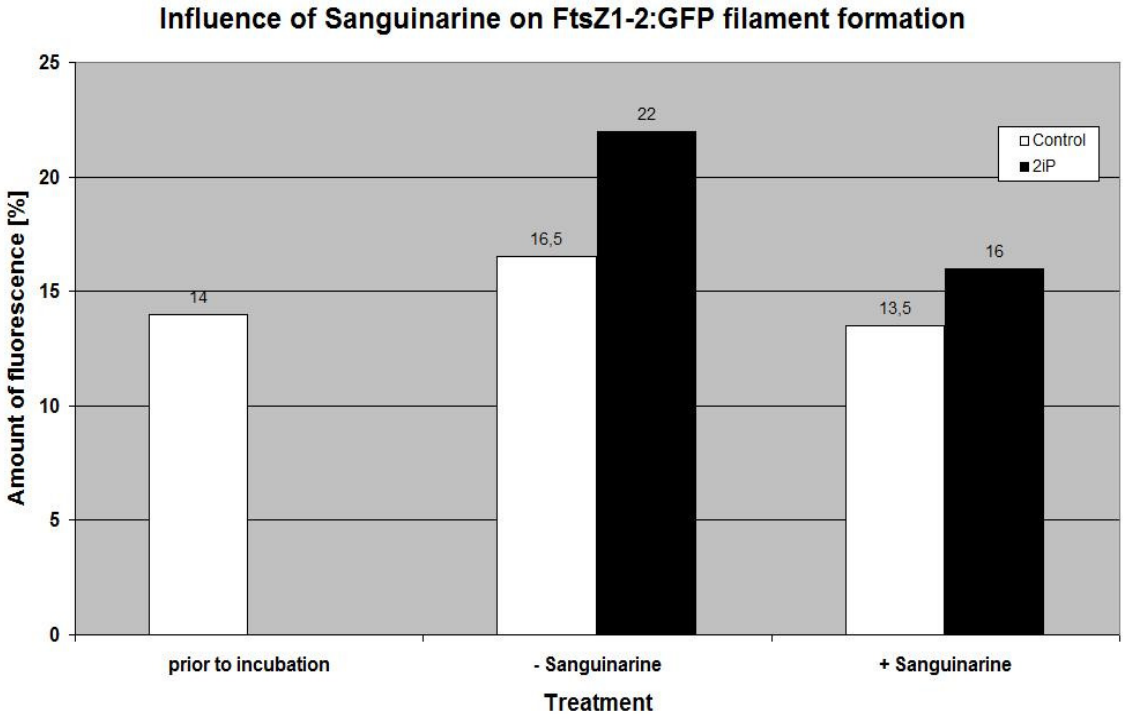

Diagram 3.6.1.1 Amount of GFP- fluorescence of FtsZ1-2 ox cell line grown under strong light conditions for three days in the presence and absence of 10 µM Sanguinarine (n = 200).

3.6.2. Influence of Zantrins on FtsZ1-2:GFP fluorescence

3.6.2.1. Influence of Z1 on FtsZ1-2:GFP fluorescence

Zantrin Z1 is a small molecule that inhibits FtsZ assembly in bacterial cells (RayChauduri 1999) and thus inhibits cell division.
To check for a direct effect of Zantrin Z1 on FtsZ1-2 filament fluorescence, 14 day old samples of the FtsZ1-2:GFP ox cell line were incubated in liquid culture in the presence of 10 µM of Z1 for 15, 30, 45 and 60 minutes and then 200 protonema were checked for fluorescence.
Control samples were treated likewise but with a corresponding amount of DMSO (2 µl DMSO to 1 ml Knop medium).

Treatment with Z1 led to a slight decrease of fluorescent filaments in the samples compared with control cells (Diagram 3.6.2.1.1). The maximal difference was 1.5% (after 60 min) compared to the amount directly after addition of Z1 (0 min). Since at 15 minutes and 30 minutes even a slight increase was observed, this might not be due to the influence of Z1, but the inhomogenity of the sample.

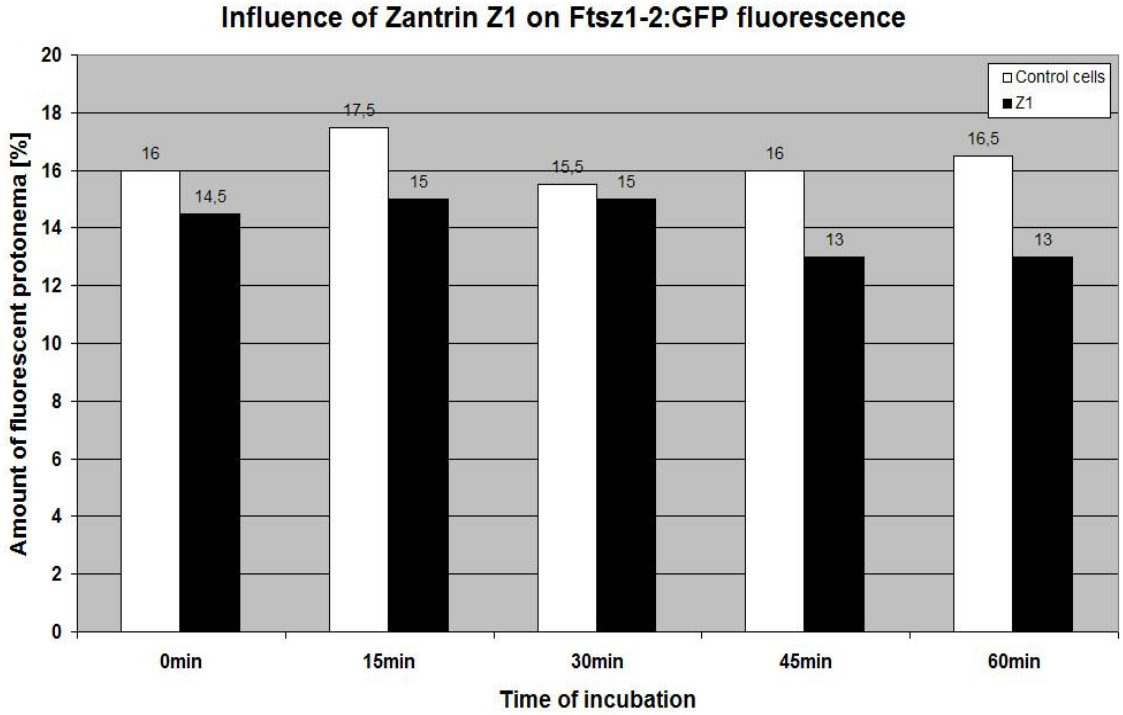

Diagram 3.6.2.1.1 Amount of fluorescent FtsZ1-2 filaments in FtsZ1-2:GFP ox cell line treated with 10 µM of Zantrin Z1 (n =200).

3.6.2.2. Influence of Z3 on FtsZ1-2:GFP fluorescence

Zantrin Z3 is a small molecule that prevents bacterial cells from dividing. It stabilizes FtsZ in bacterial cells in a manner similar to taxol and microtubules as shown by RayChauduri (1999).

To check for a direct effect of Zantrin Z3 on FtsZ1-2 filament fluorescence, 14 day old samples of the FtsZ1-2:GFP ox cell line were incubated in liquid culture in the presence of 10 µM of Z3 for 15, 30, 45 and 60 minutes and then 200 protonema were checked for fluorescence.
Control samples were treated likewise but with a corresponding amount of DMSO (2 µl DMSO to 1 ml Knop medium).

Treatment with Z3 led to a slight decrease in fluorescence compared with control samples at all checked time points. The greatest difference was visible after 15 minutes of incubation, when only 8% fluorescence could be found in the Z3 treated sample compared to 12% in the control.

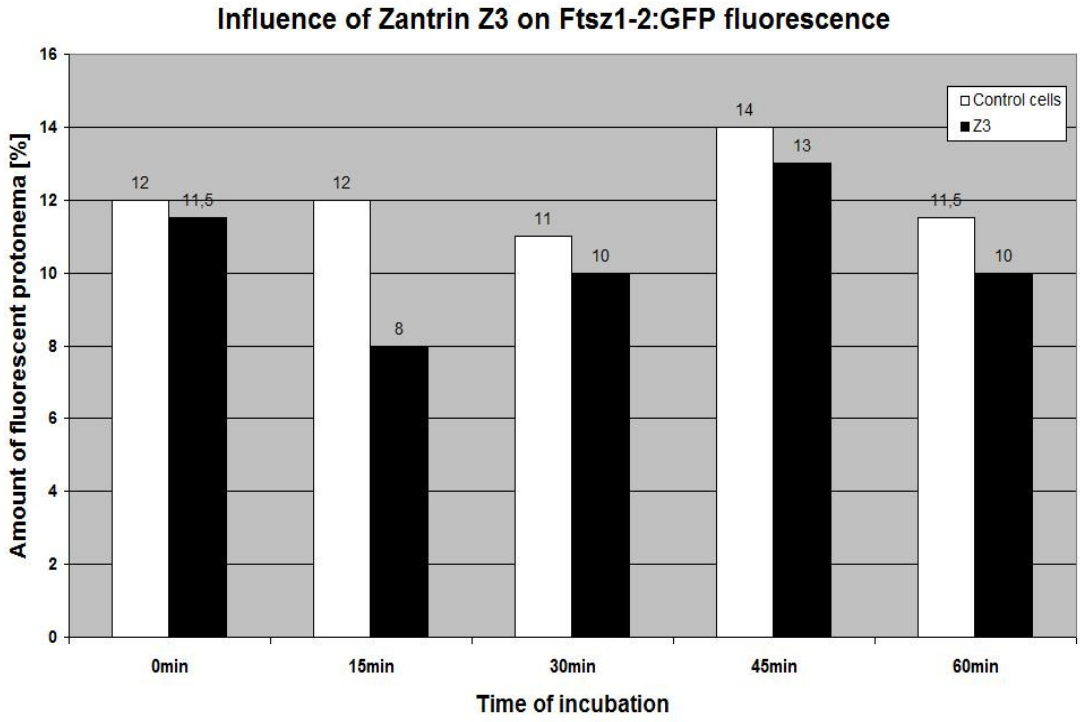

Diagram 3.6.2.2.1 Amount of fluorescent FtsZ1-2 filaments in FtsZ1-2:GFP ox cell line treated with 10 µM of Zantrin Z3 (n =200).

3.6.3. Influence of FtsZ-inhibitors on the assembly of tubulin *in vitro*

Even though the sequential homology between tubulin and FtsZ is not huge, the tertiary structure looks very similar and tubulin and FtsZ have important features in common, like the GTP binding motif, which confers the binding of the monomers to each other.
These facts make it necessary to test for interference of FtsZ inhibiting drugs with tubulin polymerization, before the results above can be conclusively interpreted. For this the protocol for microtubule coverslip nucleation assay (Zienicke, 2007) was adapted as described above.

Observation of the control samples showed that microtubules had formed in the presence of DMSO, thus confirming no influence of the solvent on polymerization (Figure 3.6.3.4).
The negative controls with colchicin only showed flakes of aggregated tubulin as expected. (Figure 3.6.3.5). Polymerization clearly did not take place.

Oryzalin which is not as effective on animal tubulins as on plant tubulins, did not inhibit assembly of tubulin, yet flaky aggregates also were formed and clung to the filaments (Figure 3.6.3.3).

Z3 did not inhibit polymerization at 10 µM. Thick bundles of microtubules as well as thin branched filaments could be observed (Figure 3.6.3.1).

Sanguinarine, that had been reported to interact with microtubules (Lopus and Panda 2006), did not inhibit polymerization, but formed thick bundles as well as very thin, straight and branching filaments (Figure 3.6.3.2).

Z1, which had led to rather strong effects in protonema cells, induced aggregation of tubulin, resembling colchicin treatment. In some samples the flakes were small and powdery and in others much bigger than in the colchicin treated samples (Figure 3.6.3.6).

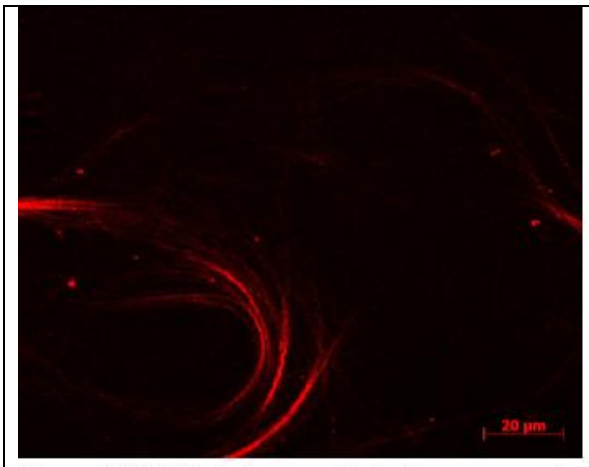

Figure 3.6.3.1 Tubulin assembly in the presence of 10 µM Z3

Figure 3.6.3.2 Tubulin assembly in the presence of 10 µM Sanguinarine

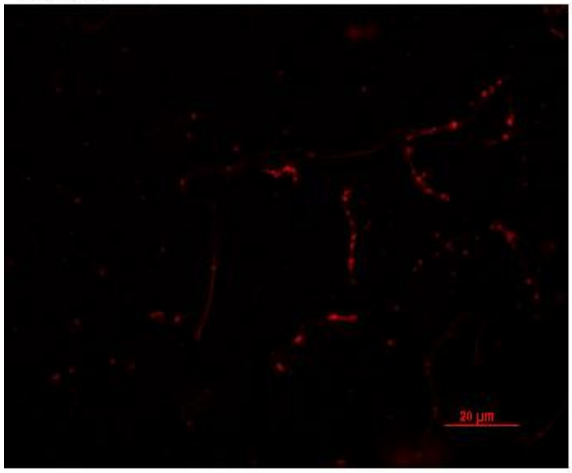

Figure 3.6.3.3 Tubulin assembly in the presence of 10 µM Oryzalin

Figure 3.6.3.4 Tubulin assembly in the presence of 10 µM DMSO

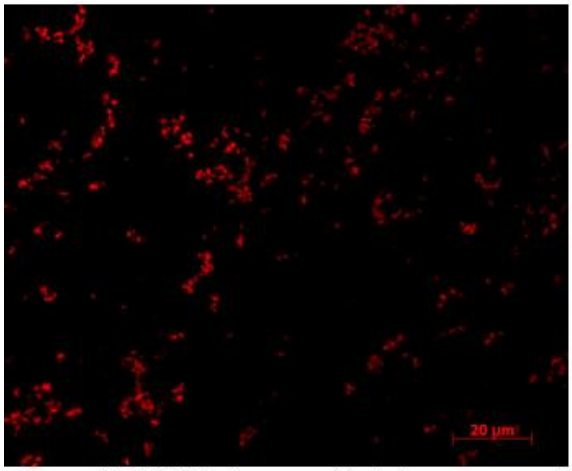

Figure 3.6.3.5 Tubulin assembly in the presence of 10 µM Colchicin

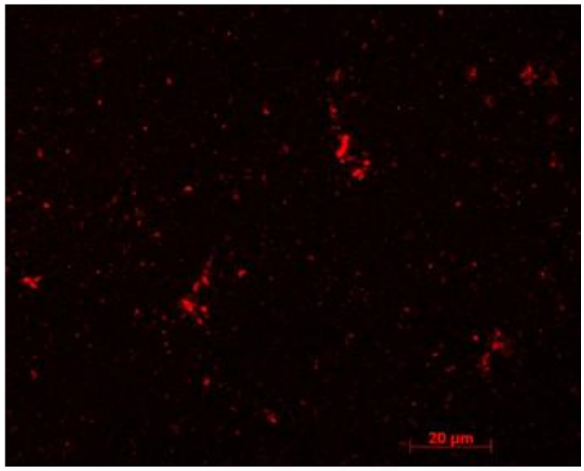

Figure 3.6.3.6 Tubulin assembly in the presence of 10 µM Z1

3.7. Influence of Ca^{2+} on growth of *P. patens* cell lines

Ca^{2+} ions were found to promote polymerisation of bacterial FtsZ filaments *in vitro* (Yu and Margolin 1997). To test for an influence of extracellular Ca^{2+} on cell growth of *P. patens* cell lines expressing different levels of FtsZ1-2, 14 day old samples of all three cell lines were incubated in Knop medium lacking Ca^{2+}. Additionally the medium included 5mM EGTA. Incubation lasted for four days under low light conditions.

Influence of intracellular Ca^{2+} transport was determined by incubating 14 day old samples of all three cell lines in Knop medium, for four days under low light conditions, with the addition of 50 µM Verapamil, a Ca^{2+} channel blocker.

As a control 14 day old samples of all three cell lines were grown for four days under low light conditions in Knop medium.

Wild type cells grew predominantly as chloronema under control conditions. Brachycytes were present (Diagram 3.7.1.2 first peak). The mode interval was at [45-55 µm]. Cells grew as long, barrel-shaped chloronema cells. Some early stage caulonemata could be found. The maximal cell length was 85 µm, also indicating growth in favor of chloronemata.

The FtsZ1-2 knock out cell line showed all three cell populations described earlier when grown under control conditions. Yet the amount of bloated and rounded cells was increased compared to samples described before. The mode interval was at [45- 55 µm]. A second peak at [65-75 µm] indicates the presence of elongated straight cells in an amount resembling previously observed ones (about 12 %). Cell files appeared knobbly and rounded, with many side branch initials. The knock out cell line showed the greatest range of cell length of the three cell lines with a maximal cell length of 140 µm.

Growth of FtsZ1-2 ox cell line was normally distributed under control conditions. The mode interval was at [55-65 µm]. Predominant growth was chloronema, yet early caulonema were abundantly formed and late stage caulonema were also observed, as was expected after 20 days without subcultivation. The cell shape was mostly barrel shaped. Chloroplast deformation was rarely observed.

Treatment with EGTA

Omission of Ca^{2+} from the medium and additional EGTA treatment led to the formation of long smooth cell walls, with a reduction of the constrictions at the cross walls, that give wild type and overexpression line their barrel shape under low light conditions (Figure 3.7.1.1 – 3.7.1.4). Predominant differentiation state was chloronema in both cell lines.
Wild type tissue formed brachycytes in the absence of Ca^{2+}, but their amount was greatly reduced compared to the control samples. The apical cells in wild type samples appeared shorter and broader. The amount of caulonema cells, especially late stage caulonema was reduced. Branching appeared to be normal for chloronema tissue.

ΔFtsZ1-2 cell line showed the greatest difference to the controls, when treated with EGTA. The amount of long, straight cells, together with the maximal cell length was strongly reduced. Also the amount of bloated cells was reduced compared to the control samples (data not quantified). The predominant growth form was in favor of cell files

containing short, straight cells with lots of side branch initials (Figure 3.7.1.5) and few interspaced bloated cells (Figure 3.7.1.6). Tmema were rare throughout the sample.

Figure 3.7.1 Wild type protonema treated with 5mM EGTA for four days showing brachycytes (arrow) and normal chloronema, scale bars corresponding to 50 µm

Figure 3.7.2 Wild type protonema treated with 5mM EGTA for four days showing short broad tipped apical cells (white arrow) , scale bar corresponding to 50 µm

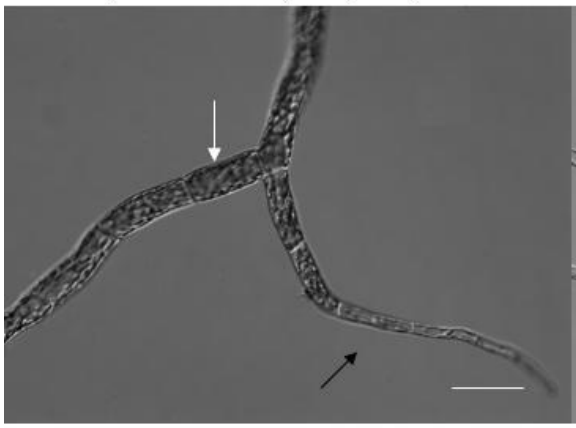

Figure 3.7.3 FtsZ1-2 ox protonema treated with 5mM EGTA for four days showing chloronema cells (white arrow) and early stage caulonema cells (black arrow)

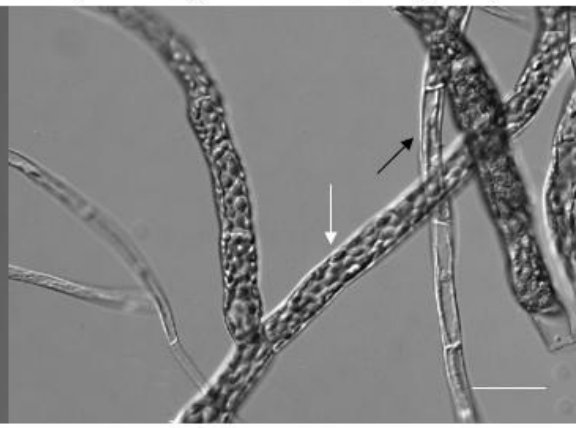

Figure 3.7.4 FtsZ1-2 ox protonema treated with 5mM EGTA for four days showing chloronema cells (white arrow) and early stage caulonema cells (black arrow)

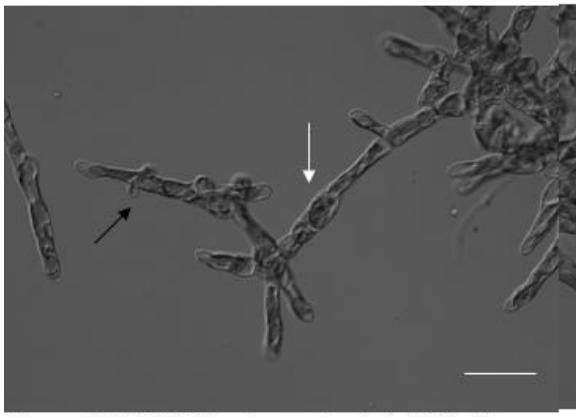

Figure 3.7.5 ΔFtsZ1-2 protonema treated with 5mM EGTA for four days showing filamentous short cells (white arrow) and branch initials (black arrow)

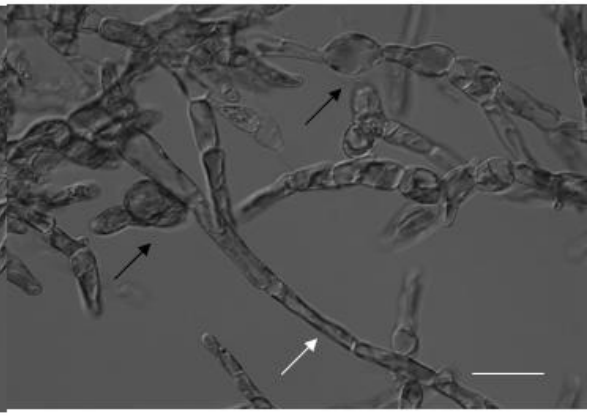

Figure 3.7.6 ΔFtsZ1-2 protonema treated with 5mM EGTA for four days showing filamentous long cells (white arrow) and bloated cells Scale bars indicate 50 µm

Treatment with EGTA caused the FtsZ1-2 ox cell line to grow mostly as chloronema. Caulonemata were present as early and late stage cell types, but markedly less so than in the control samples. Cell walls became regular and smooth, like in the wild type samples. The apical cells were not as broad at the apex as in the wild type cells, nor did they appear shorter than normal. Branching also appeared normal.

The average cell length of the knock out cell line, when treated with EGTA was 46.5 µm (± 20.3µm). Compared with the control sample (55 µm ± 22.0 µm) that means a reduction of the average cell length of 8.5 µm (Diagram 3.7.1.1). This is consistent with the observed disappearance of the "long cells" in the EGTA treated samples.
The greatest reduction in cell length was found in the FtsZ1-2 ox cell line samples, where the loss of caulonema production led to a reduction of the average cell length from 59.9 µm (± 16.08 µm) to the new average of 49,58 µm (± 14.28 µm). The comparative small standard deviation also stresses the reduction of short and long cells and is consitent with the observed reduction of caulonema differentiation in the absence of Ca^{2+}.
Wild type cells reacted to the absence of Ca^{2+} with the disappearance of brachycytes, which leads to the increase of the average cell length to 49.9 µm (± 13.22 µm) compared with control samples (46.0 µm ± 15.9 µm).

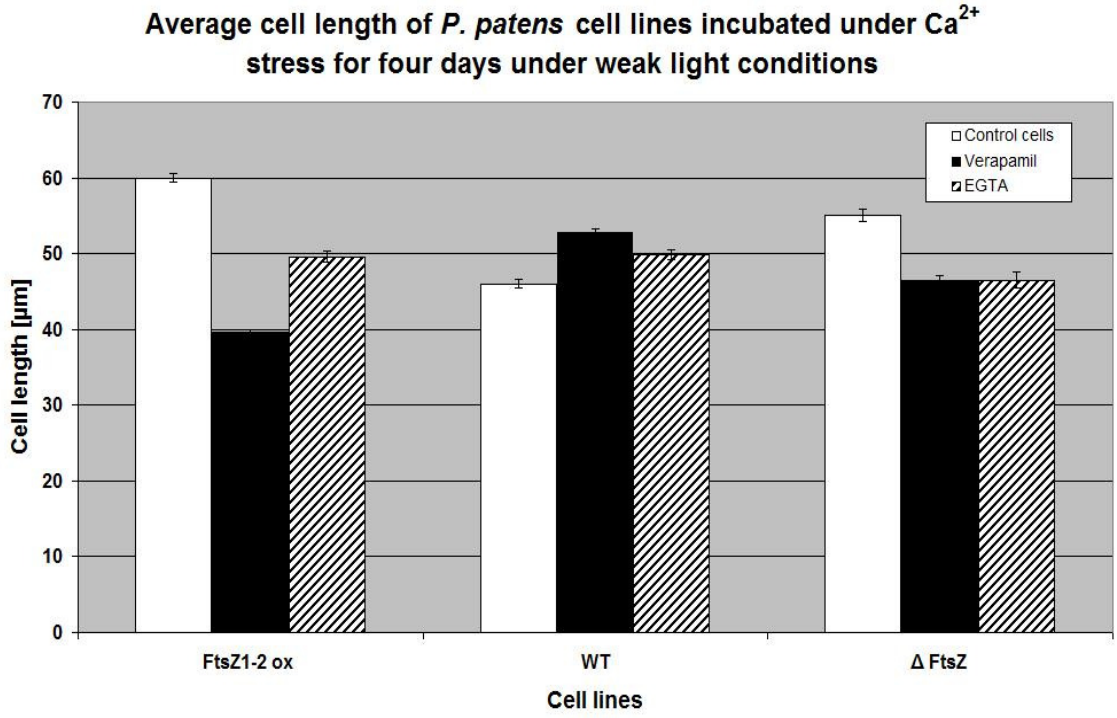

Diagram 3.7.1.1 Average cell length of protonema cells of *P. patens* under Ca^{2+} stress. Error bars indicate standard error (n = 200).

Wild type cells showed an approximately normal distribution of their cell length after treatment with EGTA. The range of the cell length did not change, but remained at a maximal length of 85 µm. The mode interval at [45- 55 µm] also stayed the same, but a mass shift from the left flank to the mode interval reduced the amount of cells in interval [25- 35 µm] from 19% in the control to 7.5% (Diagram 3.7.1.3) and increased the amount of cells that were between 45 to 55 µm long to 30% (23% in control sample). This is consistent with the observation of a reduced number of brachycytes and an increased amount of chloronema cells.

The range of cell length of the knock out line reduced as shown in Diagrams (3.7.1.2) and (3.7.1.3), indicating a strong reduction of the cell length throughout the sample. Maximal cell length was now 85 µm instead of 140 µm. The mass of the heavy tail region of the control samples shifted to the left, which fitted the observation of the increased number of cell files containing short rounded cells, as stated above.

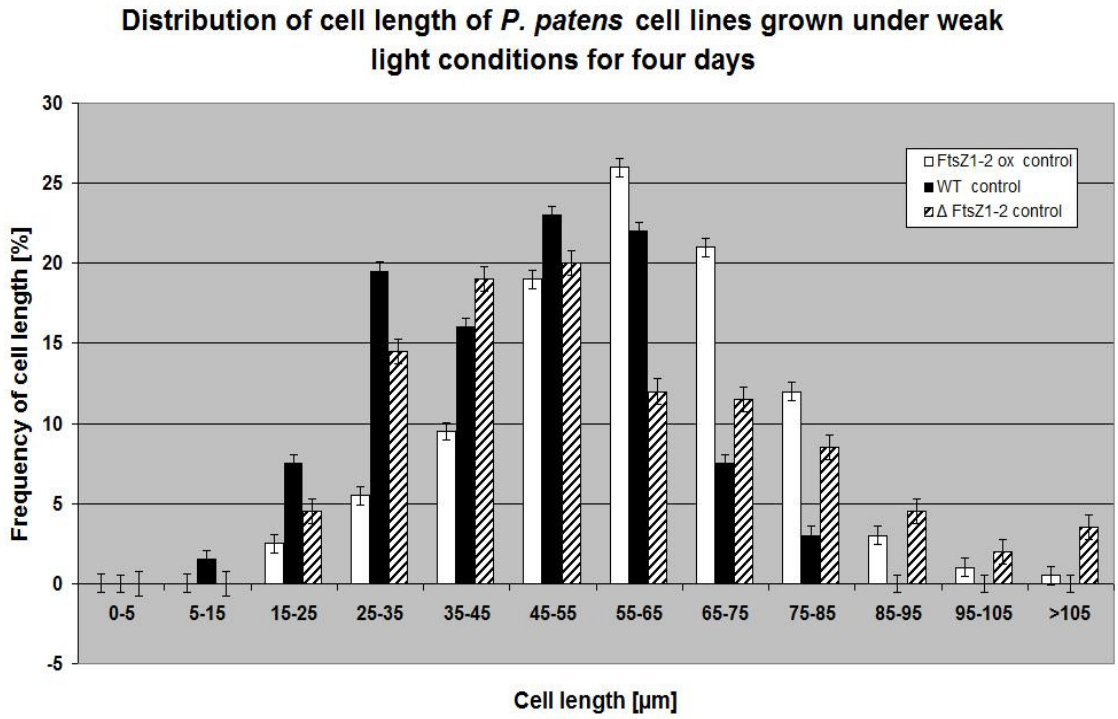

Diagram 3.7.1.2 Distribution of cell length of *P. patens* cell lines expressing different levels of FtsZ1-2 grown under low light conditions for four days.

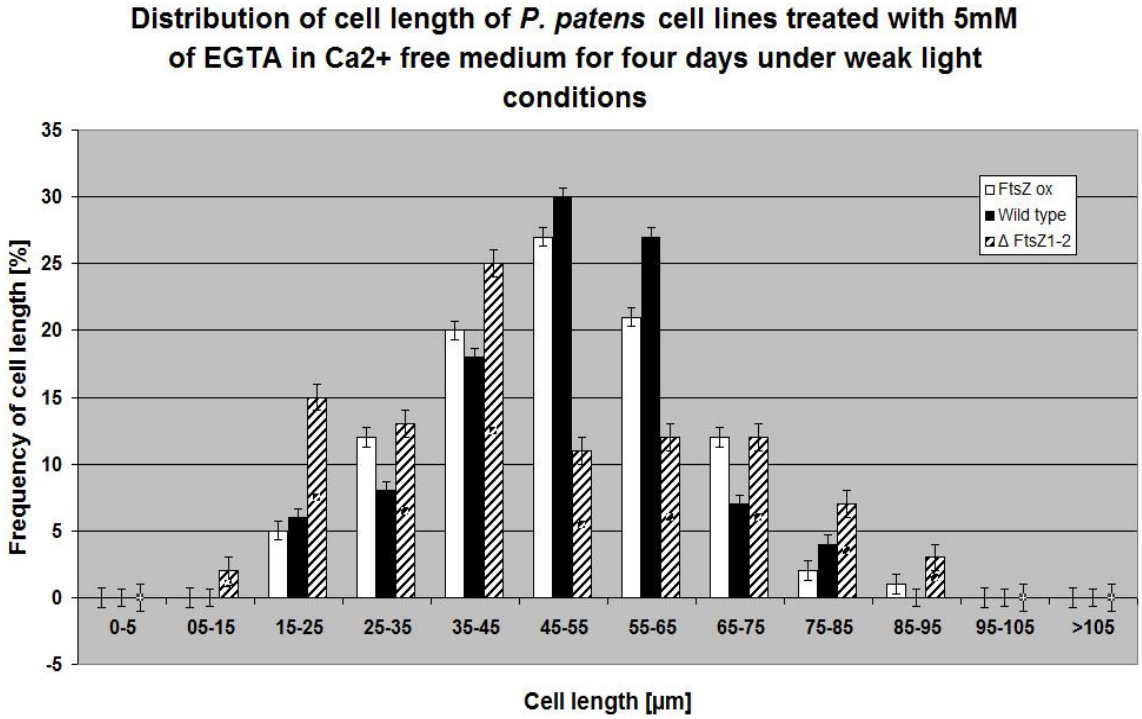

Diagram 3.7.1.3 Distribution of cell length of *P. patens* cell lines expressing different levels of FtsZ1-2 treated with 5mM of EGTA grown in Ca2+ free Knop medium under low light conditions for four days. Error bars indicate standard error (n =200)

The mode interval also shifted to the left (from 45- 55 µm in the control to 35- 45 µm). A second peak developed at [15- 25 µm]. After a steep decline following the mode interval a third peak appeared at [55-65 µm], corresponding to the decreased number of bloated cells.

The growth curve of FtsZ1-2 ox cell line again showed a normal distribution of cell length frequency, with a reduced range (85- 95 µm) compared to wild type. The mode interval was shifted to the left (45- 55 µm), indicating a decrease in the amount of caulonemata in the sample, as observed above. The symmetry of the curve (Diagram 3.7.1.3) also indicates the low amount of other developmental stages than chloronema in the absence of Ca^{2+}.

	Branching after EGTA treatment		
	K.O.	WT	OX
EGTA	55%	31%	23%
Control	42%	29%	22%

Table 3.7.1.1 Side-branches and side branch initials in [%]

Treatment with Verapamil

Treatment with Verapamil had a strong effect on the regularity of branching in the overexpression cell line. Whirls of three or more branches were formed at the same cell, usually in an apical position (Figure 3.7.1.7, Figure 3.7.1.8 and Figure 3.7.1.13). This behavior had hitherto only been seen in the knock out cell line. The predominant differentiation state was chloronema, caulonema were rarely observed. Brachyzytes and tmema cells were formed in great number, which led to a disruption of the cell files. Apart from the branching effect, the samples of the overexpression line strongly resembled the phenotype of wild type chloronema under low light conditions.

Wild type cells reacted with the production of elongated chloronema cells, which formed wavy cell files with pointy apical cells and a clear cytoplasm. In many cases the chloroplasts accumulated on one side of the cells, leaving whole patches of cytoplasm free of chloroplasts (Figure 3.7.1.11 and 3.7.1.12). In a few cases caulonema formation was observed. Branching seemed not to be affected by Verapamil treatment.

The ΔFtsZ1-2 cell line grew predominantly in dens whirls of thin cell files. Short and long cells could be observed, yet none of the cells were longer than 105 µm. Branch initials were numerous, but small (Figure 3.7.1.9). Bloated cells appeared even less often than in the EGTA treated samples, clearly stating that the bloating effect is Ca^{2+} dependent. Irregular branching effects as in the overexpression line samples also commonly occurred (Figure 3.7.1.10).

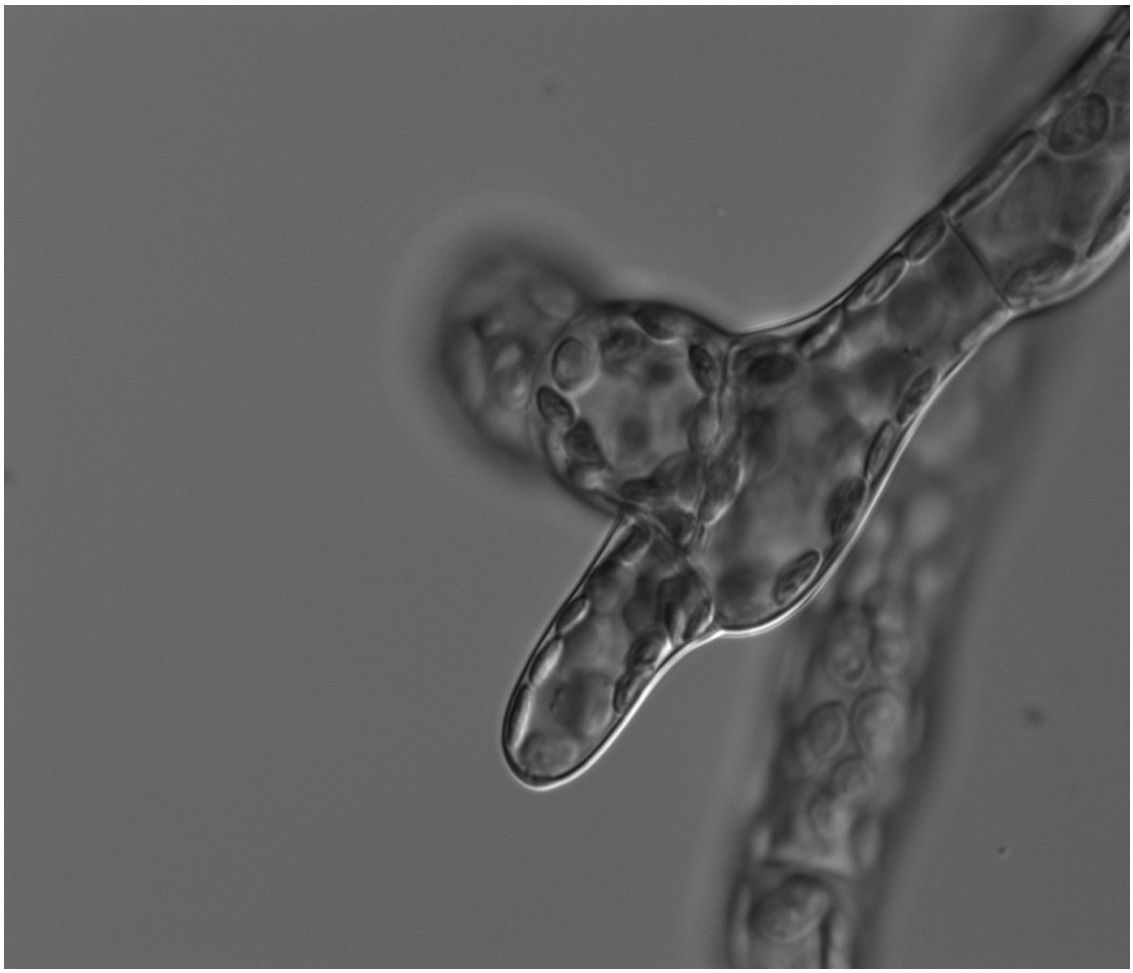

Figure 3.7.1.13 Irregular branching at the apical cell of FtsZ1-2 ox cell line chloronema in the presence of Verapamil for four days under low light conditions.

	Branching under Verapamil treatment		
	K.O.	WT	OX
Verapamil	54%	26%	27%
Control	37%	28%	20%

Table 3.7.1.2 Side-branches and side branch initials in [%]

Figure 3.7.1.7 FtsZ1-2 ox cells treated with 50µM Verapamil for 4 days showing irregular branching and rounded brachycytes (white arrow)

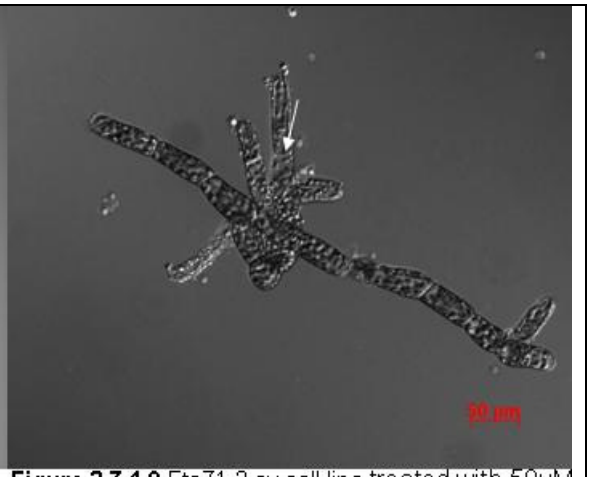

Figure 3.7.1.8 FtsZ1-2 ox cell line treated with 50µM Verapamil for 4 days showing irregular branching

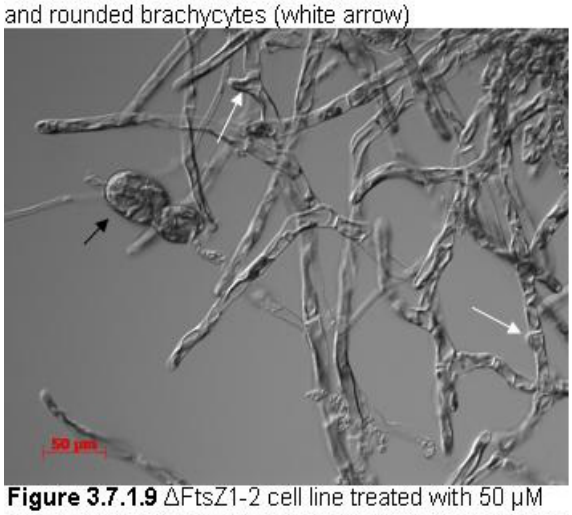

Figure 3.7.1.9 ΔFtsZ1-2 cell line treated with 50 µM Verapamil for 4 days showing long cells, bloated cells (black arrow) and branch initials (white arrows)

Figure 3.7.1.10 ΔFtsZ1-2 cell line treated with 50 µM Verapamil for 4 days showing irregular branching (white arrow) and short cells (black arrow)

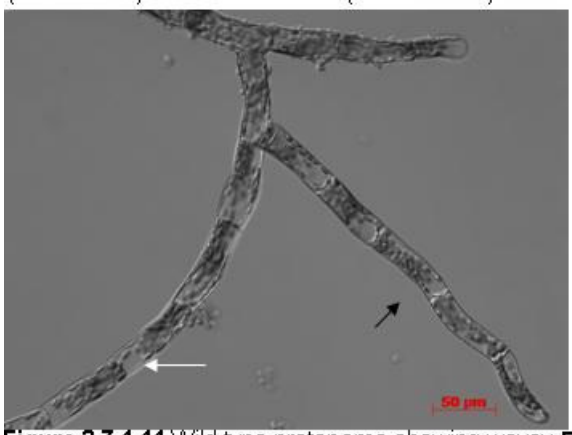

Figure 3.7.1.11 Wild type protonema showing wavey filamentous growth (black arrow) and chloroplast free clear patches of cytoplasm (white arrows)

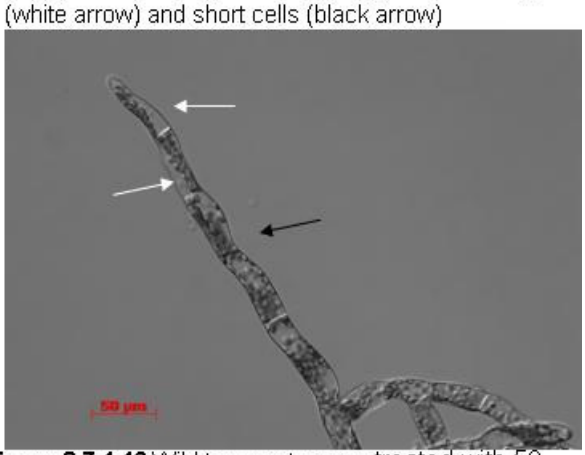

Figure 3.7.1.12 Wild type protonema treated with 50 µM Verapamil for 4 days showing wavey growth (black arrow) and chloroplast free cytoplasm (white arrows)

The distribution of the cell lengths fitted the above made observations. The normal distribution of the knock out cell line samples indicated the absence of at least one cell type population (round and bloated cells). Elongation took place, as the maximal cell length was 105 µm. The mode interval was shifted to the left compared with the

controls, which explains the reduced average cell length of 46.4 µm (±19.7 µm) (Diagram 3.7.1.1) to untreated samples.

The greatest reduction of cell length was observed in the overexpression cell line samples. The control cells were on average 59.9 µm long, while treatment with Verapamil led to an average cell length of 39,7 µm (±14.9 µm).
The growth curve of the FtsZ1-2 ox cell line shows, that the mode interval was shifted to the left compared to control (45- 55 µm to 25- 35 µm) which indicates massive physiological changes. This behavior mirrored the appearance of brachycytes as observed above. Even though the range of the sample is not reduced much (longest cell 99.9 µm instead of 106.5 in control), most of the mass is shifted to the left, which gives the growth curve the appearance of a Poisson distribution and further stresses the increase in brachycyte and chloronema development.

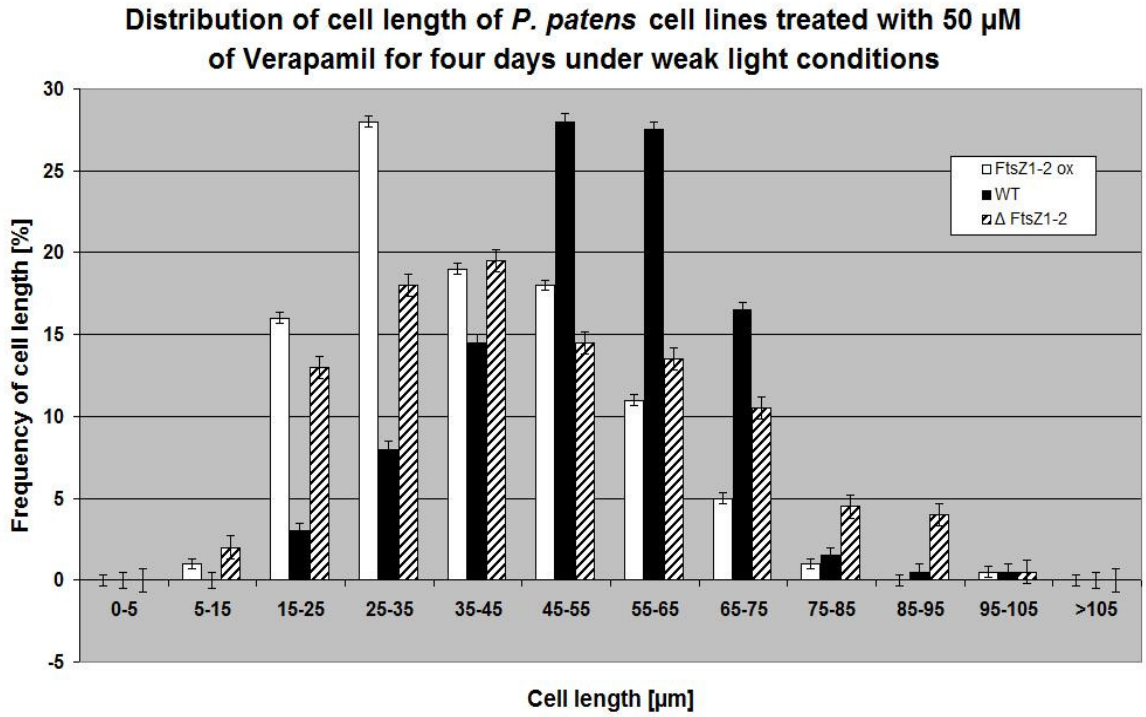

Diagram 3.7.1.4 Distribution of cell length of *P. patens* cell lines expressing different levels of FtsZ1-2 treated with 50 µM of Verapamil under low light conditions for four days. Error bars indicate standard error (n =200).

Wild type cells reacted differently to Verapamil treatment. For one they showed elongation of chloronema cells which caused an increase of the average cell length (52.8 µm to 46.0 µm). The small standard deviation of 13.4 µm indicates the concentration of most of the cells around the mode interval of [45- 55 µm]. The growth curve shows that the range of the cell length distribution is increased to a maximal cell length of 105 µm, which reflects the observed caulonema development.

3.7.1. FtsZ1-2:GFP fluorescence under influence of EGTA and Verapamil

To see if fluorescence of the FtsZ1-2:GFP cell line was affected by Ca^{2+} depletion, 200 protonemata per sample of both preparations were examined. Neither inside of chloroplasts nor in the cytoplasm could filamentous structures be observed. In the case of EGTA 7% of the protonemata showed diffuse fluorescence. The Verapamil treated samples showed 8% of protonemata with diffuse fluorescence. In both cases the fluorescence might not be GFP fluorescence, but could well be caused by dense cytoplasm of old chloronema cells, since observation with the RFP filter set also showed fluorescence. The cytoplasm appeared generally very clear except for the above mentioned examples.

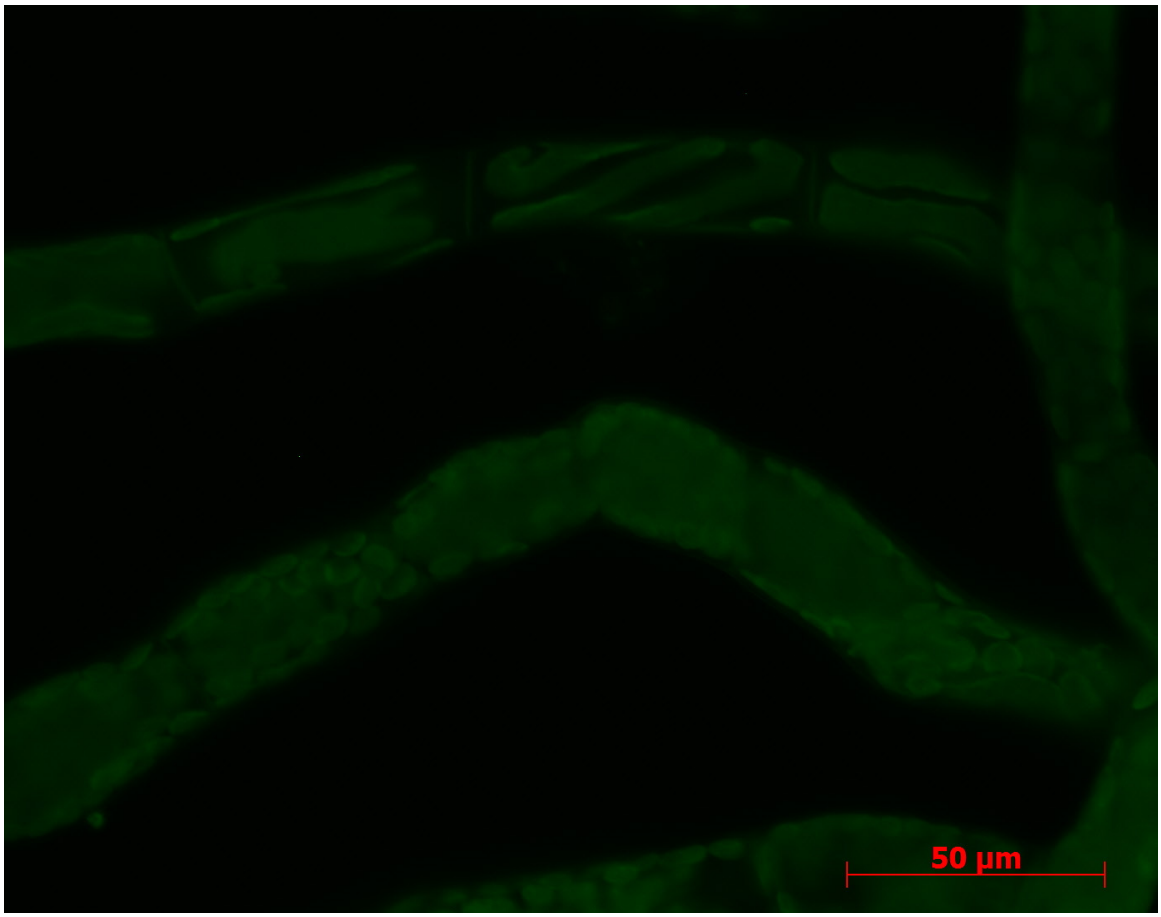

Figure 3.7.1.1 Protonema cells of FtsZ1-2:GFP ox cell line, treated with 5mM EGTA for 4 days under low light condition, showing no GFP fluorescence and very clear cytoplasm.

To summarize the results above it can be said, that treatment with EGTA attenuated low light symptoms in the wild type. Tmema formation in the knock out cell line was reduced but enhanced in the overexpression cell line. The FtsZ1-2 ox showed low light symptoms when treated with EGTA. Branching in wild type and FtsZ1-2 ox was normal. The knock out cell line showed irregular branching, reduction of brachycyte and tmema formation and increase in cell length. FtsZ1-2:GFP fluorescence was not detected.

Treatment with Verapamil caused irregular branching and low light intensity symptoms in the FtsZ1-2:GFP ox cell line. Wild type cells showed release from low light symptoms. Their cell length was increased and brachycyte and tmema formation was reduced. Branching behavior was normal. The knock out cell line showed irregular branching, reduction of brachycyte and tmema formation and increase in cell length.
FtsZ1-2:GFP fluorescence was not detected.

3.8. Interaction of FtsZ1-2 with the cytoskeleton

FtsZ1-2 has been shown to form filaments inside the cytoplasm (Kiesling *et al.* 2004). Since FtsZ is considered to be a member of the tubulin superfamily (Margolin 2005) it could be assumed that an interaction with the cytoskeleton, namely with tubulin and actin could exist, since those elements also form filamentous structures inside the same compartment. If an interaction exists, especially if direct binding of FtsZ molecules to the cytoskeleton occurs, cytoskeleton disrupting drugs should have an effect on fluorescent FtsZ filaments insofar, as either a change of filament shape should occur or the filaments should vanish altogether.
To test this, protonema of FtsZ1-2:GFP overexpression lines were incubated with cytoskeleton disrupting drugs, namely Oryzalin and Latrunculin B.

3.8.1. Interaction with tubulin

3.8.1.1. Effect of Oryzalin on filament stability

Oryzalin is a microtubule disrupting drug. It binds readily to tubulin dimers and thus inhibits further polymerisation of the existing microtubules. Since microtubules undergo treadmilling, all microtubules are depolymerised without the possibility to polymerize anew, so that after about half an hour all microtubules inside the cell disappear.

To see if depolymerisation of microtubules has an effect on cytoplasmic FtsZ filaments, a sample of protonema of FtsZ1-2:GFP overexpression lines was mounted on a glass slide. After an expressing cell was selected, a 50 µM solution of Oryzalin was added to the sample on the slide and pictures were taken every 5 minutes for 30 min.
The cytoplasmic FtsZ1-2:GFP filaments showed a slight fraying effect after 15 minutes of incubation (Figure 3.8.1.1.1), but otherwise only showed slight bleaching.

To test if longer incubation of *P. patens* FtsZ1-2:GFP overexpression lines with Oryzalin had an effect on FtsZ filament stability, agitated liquid cultures were treated with 10 µM Oryzalin (final concentration), incubated for 6 hours under low light conditions and then checked for fluorescence.
Prior to incubation 200 protonema were checked for fluorescent cytoplasmic bundles. After six hours the counting was repeated with the treated cells.
After incubation the amount of fluorescent filaments was slightly reduced from 14% prior to incubation to 12% in the presence of Oryzalin (Diagram 3.8.1.1.1). Since the protonema cells also showed a strong plasmolysis, this effect might be due to mechanical disruption rather than chemical interaction.

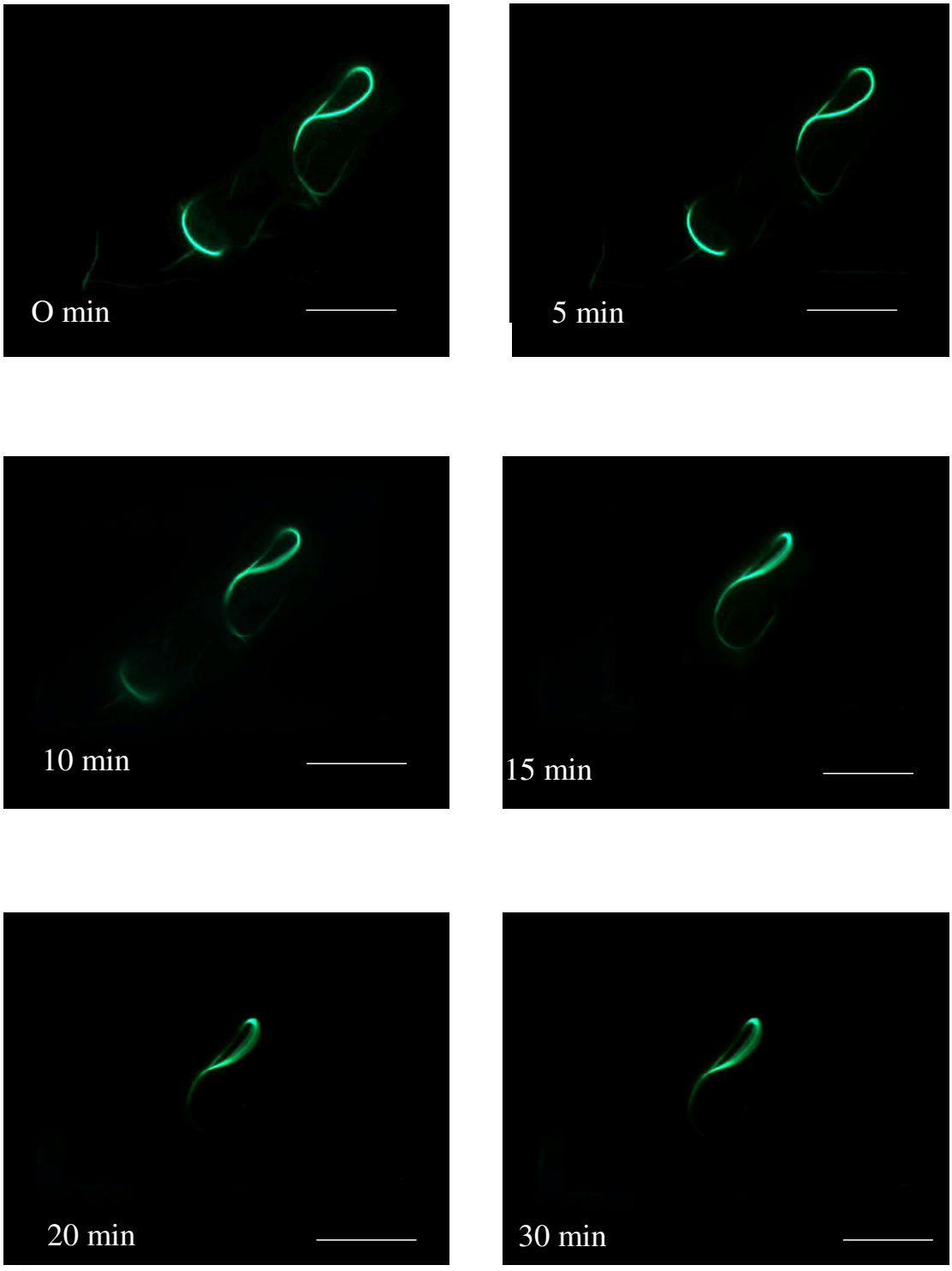

Figure 3.8.1.1.1 Image of FtsZ1-2:GFP filament inside the cytoplasm of *P. patens* protonema cell treated with Oryzalin for 30 minutes. Scale bars indicate 20 µm.

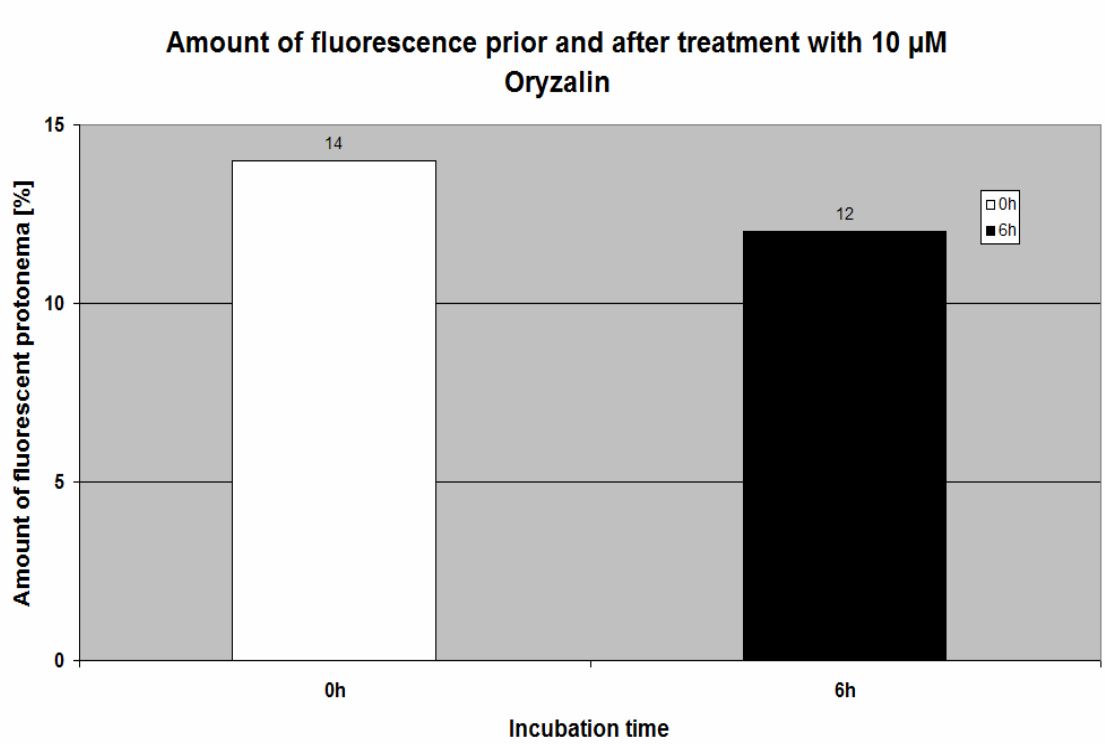

Diagram 3.8.1.1.1 FtsZ1-2:GFP ox cell line treated with 10 µM Oryzalin for 6 hours. Amount of protonema containing fluorescent cytoplasmic FtsZ1-2 filaments prior to incubation [0 h] and after incubation [6 h] (n =200).

As a conclusion it can be said, that Oryzalin had only a slight decreasing effect on FtsZ1-2:GFP fluorescence.

3.8.1.2. Effect of cold treatment on FtsZ1-2:GFP filament stability

Microtubules are dynamic sensitive structures that react to various exogenous and endogenous factors, like Ca^{2+} concentration or cold with depolymerization (Dawson, Lloyd 1987).

After incubation on ice the amount of fluorescent filaments was slightly reduced from 18% prior to incubation to 16% after 15 minutes, to 15% after 30 minutes (Diagram 3.8.1.2.1). Since Microtubules should have been completely depolymerized in the absence of stabilizing factors and FtsZ1-2 filaments were still visible, this is a strong indication of no direct binding between Microtubules and FtsZ1-2.

Diagram 3.8.1.2.1 shows, that cold treatment has only a slight decreasing effect on FtsZ1-2:GFP fluorescence.

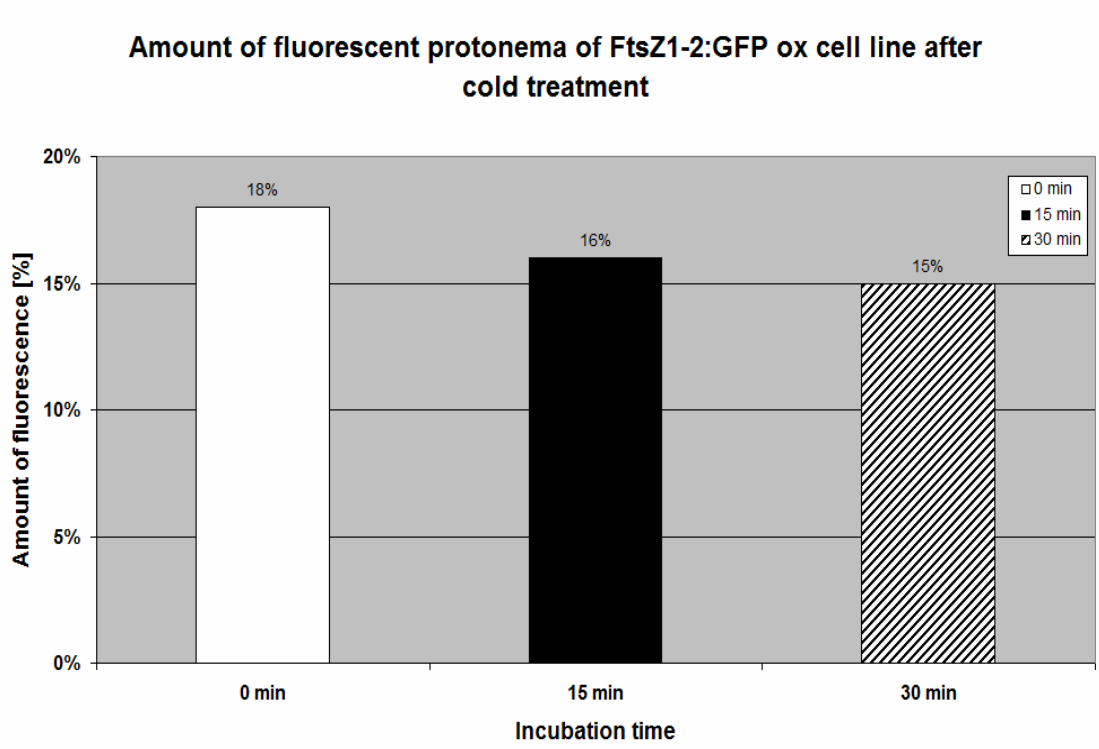

Diagram 3.8.1.2.1 FtsZ1-2:GFP ox cell line incubated on ice. Amount of protonema containing fluorescent cytoplasmic FtsZ1-2 filaments prior to incubation [0 h] and after 15 minutes and 30 minutes (n =200).

3.8.2. Interaction with Actin

3.8.2.1. Effect of Latrunculin B on filament stability

Latrunculin B is an F- actin disrupting drug, derived from the red sea sponge *Latrunculina magnifica*. It inhibits polymerisation of actin and disrupts microfilament organisation and cell growth (Spector *et al.* 1989)
A 5 µM solution of Latrunculin B dissolves actin filaments in BY-2 tobacco cells within 20 minutes (Dr. J. Maisch, verbal communication).

To see an effect on cytoplasmic FtsZ1-2:GFP filaments, a sample of 7 day old protonema of FtsZ1-2:GFP overexpression cell line was mounted on a glass slide. After an expressing cell was selected, a 5 µM solution of Latrunculin B was added to the sample and pictures were taken every 5 minutes for 45 minutes.
No effect on FtsZ1-2 filaments could be observed except for bleaching. After 45 minutes a strong plasmolysis had occurred, and the cell was dead, with the filament still visible, if somewhat weakly (Figure 3.8.2.1.1).

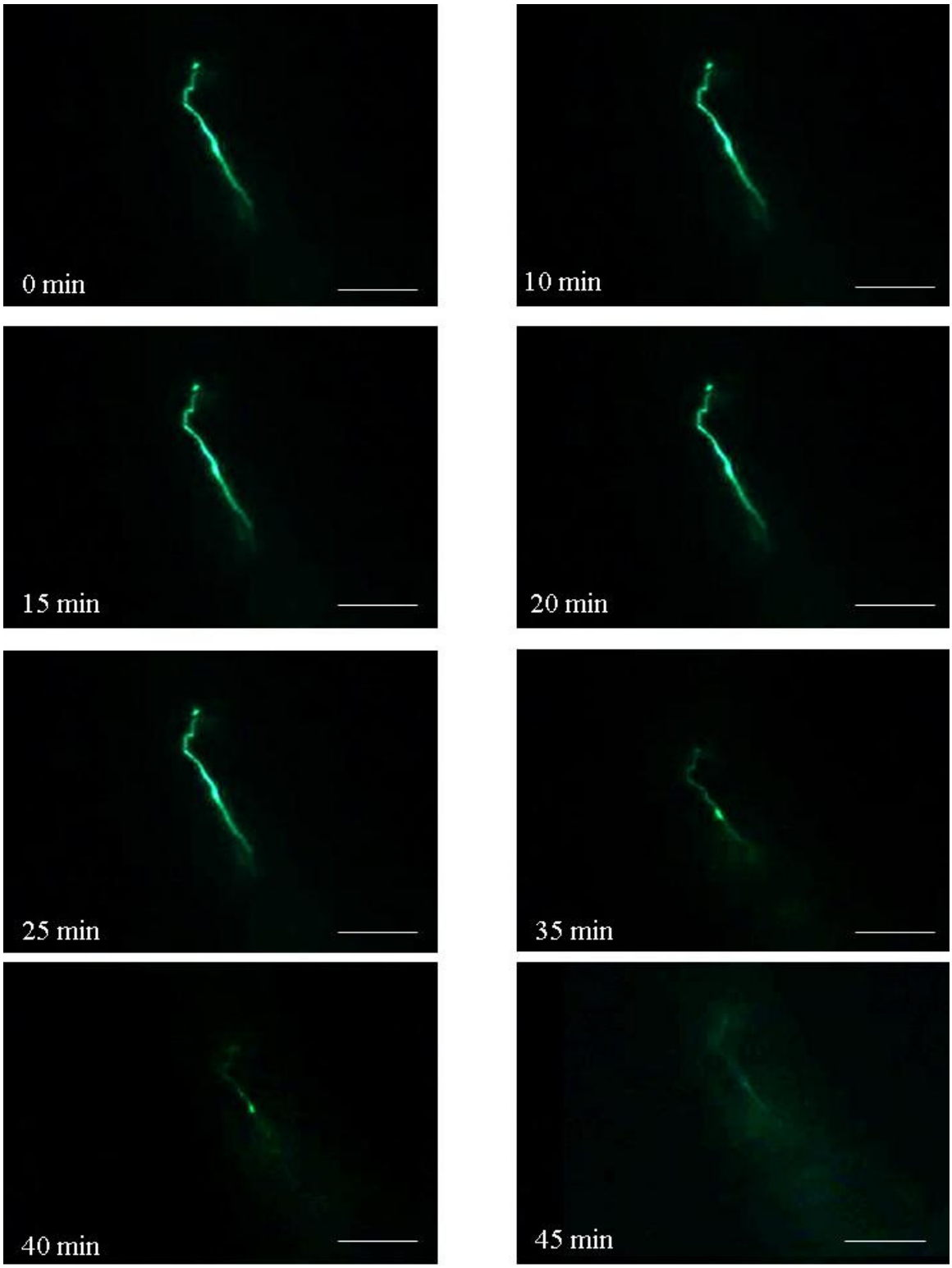

Figure 3.8.2.1 1 Image of FtsZ1-2:GFP filament inside the cytoplasm of *P. patens* protonema cell treated with Latrunculin B for 45 minutes. Scale bars indicate 20 µm

3.8.2.2. Effect of Latrunculin B on fluorescent filament induction

To test if Latrunculin B has an effect on the formation of cytoplasmic FtsZ1-2:GFP filaments, a sample of *P. patens* FtsZ1-2:GFP overexpression cell line grown under low light conditions for 10 days was treated with Latrunculin B at a final concentration of 1

µM and incubated under strong light conditions for 3 days. The control was also treated with Latrunculin B and incubated for 3 days under low light conditions, so that no increased filament induction could take place.
Of those cultures, samples were taken and 200 protonemata checked for fluorescence.

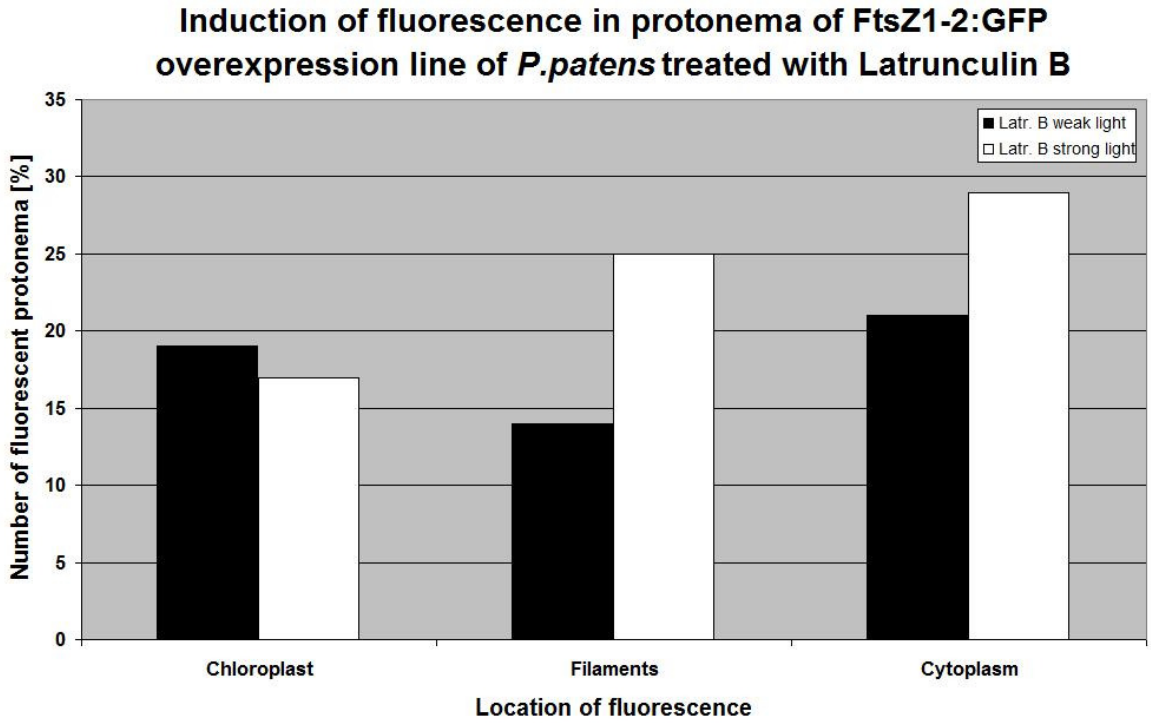

Diagram 3.8.2.2.1 Number of protonema of *P. patens* FtsZ1-2:GFP overexpression line treated with Latrunculin B for 3 days under strong light and low-light conditions.

After 3 days under strong light conditions induction of filament formation was not inhibited. 17% of the tested protonema contained chloroplasts with fluorescent structures, 29% showed a diffuse fluorescence inside the cytoplasm and 25% contained cytoplasmic FtsZ1-2:GFP filaments. The control showed 2% more protonema with fluorescent structures on chloroplasts, but only 21% protonema with diffuse fluorescence and only 14% protonema with cytoplasmic filaments inside the cytoplasm. This implies that the increase in fluorescent filaments under strong light conditions is not impaired by Latrunculin B.

As a summary of the results above it can be said that

1. Latrunculin B did not inhibit high light intensity induced FtsZ1-2:GFP filament formation.
2. Treatment with Latrunculin B had no disrupting effect on pre-existing FtsZ1-2:GFP filaments.

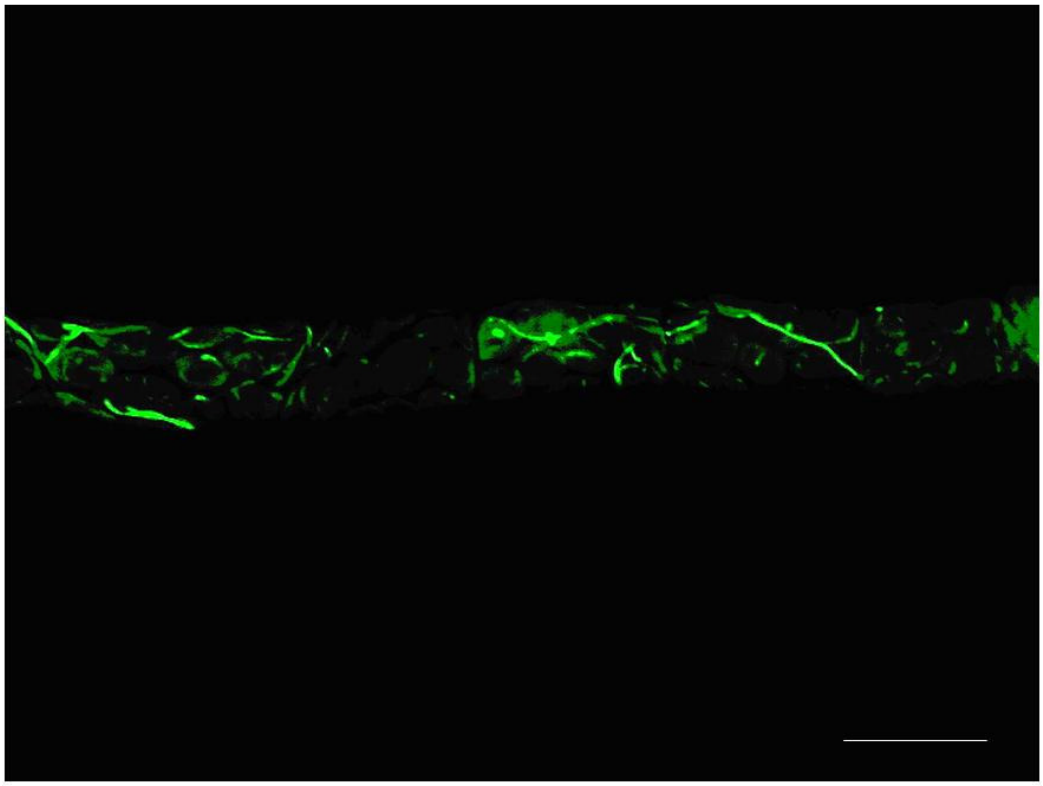

Figure 3.8.2.2.1 Renderimage of *P. patens* FtsZ1-2:GFP overexpression line treated with Latrunculin B for 3 days under low light. Scalebar corresponds to 20 µm.

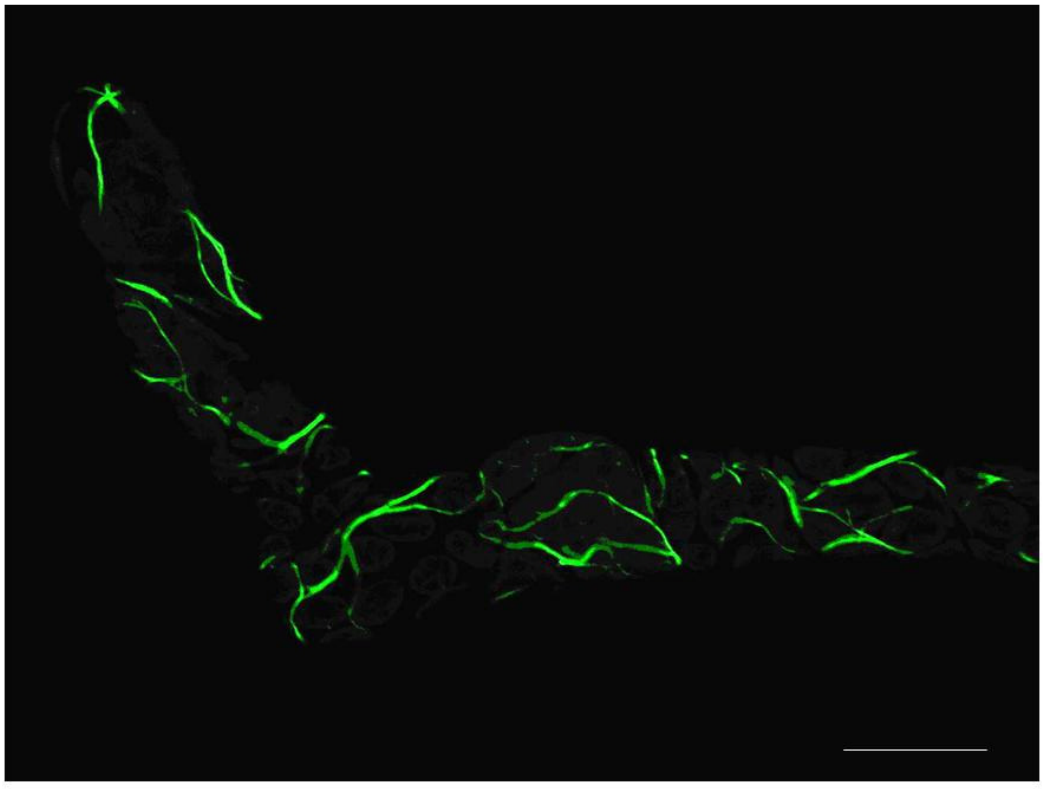

Figure 3.8.2.2.2 Renderimage of Protonema of *P. patens* FtsZ1-2:GFP overexpression line treated with Latrunculin B for 3 days under strong light conditions. Scalebar corresponds to 20 µm.

3.9. Summary of the results

Auxin

Under low light conditions the reduction of FtsZ1-2 concentration led to a decrease of chloronema cell length and the abundant production of brachycytes. The morphology of the knockout line was not visibly changed by treatment with auxin. Differentiation to caulonema was blocked in the presence of high amounts of exogenous auxin. Blocked auxin efflux additionally increased branch initial formation.

Cytokinin

In FtsZ1-2 over-expressing protonema cytokinin treatment reduced caulonema development when grown under low light intensity. In wild type protonema grown under low light intensity, cytokinin increased caulonema development
Exogenous cytokinin did not induce bud formation in the FtsZ1-2 knock out cell line after 6 days of incubation but reduced the amount of branching and increased cell length.
Exogenous Cytokinin decreased cell length in the protonema of the FtsZ1-2 overexpression line and wild type.

Abscisic acid

ABA treatment did not change cell morphology of ΔFtsZ1-2 protonema further except for an increased tmema formation and increased branch-initial formation. Overexpression of FtsZ1-2 attenuated ABA induced short cell formation.

Light intensity

FtsZ1-2 overexpression led to a faster differentiation response to strong light conditions.In wild type and the FtsZ1-2 knock out cell line caulonema formation was slowed compared to protonemata overexpressing FtsZ1-2.

Blue light

Treatment with blue light slightly decreased branching in the FtsZ1-2ox cell line and did not hinder caulonema formation. In wild type and knock out samples no caulonemata were observed but an increase in cell length was noticed.

Red light

Treatment with high intensity red light led to an increase in cell-length in the FtsZ1-2 overexpression cell line and in wild type. It also increased the amount of deformed chloroplasts in the FtsZ1-2 overexpression cell line.
The ΔFtsZ1-2 cell line showed a large amount of incorrectly placed side branch initials and a general increase in branching, also cell length was reduced.

Zantrins Z3

Treatment with Z3 led to a decrease in cell length in the FtsZ1-2:GFP ox cell line and wild type, while the knock out cell line showed no change in its average cell length. Caulonema differentiation was not observed in all three cell-lines.

Sanguinarine

Sanguinarine treatment decreased the cell length in all three cell lines, but the effect on the FtsZ1-2:GFP ox cell line was weakest.

Calcium

To summarize the results above it can be said, that treatment with EGTA attenuated low light symptoms in the wild type. Tmema formation in the knock out cell line was reduced but enhanced in the overexpression cell line. The FtsZ1-2 ox showed low light symptoms when treated with EGTA. Branching in wild type and FtsZ1-2 ox was normal. The knock out cell line showed irregular branching, reduction of brachycyte and tmema formation and increase in cell length. FtsZ1-2:GFP fluorescence was not detected.

Treatment with Verapamil caused irregular branching and low light intensity symptoms in the FtsZ1-2:GFP ox cell line. Cell length of wild type was increased and brachycyte and tmema formation was reduced. Branching behavior was normal. The knock out cell line showed irregular branching, reduction of brachycyte and tmema formation and increase in cell length.FtsZ1-2:GFP fluorescence was not detected.

Microtubul inhibitors

Cold treatment had only a slight decreasing effect on FtsZ1-2:GFP fluorescence

Oryzalin had only a slight decreasing effect on FtsZ1-2:GFP fluorescence

Latrunculin B

Latrunculin B did not inhibit high light intensity induced FtsZ1-2:GFP filament formation.
Treatment with Latrunculin B did not disrupt pre-existing FtsZ1-2:GFP filaments.

Summary of the effects on fluorescence:

Key for the following tables:

/ = no data available 0 = no change (-) = values inconclusive

(+) = slight increase + = increase ++ = strong increase

- = decrease -- = strong decrease

OX = overexpression cell line WT = Wild type K.O. = Knock out cell line

The effect of hormone treatment on fluorescence compared with control samples is

	Location of fluorescence under the influence of different hormones			
	Chloroplast	Diffuse cytoplasm	Filaments cytoplasm	Total amount of fluorescent protonema
NPA	**++**	**-**	**-**	**+**
IAA	**+**	**++**	**+**	**++**
2iP	**++**	**+**	**++**	**++**
ABA	**(-)**	**++**	**-**	**-**

Table 3.9.1 **(+)** = increase, ++ = strong increase, - = decrease, **(-) =** values inconclusive.

The effect of light quality on fluorescence in the presence of Cytokinin compared to control samples

	Location of fluorescence under the influence of light quality			
	Chloroplast	Diffuse cytoplasm	Filaments cytoplasm	Total amount of fluorescent protonema
Low light	**-**	**-**	**+**	**-**
White light	**++**	**+**	**-**	**+**
Blue light	**+**	**++**	**-**	**+**
Red light	**+**	**++**	**-**	**++**

Table 3.9.2 **+** = increase, **++** = strong increase, **-** = decrease, **--** = strong decrease.

	Location of fluorescence under the influence of light quality in the presence of 2iP			
	Chloroplast	Diffuse cytoplasm	Filaments cytoplasm	Total amount of fluorescent protonema
Low light	**-**	**+**	**+**	**-**
White light	**++**	**+**	**++**	**+**
Blue light	**-**	**-**	**-**	**+**
Red light	**+**	**++**	**++**	**++**

Table 3.9.3 + = increase, ++ = strong increase, - = decrease, -- = strong decrease.

Table: Overview of FtsZ1-2 effects on differentiation and cell growth

	Cytokinin						
	Caulonema	Shoot bud	Chloronema	Brachyzytes	Fluorescence	Cell length	Branching
OX	**-**	**++**	**(-)**	**-**	**++**	**(+)**	**-**
WT	**+**	**+**	**+**	**-**	/	**-**	**-**
K.O.	**(-)**	**-**	**+**	**+**	/	**+**	**-**
	Abscisic acid						
	Caulonema	Shoot bud	Chloronema	Brachyzytes	Fluorescence	Cell length	Branching
OX	**-**	/	**+**	**-**	**(-)**	**(+)**	**(+)**
WT	**-**	/	**+**	**+**	/	**-**	**-**
K.O.	**(-)**	/	**+**	**++**	/	**-**	**(+)**
	Auxin						
	Caulonema	Shoot bud	Chloronema	Brachyzytes	Fluorescence	Cell length	Branching
OX	**-**	/	**+**	**+**	**-**	**+**	**-**
WT	**-**	/	**+**	**+**	/	**+**	**-**
K.O.	**(-)**	/	**+**	**+**	/	**0**	**-**
	Red light						
	Caulonema	Shoot bud	Chloronema	Brachyzytes	Fluorescence	Cell length	Branching
OX	**++**	/	**+**	**-**	**++**	**+**	**-**
WT	**+**	/	**+**	**-**	/	**-**	**+**
K.O.	**(-)**	/	**+**	**-**	/	**-**	**++**
	Blue light						
	Caulonema	Shoot bud	Chloronema	Brachyzytes	Fluorescence	Cell length	Branching
OX	**(+)**	/	**+**	**+**	**-**	**0**	**+**
WT	**-**	/	**++**	**-**	/	**-**	**++**
K.O.	**(-)**	/	**+**	**+**	/	**+**	**(+)**
	White light						
	Caulonema	Shoot bud	Chloronema	Brachyzytes	Fluorescence	Cell length	Branching
OX	**++**	/	**(-)**	**(+)**	**+**	**(+)**	**+**
WT	**+**	/	**(+)**	**-**	/	**+**	**(+)**
K.O.	**(+)**	/	**+**	**-**	/	**++**	**-**
	EGTA						
	Caulonema	Shoot bud	Chloronema	Brachyzytes	Fluorescence	Cell length	Branching
OX	**+**	/	**+**	**(-)**	**--**	**-**	**(+)**
WT	**-**	/	**+**	**(+)**	/	**+**	**(+)**
K.O.	**(-)**	/	**+**	**(+)**	/	**-**	**++**
	Verapamil						
	Caulonema	Shoot bud	Chloronema	Brachyzytes	Fluorescence	Cell length	Branching
OX	**(+)**	/	**+**	**++**	**--**	**-**	**++**
WT	**(+)**	/	**+**	**(+)**	/	**+**	**-**
K.O.	**(+)**	/	**+**	**-**	/	**-**	**++**

Table 3.9.4

(/) no value available, 0 = no change, **(+)** = slight increase + = increase, **++** = strong increase, **-** = decrease, -- = strong decrease, **(-)** = values inconclusive.

4. Discussion

Plant cells rely on sunlight as their energy source. Ensuring that cell division will not deplete a daughter-cell of chloroplasts is therefore one of the most important processes during plant cell development. Cell division and chloroplast division have to be synchronized and tightly controlled by the cell.
By an as yet unknown mechanism the cell gains information on the condition of its plastids and reacts with appropriate changes to its morphology and growth. A regulating variable that mediates between the plant cell and the chloroplasts would therefore influence chloroplast division as well as cell growth and cell division and differentiation. The central role of FtsZ proteins in chloroplast division makes it the ideal target for control mechanisms of the cell to regulate chloroplast division. Since FtsZ1-2 occurs in the chloroplast and the cytoplasm it might be this correcting variable.
FtsZ1-2 knock out cell lines have been shown to possess an altered morphology compared to wild type cells of *P. patens* (Martin 2007). Cell morphology results from the interaction of all stimuli affecting the cell during growth and differentiation. If a factor influences cell morphology, the variation of exogenous stimuli will most likely result in an altered reaction of said factor. The possibility to vary one stimulus in dose-dependent manner will also provide important insights into the functionality of the target factor. The target in this study was *Pp*FtsZ1-2, the only FtsZ paralogue with a peptide motive addressing it to the cytoplasm as well as the chloroplast so far discovered. The dose variation was achieved by using three cell lines of *P. patens*, expressing different levels of *Pp*FtsZ1-2.

The exogenous stimuli came in four groups:

1. Light, possibly the most important growth factor of plant cells.

2. Hormones, the plants way of mediating environmental and cellular changes to the component parts of its body.

3. Calcium, an important plant signaling component that also promotes FtsZ polymerisation i*n vitro* (Erickson *et al.* 1996)

4. FtsZ inhibitors Zantrin Z3 and Sanguinarine, both shown to inhibit Z- ring formation in bacteria (Margalit *et al.* 2004, Beuria *et al.* 2005).

4.1 FtsZ1-2 is differentially affected by light quality and quantity

4.1.1. FtsZ1-2 influences differentiation under low light intensity

The differentiation of chloronema to caulonema cells has been shown to need an increase in light intensity as a trigger in the absence of exogenous auxin (Cove *et al.* 1978, Review by Schumaker and Dietrich 1997). Under low light conditions the protonemal tissues will stay in chloronema state, because the triggering light intensity is not reached (Klebs, (1893); Review by Bopp, (2000)). Therefore chloronemal growth

was expected under low light culture conditions. This led to the first observed difference between the cell lines, because they showed different phenotypes under low light intensity. Wild type cells acted as described above and the cells grew mainly as chloronema interspaced with short, slightly rounded brachycytes.
FtsZ1-2 overexpression seemed to attenuate the inhibitory effect of low light on protonema differentiation. Cell length analysis showed that the protonemata were not only longer than the wild type cells, but were also starting to differentiate into caulonemata. Only few brachycytes were observed.
Under high intensity white light the growth of the overexpression cell line changed from predominantly chloronema to caulonema growth with a large number of long thin caulonema filaments.
For the knock out line, growth under low light conditions resulted in a change of appearance. Cells were bloated, rounded and short, resembling brachycytes. Cell files were only rarely formed. Differentiation into caulonema was not observed and filamentous growth was disrupted by the abundant production of tmema cells.
These low light symptoms could be healed by treatment with high intensity white light.
The knock out cell line started producing long thin filaments resembling chloronema cells and even thinner and longer cells that resembled late stage caulonema except that they did not possess oblique cross walls. This indicates that caulonema formation is not blocked, but that tissue of FtsZ1-2 knock out cell lines in G1 phase is morphologically different from normal caulonema tissue. This has also been suggested by flow cytometric analysis data, which showed, that the number of cells in G1 phase are even increased in the knock out cell line, compared with wild type, grown under standard light conditions (Martin 2007). Under low light conditions, cells in G1 could not be distinguished from other cells of the knock out cell line by microscopy only

Wild type protonema differentiated much slower under high intensity white light than the overexpression line. The reason for this could be the arrest in G2 phase and the high amount of brachycytes induced by low light intensity, which means that the cells had to progress through two differentiation states instead of only one to reach caulonema state. Compared with wild type-cells under low light conditions, a slight increase of chloronema cell-length was observed. Also early stages of caulonema development were present. Caulonema differentiation starts with elongation of chloronema-cells. The cross-walls start inclining slowly until the typical oblique orientation is reached. This slow elongation of protonemal cells at caulonema induction has been reviewed by Bopp (2000) and is typical for caulonema development. Because of that, cell length could be used as a measure for differentiation in this study.

From these differences in cell morphology and differentiation it is possible that FtsZ1-2 is involved in mediating the different phenotypes under low light conditions and is necessary for the correct morphological changes that accompany transition to G1 phase. Especially the correct placement of the cross-walls seems to be strongly influenced by the amount of FtsZ1-2 present in the cytoplasm, as observed in the FtsZ1-2 knock out cell-line.
The formation of brachycytes is another difference observed in the development of the three cell lines. Brachycytes are a differentiation state that allows the cell to endure adverse surrounding conditions like salt stress, draught and low light intensities. They are usually induced and accompanied by rising ABA levels (Bopp 2000, Tintelnot, 2006). The amount of these cells varied strongly between the three cell lines. The highest amount was found in the knock out cell line. The abundant production of cells

resembling brachycytes in the knock out cell line indicates a higher sensitivity to low light conditions than possessed by cells over-expressing FtsZ1-2.
In the wild type they were formed abundantly but not as much as in the knock outs and in the overexpression cell line they were rare. The absence of this cell type from samples overexpressing FtsZ1-2 could indicate that the cells are less sensitive to low light intensity so that they are unable to react in the normal way.
The reaction of FtsZ1-2 overexpressing cells to high light intensity shows that light perception is not impaired. The reaction to low light intensity must therefore be due to another factor which is also triggered by low light conditions. ABA concentration has been shown to be increased by dark treatment of *Lemna* and *Arabidopsis* plants by Weatherwax et al (1996) and might thus be this second factor. Influence of ABA on the different FtsZ1-2 mutants was therefore tested (see below).

4.1.2. FtsZ1-2 is involved in caulonema differentiation and correct positioning of branch initials under irradiation with high intensity red light

Another light induced differentiation step is the generation of side branches under influence of red light. Irradiation with high intensity white light led to only a slight increase in branching depending on the level of FtsZ1-2 expression.
Irradiation with high intensity red light increased branching in the wild type cells. These findings are affirmed by Kagawal *et al* (1997) who found, that that dark adapted protonema of *Ceratodon purpureus* increased their branch initial production about 72% after irradiation with red light.
Irregular and cumulative branching was observed in the knock- out cell line. Red light treatment had the most disrupting effect on the growth pattern of the knock out cell line in this study. Usually side branch formation is a highly controlled and regular process with the frequency of the position of the branch initial depending on the age of the cell (Kagawal *et al.,* 1997). Also under normal circumstances only one branch per cell is produced. The FtsZ1-2 knock out cell line did not show such a preference of branch initial position, but produced many initials at one cell (up to five branch initials per cell Figure 3.3.3.2) Branch initial formation is induced by low levels of cytokinin in combination with the correct concentration of auxin. Branch initial position depends on the position of the nucleus (Schmiedel and Schnepf, 1979). Since the amount of nuclei per cell was not increased in the knock out cell line (DNA staining with HOECHST 33258, Data not shown), this indicates another mechanism, that overrides the information from the nucleus and lets the cell produce abundant branch initials in one cell.
Amazingly the exact opposite effect was observed with red light irradiation of the overexpression cell line. In this case the branching events decreased strongly, while caulonema development increased. This observation hints at auxin influence. Resli (1998) and Schumaker and Dietrich (1998) reported that high levels of auxin induced caulonema development. Caulonema grow faster than chloronema cells and
These events let it appear possible, that red light influences branch initial formation at low levels or absence of FtsZ1-2. The protein seems to be necessary for correct placement of side branches. It could be assumed, that FtsZ1-2 is necessary for the perception of the nucleus position under red light, or that red light induces some unknown mechanism that triggers uncontrolled branching in the absence of FtsZ1-2.
Differentiation to caulonema was strongly increased in the overexpression cell line under red light irradiation. The wild type cells did not show this extent of caulonema

production. Possibly their differentiation was slowed, since the growth curve of the control samples, treated with high intensity white light, suggested differentiation in progress. The knock out cell line did not grow into caulonema like structures. This would mean that FtsZ1-2 is necessary for the red light induced caulonema differentiation. This suggestion should be further verified by flow cytometric analysis, to determine the definite cell cycle phase of the protonema under red light treatment, since the absence of late stage caulonema like structures of the knock out cell line makes it impossible to determine the developmental state by microscopy. Even so the distribution of the cell length gives a nice hint at the developmental states of the samples.

4.1.3. Side branch formation in the presence of blue light is influenced by FtsZ1-2 expression

Auxin and high light intensity are needed for caulonema differentiation (Reski 1998). It has been reported that blue light via the cryptochrome system blocks auxin induced differentiation in moss protonema cells (Imaizumi *et al.* 2002). This could be the reason why the wild type cells showed no differentiation to caulonema when irradiated with blue light, yet caulonema differentiation was present in FtsZ1-2 ox cell line tissue implying that FtsZ1-2 attenuates cryptochrome induced inhibition of caulonema development.
The cell walls of the knock out cell line appeared smoother than normal and branching was decreased (see figure 3.3.3.2.). The growth curve with its heavy tail region implies differentiation in progress though. If caulonema development is not impaired in the knock out cell line, this would indicate, that caulonema development depends on the right amount of FtsZ1-2 instead of just the presence of FtsZ1-2 inside the cytoplasm.
The highest amount of branching was observed in wild type. Since the protonema contained numerous brachycytes which had been formed prior to irradiation with blue light, it could be possible that the observed branching is a consequence of the starting differentiation of the wild type protonemata from brachycytes to chloronema. On the other hand, Imaizumi *et al* (2002) propose that side branch formation is dependant on cryptochrome signals. The overexpression line showed only a slight increase in branching. From this it could be proposed, that branching under blue light conditions is promoted in the presence of FtsZ1-2.

4.2. Phytohormones differentially affect FtsZ1-2

4.2.1. Cytokinin induces cytoplasmic FtsZ1-2:GFP filament formation and FtsZ1-2 is necessary for shoot bud development under low light

Cytokinin has been the centre of many moss related studies. It was found to mediate two very important stages in the life of protonema cells. First it induces shoot bud formation and second cytokinin has been shown to influence chloroplast division (e.g. Schumaker and Dietrich 1998). Table 3.9.1 shows, that bud formation is correlated to FtsZ1-2 expression level under low light conditions. These results indicate that FtsZ1-2

appears to be necessary for the differentiation of the caulonema to the adult gametophyte. Under the microscope first shoot buds could be observed on protonema of the overexpression line 48 hours after inoculation. At the same time fluorescent rings at the division site of chloronema appeared and 72 hours after inoculation the first increase of FtsZ1-2:GFP fluorescent filaments inside the cytoplasm was noted. The increase in GFP fluorescence could be enhanced further by incubation under strong white light in the presence of cytokinin. These findings indicate that the formation of fluorescent FtsZ1-2:GFP structures is brought about by two factors that enhance each other in a multiplicative way, light intensity and cytokinin. This again implies that both factors are likely to influence the same signal cascade.

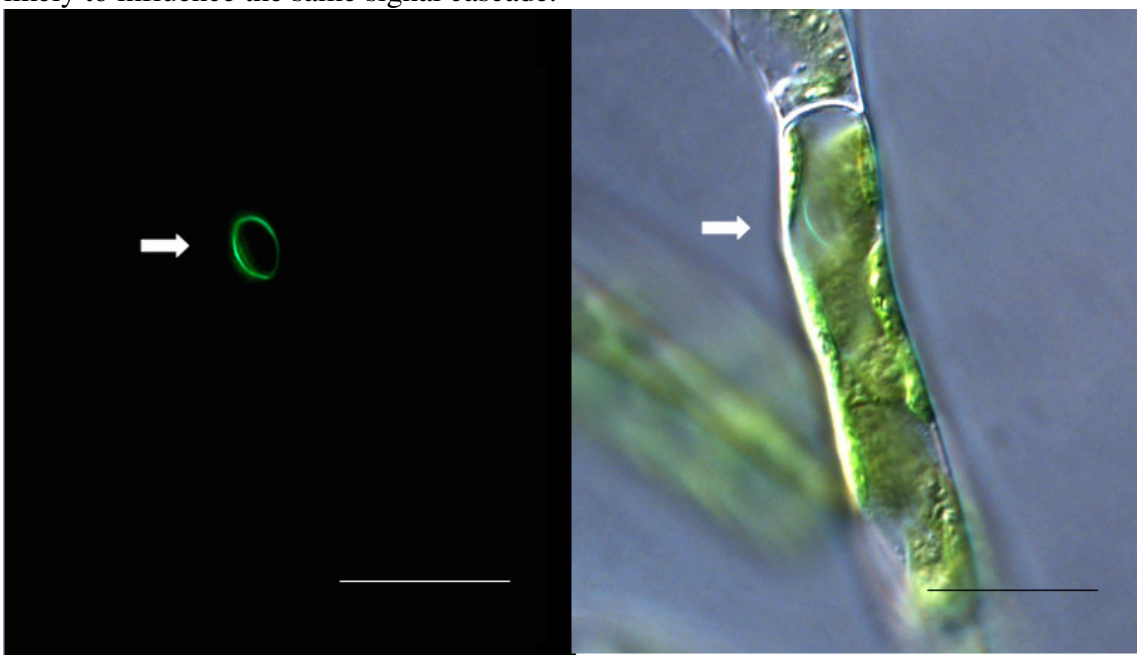

Figure 4.2.1 Overlay picture of green fluorescence with the mother cell, FtsZ1-2:GFP ring assembly at the possible site of branch initial formation in caulonema cell of FtsZ1-2:GFP ox cell line grown under day light. Scale bars indicate 20 µm

It is known, that treatment with cytokinin leads to a transient increase of the cytosolic Ca^{2+} concentration in dependence of dihydropyridin sensitive channels (Schumaker, Gizinsky 1993). It has been shown that bacterial FtsZ polymerises in the presence of 10 mM Ca^{2+}. Calcium is a prerequisite for FtsZ polymerisation, *in vitro* (Yu, Margolin 1997). These concentrations were not reached in the Schumaker, Gizinsky experiment. But only little is known about assembly behavior of plant FtsZ *in vivo*. What further strengthens the position of Ca^{2+} in the increase of FtsZ1-2:GFP fluorescence is, that Yu and Margolin (1997) propose a role in Ca^{2+} concentration in the assembly and disassembly of FtsZ in bacteria. Typically GTP is also needed for polymerization of FtsZ. That means that assembly is a high energetic event, which reduces the possibility of random, meaningless polymerization. Cytokinin has been shown to up-regulate essential chloroplast genes, within a few hours of treatment (Nakano *et al.* 1999 Reviewed). Another mechanism of fluorescence induction is of course the upregulation of the FtsZ genes for chloroplast division. This in return is influenced by the presence and concentration of cytokinin. This fits the observation, that after cytokinin treatment the fluorescent structures to be observed were inside the chloroplasts.

4.2.2. FtsZ1-2 overexpression inhibits abscisic acid induced brachycyte development.

The presence of abscisic acid leads to an increase of brachycyte formation in wild type cells. The overexpression of FtsZ1-2 protected the cells from the mechanism that led to the short cell formation, whiche means, that brachycytes formation was strongly reduced. The knock out line was already maximal stressed from low light, so that no changes in cell shape occurred under hormone treatment.
ABA is a phytohormone that regulates stress responses in plant cells, like chloroplast avoidance movement and cold or draught resistance. Long term effects in mosses lead to short cell formation, brachycyte and tmema formation, arrest in G2 phase and chloronema growth, which is the direct result of G2 phase arrest. Also the cytoplasmic architecture is greatly changed after ABA treatment. The cytoplasm becomes denser, the chloroplasts fill the whole surface of the cell and the vacuole divides into many small ones. (Tintelnot 2006) All this starts with the efflux of Ca^{2+} from internal calcium stores. Since the samples were grown under low light intensities their reaction to ABA treatment was rather transient at first. In contrast to wildtype cells, the response of the overexpression line was completely reduced to transient effects (Chloroplast movement, condensation of cytoplasm, reduction of vacuole size). Increase in cell length was not inhibited. This might mean that FtsZ1-2 transfers resistance to ABA induced short cell- and brachycyte formation.

Fluorescent analysis showed a strong increase in diffuse cytoplasmic fluorescence (see Figure 3.2.3.1). This could be brought about by a increased level of Ca^{2+} in the cytoplasm, which might lead to the formation of short FtsZ1-2:GFP bundles or short strands of only a few monomers, that increases the diffuse cytoplasmic fluorescence. On the other hand, the dense cytoplasm might bring the FtsZ1-2:GFP monomers and polymers into close proximity, so that fluorescence is enhanced without conformational change to the filaments or solvable FtsZ populations inside the plasma. To clear this point satisfactorily, more research is needed.

4.2.3. High concentrations of auxin inhibit increase in cell length and differentiation under low light conditions.

Treatment with exogenous auxin induced short cell development in the overexpression cell line. The cell length of the wild type was also reduced. The knock- out cell line again showed the least response to the hormone treatment, possibly, because it was already maximally stressed and the low light symptoms could not be distinguished from auxin stress symptoms. High levels of extrcellular auxin, Have been described to inhibit cell length and differentiation in mosses (Johri *et al*. (1973); Bopp (2000)). Under high light or day light, exogenous auxin stimulates caulonema differentiation and promotes shoot bud formation in the right concentration ratio to cytokinin (Bopp (2000), Schumaker Dietrich (1997), Reski (1998)). This response could not be observed here. Oddly the response to the auxin transport inhibitor NPA was less drastic, than the response to high amounts of auxin itself. Even though the reaction to auxin stress appears to be an enhanced low light intensity reaction, and could be interpreted as a result of the ability of auxin to enhance the acidity of the cell wall and change the Ca^{2+} flux from the Calcium store inside the apoplastic room into the cytoplasm (Bush 1995), it is most likely, that the reduced cell length results from intercalary divisions. Bopp

(2000) reviewed this phenomenon, stating that the inhibition of apical growth stimulates intercalary divisions in early stage caulonema cells of mosses. The destruction of basipetal auxin transport is one of the stated factors. This fits the observation, that NPA had the same effect as auxin in high concentrations. Other factors increasing the cytoplasmic Ca^{2+} concentration is low light, red light, where a strong increase in cytoplasmic FtsZ1-2 fluorescence had been observed, and abscisic acid where the same effect was seen.

4.3. Calcium perception is mediated by FtsZ1-2

Calcium is one of the most versatile signaling factors in the plant cell. In mosses, calcium is influenced by red and blue light and reacts to unidirectional light. It is involved in side branch formation, and a Ca^{2+} gradient is necessary for tip growth (see below). Herth *et al*. (1990) showed that apical growth of *Ceratodon purpureus* was inhibited by calcium chelators.
Treatment with EGTA in Ca^{2+} free medium resulted in stunted growth of the apical cells of wild type chloronema. The apical cells were short and broad across the tip, while the rest of the cell file was very straight (resembling blue light treatment). The Over expression cell line grew in caulonema state and was not impaired in apical division. The knock- out line grew in tight bunches of branching protonema with many irregular branch initials. That tip cell growth was not inhibited, might have had its reason in the high amount of Ca^{2+} in the cell walls of the wild type protonema cells, brought about by low light intensity treatment. The Calcium- store is depleted over time, so it is possible that longer incubation would have resulted in the inhibition of tip growth.

Verapamil treatment induced sudden release from low light symptoms in the wild type protonema. The cells were elongated, and grew wavy with few branches. The most important observation is the sudden loss of polar growth in the over expression cell line. The apical cells divided irregularly and then changed their growth in the opposite direction of their cell axis. Wacker & Schnepf (1990) saw something similar in *Funaria hygrometrica,* when they screened for Ca^{2+} channels. Apical growth is depending on a constant perception of a Ca^{2+} gradient in the tip to the base of the cell. This body was destroyed after treatment with Verapamil in *Funari*a and also in *Physcomitrella* FtsZ1-2:GFP overexpression cell line, but not in the *Physcomitrella* wild type. When the perception is inhibited, growth direction can no longer be perceived and polarity is lost or perturbed. The wild type was in a Ca^{2+} enriched developmental state (brachycyte) when the treatment started. This may be the cause for its comparably normal growth.

Analysis of fluorescence showed that no GFP fluorescence was retained after depletion of exogenous and endogenous Ca^{2+}. EGTA and Verapamil were the only drugs tested in this study, that had a secure negative effect on FtsZ1-2:GFP fluorescence.

From this it can be gathered that Ca^{2+} is necessary for filamentatious polymerisation of FtsZ1-2 in the cytoplasm and thus for any function incumbent in those filamtatious structures inside the cytoplasm.

4.4. Inhibitors do not disturb FtsZ1-2:GFP fluorescence significantly

4.4.1. Cytoskeletal drugs do not relevantly destroy FtsZ1-2:GFP fluorescence

Treatment with Oryzalin, a strong plant microtubule disrupting drug, and Latrunculin B, an F- actin disrupting drug did not result in significantly less fluorescent structures inside the cytoplasm of *P. patens*. Also the high light intensity induced rise of fluorescence was not inhibited during Latrunculin B treatment.
From these data it can be gathered, that a direct interaction of the FtsZ1-2 filaments with the cytoskeleton is not probable, because no disruptive effects could be observed. An indirect effect over one or more different factors like MAPs can not be excluded and will be an interesting point in further research.

4.4.2. FtsZ inhibitors affect cell morphology, but do not significantly disturb FtsZ1-2:GFP fluorescence

The Data showed that fluorescence inside the cytoplasm was not significantly disturbed by treatment with Zantrins Z1 and Z3. Treatment with Sanguinarine also did not inhibit development of fluorescence. Cell growth was considerably disturbed after treatment with Z3, but the lack of reaction of the knock out strain to Z3 may indicate specific interaction of Zantrin Z3 and FtsZ1-2. Sanguinarine showed fascinating properties in that it differentially stained future branch initial sites at the outer caulonema wall and that cross walls were differentially stained in the overexpression cell line. From the strong fluorescence it can be surmised that specific binding with FtsZ1-2:GFP may have occurred at the cross walls, and that FtsZ1-2:GFP was concentrated there.
The growth curve of Sanguinarine treated cells indicates that a second cytoskeletal target may exist. This may concur with recent findings that Sanguinarine binds microtubules as well as bacterial FtsZ (Beuria *et al.*2005, Lopus, Panda,2006) and inhibits turnover through a steric hindrance of the GTP-binding site. On the other hand pig brain neurotubulin assembly was not inhibited by Sanguinarine in this study.

4.5. Conclusion

This study has provided many factors that influence FtsZ1-2 mediated cell morphology. First, there is the influence of light on branch initiation in the absence and presence of FtsZ1-2. Second the differential developmental influences of FtsZ1-2 under hormone treatment could be observed. Third the influence of cytoskeletal and FtsZ inhibiting drugs had been tested, and fourth the influence of calcium on the morphology of *P. patens* could be shown to be influenced by the expression level of FtsZ1-2. All in all the greatest impact on growth and cell shape had those factors that initiated a change of Ca^{2+} concentration inside the cytoplasm, like red light, ABA, cytokinin, EGTA and Verapamil. In the latter cases fluorescence was completely blocked in the absence of

calcium, in the first cases, a strong diffuse GFP fluorescence could be observed, which proposes an influence of Ca^{2+} on assembly of Ftsz1-2 in the cytoplasm.
It could be shown, that correct side branch positioning is mediated by FtsZ1-2, also that FtsZ1-2:GFP filaments in the cytoplasm could only be formed in the presence of strong white light or 2iP indicating a functionality of those fluorescent structures observed inside the cytoplasm. Shoot bud formation which very much depends on the presence of cytokinin, also is influenced by the correct amount of FtsZ1-2 under low light conditions.

From these results the following is surmised:

FtsZ1-2 is a means of the plant to measure and translate information on growth-conditions by polymerizing and depolymerizing. Polymerisation depends on protein concentration and calcium concentration, which in return are brought about and influenced by changes in hormone concentration and -ratio and light quality and quantity. Thus cell growth, chloroplast division, developmental fate and reproduction are influenced and possibly synchronized and directed. A possible mechanism for this could be the measurement of the amount of polymerized and/ or unbound, solvable FtsZ1-2 monomeres inside the cytoplasm by a binding-partner, which again could interact (or could be prevented from interacting) with other components of the cytoplasm like microtubuli and microfilaments in the manner of MAPs. Another possible mechanism could be the binding of calcium to FtsZ1-2 filaments. This binding could deplete the cytoplasm of calcium and prevent other functions like e.g. the opening of calcium channels. Since in wild type cells of *Physcomitrella* FtsZ1-2 is in rather low supply, and calcium can be present in mM concentrations, this last suggestion seems not feasible though and has only been added for completeness.

4.6. Outlook

To verify some still open questions and surmises, various experiments need still to be conducted.

1. The interaction of the cytoskeleton elements with FtsZ1-2 will have to be analysed with protein biochemical methods. This is probably the only way to get a dependable proof for binding proteins.
2. The interaction and dependence of FtsZ1-2 mediated developmental progresses need to be further analysed and the interaction with calcium still needs further proof.
3. Even though a direct influence of light intensity, light quality and cytokinin on fluorescence development of FtsZ1-2:GFP filaments could be shown, the function of said filaments is still open. Covizualisation with cytoskeletal elements might be of help in understanding the function of these structures and need to be tested under the appropriate culture conditions.

5. References

Anderson, D.E., Trujillo, K.M., Sung, P. and Erickson, H.P. (2001) Structure of the Rad50 x Mre11 DNA repair complex from Saccharomyces cerevisiae by electron microscopy. J.Biol.Chem. **276**, 37027-33.

Bernardt, T.G. and de Boer, P. (2005). SlmA, A Nucleoid Associated, FtsZ-Binding Protein Required for Blocking Septal Ring Assembly Over Chromosomes in *E. coli*. Mol. Cell. **Vol.18.** 555–564.

Beuria, T.K., Santra, M.K. and Panda, D. (2005). Sanguinarine Blocks Cytokinesis in Bacteria by Inhibiting FtsZ Assembly and Bundling. Biochemistry, **44**, 16584-16593.

Bopp, M., Atzorn, R. (1992), Hormonelle Regulation der Moosentwicklung, Naturwissenschaften **79**, 337- 346

Bopp, M., Bohrs, L. (1965). Versuche zur Analyse der Protonemaentwicklung der Laubermoose. Die Regeneration der Caulonemen von *Funaria hygrometrica*. Planta **67,** 357–374.

Bopp, M., Jacob, H.J. (1986). Cytokinin effect on branching and bud formation in Funaria. Planta **169,** 462–464.

Bopp, M. (2000). 50 years of the moss story. Progr. Bot. **61,** 3–34.

Briegel A., Dias D.P., Li Z., Jensen R.B., Frangakis A.S. and Jensen G.J. (2006) Multiple large filament bundles observed in *Caulobacter crescentus* by electron cryotomography. Mol Microbiol. **62**, 5-14.

Bopp M, Quader H, Thoni C, S awidis T, Schnepf E (199 I) Filament disruption in *Funaria* protonemata: formation and disintegration of tmema cells. J Plant Physiol 137:273-284

Buddelmeijer, N. and Beckwith, J. (2004). A complex of the *Escherichia coli* cell division proteins FtsL, FtsB and FtsQ forms independently of its localization to the septal region. Mol Microbiol. **52,** 1315-1327.

Burns, R. (1998). Synchronized division proteins. Nature. **391**, 121-123.

Bush, D.S. (1995). Calcium regulation in plant cells and its roll in signaling. Annu. Rev. Plant Physiol. Plant Mol. Biol., **46**, 95-122.

Chen, J.C., Weiss, D.S., Ghigo, J. and Beckwith, J. (1999). Septal localization of FtsQ, an essential cell division protein in *Escherichia coli*. Journal of Bacteriology. **181,** 521-520.

Christianson, M.L. (2000) ABA Prevents the Second Cytokinin-Mediated Event During the Induction of Shoot Buds in the Moss *Funaria* hygrometrica. American Journal of Botany **87(10),** 1540–1545.

Colletti, K.S., Tattersall, E.A., Pyke, K.A., Froelich, J.E., Stokes, K.D. and Osteryoung, K.W. (2000). A homologue of the bacterial cell division site-determining factor MinD mediates placement of the chloroplast division apparatus. Curr. Biol. **10,** 507-516.

Cove, D.J., Schild, A., Ashton, N. W. and Hartmann, E. (1978). Genetic and physiological studies of the effect of light on the development of the moss, *P. Patens*. Photochemistry and Photobiology **27 (2)**, 249–254.

Dai, K. and Lutkenhaus, J. (1992). The proper ratio of FtsZ to FtsA is required for cell division to occur in *Escherichia coli*. J. Bacteriol. **174,** 6145-6151.

De Boer, P., Crossley, R. and Rothfield, L. (1992). The essential bacterial cell-division protein FtsZ is a GTPase. Nature. **359,** 254-256.

De Veylder, L., Beeckman, T., Beemster, G.T., de Almeida Engler, J., Ormenese, S., Maes, S., Naudts, M., Van Der Schueren, E., Jacqmard, A., Engler, G., and Inze, D. (2002). Control of proliferation, endoreduplication and differentiation by the Arabidopsis E2Fa-Dpa transcription factor. EMBO J **21**, 1360-1368.

Di Lallo, G., Anderluzzi, D., Ghelardini, P. and Paolozzi, L. (1999). FtsZ dimerization *in vivo*. Molecular Microbiology. **32**, 265-274.

Din, N., Quardokus, E.M., Sackett, M. J. and Brun, Y.V. (1998). Dominant C-terminal deletions of FtsZ that affect its ability to localize in *Caulobacter* and its interaction with FtsA. Molecular Microbiology. **27,** 1051-1063.

Dinkins, R., Reddy, M.S., Leng, M. and Collins, G.B. (2001). Overexpression of the Arabidopsis thaliana MinD1 gene alters chloroplast size and number in transgenic tobacco plants. Planta **214,** 180-8.

El-Kafafi, E.S., Mukherjee, S., El-Shami, M., Putaux, J.L., Block, M.A., Pignot-Paintrand, I., *et al.* (2005). The plastid division proteins, FtsZ1 and FtsZ2: differ in their biochemical properties and sub-plastidial localization. Biochemical Journal **387,** 669–676.

Erickson , H.P. (1995). FtsZ, a prokaryotic homolog of tubulin? Cell. **80,** 367-370.

Erickson, H.P., Taylor, D.W., Taylor, K.A. and Bramhill, D. (1996). Bacterial cell division protein FtsZ assembles into protofilament sheets and minirings, structural homologues of tubulin polymers. Proc Natl Acad Sci USA **93,** 519-523.

Erickson , H.P. (1997). FtsZ, a tubulin homologue in prokaryotic cell division. Trends in Cell Biology. **7,** 362-367.

Erickson, H.P. (1998). Atomic structures of tubulin and FtsZ. Trends in Cell Biology. **8**, 133-137.

Erickson, H.P. (2001) Cytoskeleton - Evolution in bacteria. Nature **413,** 30.

Erickson, H.P. (2001) The FtsZ protofilament and attachment of ZipA-structural constraints on the FtsZ power stroke. Curr Opin Cell Biol. **13**, 55-60.

Esch, H., Hartmann, E., Cove, D., Wada, M. and Lamparter, T. (1999). Phytochrome-controlled phototropism of protonemata of the moss Ceratodon purpureus: physiology of wild type and class 2 ptr mutants. Planta **209**, 290-298.

Gao, H., Kadirjan-Kalbach, D., Froehlich, J.E. and Osteryoung, K.W. (2003). ARC5, a cytosolic dynamin-like protein from plants, is part of the chloroplast division machinery. Proc Natl Acad Sci USA **100,** 4328–4333.

Ghigo, J. and Beckwith, J. (2000). Cell division in *Eschericia coli*: Role of FtsL domains in septal localization, function, and oligomerization. Journal of Bacteriology. **182,** 116-129.

Goodwin, R.H. (1953). Fluorescent Substances in Plants. Annual Review of Plant Physiology, **Vol.4**, 83-304.

Goode, J.; Alfano, F.; Stead, A.; Duckett, J. G. (1993) The formation of aplastidic abscission (tmema) cells and protonemal disruption in the moss *Bryum tenuisetum* Limpr. is associated with transverse arrays of microtubules and microfilaments Protoplasma 174:158-172

Gremillon, L., Kiessling, J., Hause, B., Decker, E.L., Reski, R. and Sarnighausen, E. (2007a). FtsZ isoforms specifically interact in the chloroplasts and in the cytosol of *Physcomitrella patens*. New Phytologist, accepted for publication

Gremillon, L. (2007b). Protein-protein interaction analysis and subcellular localization of plastid division proteins FtsZ in the moss *Physcomitrella patens.* PhD thesis

Hale, C.A. and de Boer, P.A. (1997). Direct binding of FtsZ to ZipA, an essential component of the septal ring structure that mediates cell division in *E. coli*. Cell. **88,** 175-185.

Hashimoto, H. (1986). Double ring structure around the constricting neck of dividing plastids of *Avena sativa*. Protoplasma **135** 166-172.

Howard, M., Rutenberg, A. D. and de Vet, S. (2001). Dynamic compartmentalization of bacteria: accurate division in *E. coli*. Physical Review Letters. **87**, 278102.

Imaizumi, T., Kadota, A., Hasebe, M. and Wada, M. (2002). Cryptochrome Light Signals Control Development to Suppress Auxin Sensitivity in the Moss *P. patens.* The Plant Cell, **Vol.14**, 373–386.

Johri,M.; Desai, S. (1973).Auxin regulation of cell differentiation in moss protonema. Nature (Lond) New Biol. 245:223-224

Joseleau-Petit, D., Vinella, D. and D'ari, R. (1999). Metabolic alarms and cell division in *Escherichia coli*. Journal of Bacteriology. **181**, 9-14.

Kagawa1,T.; Lamparter, T.; Hartman, E. and Wada, M. (1997) Phytochrome-mediated branch formation in protonemata of the moss *Ceratodon purpureus.* Journal of plant research, Vol. 10, no3, 363-370

Kuroiwa, T., Kuroiwa, H., Sakai, A., Takahashi, H., Toda, K. and Itoh, R. (1998). The division apparatus of plastids and mitochondria. Int. Rev. Cytol. **181,** 1–41

Larsen R.A., Cusumano C., Fujioka A., Lim-Fong G., Patterson P. and Pogliano J. (2007) Treadmilling of a prokaryotic tubulin-like protein, TubZ, required for plasmid stability in *Bacillus thuringiensis*. Genes Dev. **21**,1340-1352.

Li Z., Trimble M.J., Brun Y.V. and Jensen G.J. (2007) The structure of FtsZ filaments in vivo suggests a force-generating role in cell division. EMBO J. **26**, 4694-4708.

Lopus, M. and Panda, D. (2006). The benzophenanthridine alkaloid sanguinarine perturbs microtubule assembly dynamics through tubulin binding. A possible mechanism for its antiproliferative activity. FEBS Journal, **273**, 2139-2150.

Löwe, J. and Amos, L.A. (1998) Crystal structure of the bacterial cell-division protein FtsZ. Nature **391**, 203–206.

Löwe, J. (1998). Crystal structure determination of FtsZ from *Methanococcus jannaschii*. Journal of Structural Biology. **124,** 235-243.

Löwe, J. and Amos, L.A. (1998). Crystal structure of the bacterial cell-division protein FtsZ. Nature. **391**, 203–206

Lu, C., Reedy, M., and Erickson, H.P. (2000). Straight and curved conformations of FtsZ are regulated by GTP hydrolysis. Journal of Bacteriology. **182,** 164-170.

Lu, C., Stricker, J. and Erickson, H.P. (2001) Site-specific mutations of FtsZ - effects on GTPase and in vitro assembly. BMC Microbiol. **1**, 7.

Lutkenhaus, J., and Addinall, S.G. (1997). Bacterial cell division and the Z ring. Annual Review of Biochemistry. **66**, 93-116.

Ma, S. and Margolin, W. (1999). Genetic and functional analyses of the conserved C-terminal core domain of *Escherichia coli* FtsZ. Journal of Bacteriology. **181,** 7531-7544.

Ma, X., Ehrhardt, D.W., and Margolin, W. (1996). Colocalization of cell division proteins FtsZ and FtsA to cytoskeletal structures in living *Escherichia coli* cells by using the green fluorescent protein. Proceedings of the National Academy of Sciences, USA. **93**, 12998-13003.

Maisch, J. (2006). Auxin, Actin and polar patterning in tobacco cells. PhD thesis.

Maisch, J. and Nick, P. (2007). Actin is involved in auxin-dependant patterning. Plant Physiol. **143**, 1695-1704.

Maple, J., Fujiwara, M.T., Kitahata, N., Lawson, T., Baker, N.R., Yoshida, S. and Moller, S.G. (2004) GIANT CHLOROPLAST 1 Is essential for correct plastid division in Arabidopsis. Curr Biol, **14,** 776–781.

Margalit, D.N., Romberg, L., Mets, R.B., Hebert, A.M., Mitchison, T.J., Kirschner, M.W. and RayChaudhuri, D. (2004). Targeting cell division: Small-molecule inhibitors of FtsZ GTPase perturb cytokinetic ring assembly and induce bacterial lethality. Proc Natl Acad Sci U S A, **101(32)**, 11821–11826.

Martin, A. (2007). Functional analysis of plastid division proteins FtsZ in the moss *Physcomitrella patens* (Hedw.) B.S.G. PhD thesis

McFadden, G.I. (2001). Primary and secondary endosymbiosis and the origin of plastids. J. Phycol. **37,** 951- 959

Menand, B., Calder, G. and Dolan, L. (2007). Both chloronemal and caulonemal cells expand by tip growth in the moss *Physcomitrella patens*. Journal of experimental botany, **Vol.58 (7),** 1843-1849.

Mita, T., Kanbe, T., Tanaka, K., and Kuroiwa, T. (1986). A ring structure around the dividing plane of the *Cyanidium caldarium* chloroplast. Protoplasma **130,** 211-213.

Miyagishima, S., Kuroiwa, H., and Kuroiwa, T. (2001 a). The timing and manner of disassembly of the apparatuses for chloroplast and mitochondrial division in the red alga *Cyanidioschyzon merolae*. Planta **212,** 517-528.

Miyagishima, S-Y, Takahara, M., Mori, T., Kuroiwa, H., Higashiyama, T. and Kuroiwa, T. (2001 b). Plastid division is driven by a complex mechanism that involves differential transition of the bacterial and eukaryotic division rings. Plant Cell **13,** 2257–2268.

Miyagishima, S.Y., Nishida, K., Mori, T., Matsuzaki, M., Higashiyama, T., Kuroiwa, H. and Kuroiwa, T. (2003). A plant-specific dynamin-related protein forms a ring at the chloroplast division site. Plant Cell **15,** 655-665**.**

Miyagishima, S.Y., Nozaki, H., Nishida, K., Matsuzaki, M. and Kuroiwa, T. (2004). Two types of FtsZ proteins in mitochondria and red-lineage chloroplasts: the duplication of FtsZ is implicated in endosymbiosis. J. Mol. Evol. **58**, 291–303.

Miyagishima, S-Y, Froehlich, J.E. and Osteryoung, K.W. (2006). PDV1 and PDV2 Mediate Recruitment of the Dynamin-Related Protein ARC5 to the Plastid Division Site. The Plant Cell. **18**, 2517-2530.

Niu, L. and Yu, J. (2008). Investigating intracellular dynamics of FtsZ cytoskeleton with photo-activation single-molecule tracking. Biophys. J. **108.128751**.

Nogales, E., Wolf, S.G. and Downing, K.H. (1998). Structure of the alpha/beta tubulin dimer by electron crystallography. Nature. **391,** 199-202.

Raynaud, C., Cassier-Chauvat, C., Perennes, C. and Bergounioux, C. (2004) An Arabidopsis homolog of the bacterial cell division inhibitor SulA is involved in plastid division. Plant Cell **16,** 1801–1811.

Reddy, M.S., Dinkins, R. and Collins, G.B. (2002).Overexpression of the Arabidopsis thaliana MinE1 bacterial division inhibitor homologue gene alters chloroplast size and morphology in transgenic Arabidopsis and tobacco plants. Planta **215,** 167-76.

Rensing, S.A., Kiessling, J., Reski, R., and Decker, E.L. (2004). Diversification of ftsZ during early land plant evolution. J. Mol. Evol. **58,** 154-162.

Reski, R. and Abel, W.O. (1985). Induction of budding on chloronemata and caulonemata of the moss, *Physcomitrella patens*, using Isopentenyladenine. Planta **165**, 354-358.

Reski, R. (1998). Development, genetics and molecular biology of mosses. Bot. Acta **111**, 1-15.

Reski, R. (2002). Rings and networks: the amazing complexity of FtsZ in chloroplasts. Trends in Plant Science **7**, 103-105.

Reski, R., and Cove, D.J. (2004). *Physcomitrella patens*. Curr Biol **14,** R261-262.

Rothfield, L., Justice, S. and Garcia-Lara, J. (1999). Bacterial cell division. Annu. Rev. Genet. **33**, 423-48.

Saunders, M.J. and Hepler, P.K. (1982). Calcium ionophore A23187 stimulates cytokinin-like mitosis in *Funaria.* Science **217,** 943–945.

Saunders, M.J. and Hepler, P.K. (1983). Calcium antagonists and calmodulin inhibitors block cytokinin-induced bud formation in *Funaria.* Developmental Biology **99,** 41–49.

Saunders, M.J. (1986). Cytokinin-activation and redistribution of plasmamembrane ion channels in *Funaria.* Planta **167,** 402–409.

Schimper, A.F.W. (1883). Über die Entwicklung der Chlorophyllkörner und Farbkörper. Bot. Zeitung **41,** 105-162.

Schmiedel, G. and Schnepf, E. (1979). Side branch formation and orientation in the caulonema of the moss,Funaria hygrometrica: Normal development and fine structure. Protoplasma, **Vol.100 (3-4)**, 367-383.

Schumaker, K.S. and Gizinski, M.J. (1993). Cytokinin stimulates dihydropyridine-sensitive calcium uptake in moss protoplasts. Proceedings of the National Academy of Sciences, USA **90**, 10937–10941.

Schumaker, K.S. and Gizinski, M.J. (1996). G proteins regulate dihydropyridine binding to moss plasma membranes. Journal of Biological Chemistry **271,** 21292–21296.

Shimada, H., Koizumi, M., Kuroki, K., Mochizuki, M., Fujimoto, H., Ohta, H., Masuda, T. and Takamiya, K. (2004) ARC3, a chloroplast division factor, is a chimera of prokaryotic FtsZ and part of eukaryotic phosphatidylinositol-4-phosphate 5-kinase. Plant Cell Physiol **45,** 960–967.

Soll, J., and Schleiff, E. (2004). Protein import into chloroplasts. Nat Rev Mol Cell Biol. **5**, 198-208.

Spector, I., Shochet, N., Blasberger, D. and Kashman, Y. (1989) Latrunculins—novel marine macrolides that disrupt microfilament organization and affect cell growth: I. Comparison with cytochalasin D. Cell Motil Cytoskel **13**, 127-144

Stokes, K.D. and Osteryoung, K.W. (2003). Early divergence of the FtsZ1 and FtsZ2 plastid division gene families in photosynthetic eukaryotes. Gene. **320**, 97–108.

Thanedar, S., and Margolin, W. (2004). FtsZ exhibits rapid movement and oscillation waves in helixlike patterns in *Escherichia coli*. Curr Biol **14,** 1167-1173.

Tintelnot, S. (2006). Der Einfluss von Abscisinsäure auf die pflanzliche Zellwand: Untersuchung extrazellulärer Proteine beim Laubmoos *Physcomitrella patens*. PhD thesis.

Tucker, E.B., Lee, M., Alli, S., Sookhdeo, V., Wada, M., Imaizumi, T., Kasahara, M. and Hepler, P.K. (2005). UV-A Induces Two Calcium Waves in *P. patens.* Plant and Cell Physiology, **46(8)**, 1226-1236.

Ullanat, R. and Jayabaskaran C. (2002). Light- and cytokinin-regulated *ftsZ* gene expression in excised cucumber cotyledons (Cucumis sativus). Plant growth regulation, **Vol. 38 (3)**, 209-218.

Vaughan, S., Wickstead, B., Gull, K. and Addinall, S.G. (2004) Molecular evolution of FtsZ protein sequences encoded within the genomes of archaea, bacteria, and eukaryota. J. Mol. Evol. **58**, 19–29.

Vicente, M., Rico, A. I., Martınez-Arteaga and R., Mingorance, J. (2006) Minireview Septum Enlightenment: Assembly of Bacterial Division Proteins; J. Bacteriol. **Vol.188,** 19- 27.

Vishnyakov and S. N. Borchsenius (2007). FtsZ and Bacterial Cell Division. Cell and Tissue Biology, **Vol.1, No.3**, 206–214.

Vitha, S., McAndrew, R.S., and Osteryoung, K.W. (2001). FtsZ ring formation at the chloroplast division site in plants. J Cell Biol **153,** 111-120.

Vitha, S., Froehlich, J.E., Koksharova, O., Pyke, K.A., van Erp, H. and Osteryoung, K.W. (2003) ARC6 is a J-domain plastid division protein and an

evolutionary descendant of the cyanobacterial cell division protein Ftn2. Plant Cell **15,** 1918–1933.

Vollmer, W. (2006). The prokaryotic cytoskeleton: a putative target for inhibitors and antibiotics? Applied Microbiology and Biotechnology, **Vol.73 (1)**, Mini-Review.

Wacker, I. and Schnepf, E. (1990). Effects of nifedipine verapamil and diltiazem on Tipp growth in Funaria hygrmetrica. Planta, **180**, 492-501.

Wang, X., Huang, J., Mukherjee, A., Cao, C., and Lutkenhaus, J. (1997). Analysis of the interaction of FtsZ with itself, GTP, and FtsA. Journal of Bacteriology. **179,** 5551-5559.

Ward, J.E., Jr., and Lutkenhaus, J. (1985). Overproduction of FtsZ induces minicell formation in *E. coli*. Cell. **42,** 941-949.

Weiss, D.S., Chen, J.C., Ghigo, J., Boyd, D., and Beckwith, J. (1999). Localization of FtsI (PBP3) to the septal ring requires its membrane anchor, the Z ring, FtsA, FtsQ, and FtsL. Journal of Bacteriology. **181,** 508-520.

Wellman, C.H., Osterloff, P.L. and Mohiuddin, U. (2003). Fragments of the earliest land plants. Nature **425**, 282-285.

Woldringh, C.L., Mulder, E., Valkenburg, J.A., Wientjes, F.B., Zaritsky, A., and Nanninga, N. (1990). Role of the nucleoid in the toporegulation of division. Res. Microbiol. **141,** 39-49.

Yoshida, Y., Kuroiwa, H., Misumi, O., Nishida, K., Yagisawa, F., Fujiwara, T., Nanamiya, H., Kawamura, F. and Kuroiwa, T. (2006). Isolated chloroplast division machinery can actively constrict after stretching. Science **313**, 1435-1438.

Yu, X. and Margolin, W. (1997). Ca^{2+}-mediated GTP-dependent dynamic assembly of bacterial cell division protein FtsZ into asters and polymer networks *in vitro*. The EMBO Journal. **16**, 5455-5463.

6. Appendix

6.1 List of abbreviations

ABA	abscisic acid
cDNA	complementary DNA
DMSO	Dimethylsulfoxide
DNA	desoxyribonucleic acid
EGTA	ethylene glycol tetraacetic acid
FRET	fluorescence resonance energy transfer
FtsZ	“Filamentous temperature sensitive Z”
GFP	green fluorescent protein
GTP	Guanosin-5’-triphosphat
*npt*II	*nptII* neomycin phosphotransferase II
NPA	1-*N*-naphthylphthalamic acid
IAA	indole-3-acetic acid
2iP	N^6- Δ^2- isopentenyladenine,
LatB	Latrunculin B
Z1	4-chloro-2,6-bis(5-chloro-2-hydroxybenzyl) phenol
Z3	N'-{2-[2-(4-chlorophenyl)vinyl]benzo[g]quinazolin-4-yl}-N,N-diethyl-1,2-ethanediamine
ox	overexpression line
KO	knock out
WT	wild type
Δ*fts*Z1-2	knock out

6.2 List of Figures

1.1.1.1 List of Diagrams

1.1.1.2 List of Tables

Acknowledgments

I want to thank Prof. Peter Nick for the chance of doing this study under his supervision.

Also I want to thank Priv.Doz. Frank Hartung for agreeing to be my coexaminer.

I especially thank Dr. Anja Martin for her help with the mosses.

And at the very last, I want to thank those that are not last in my heart: my colleagues, who went with me the last years and never once sent me away when I was in need of them.

Especially Aleksandra Jovanovic, who made live exiting in the attic and always lend a helping hand, Kai Eggenberger who was always there and Dr. Maurice Ouko, who made the best fantastic fourth.

Thank you all!